CATALYTIC TRANSFORMATION OF BIOMASS-DERIVED CARVONE OVER SUPPORTED METAL CATALYSTS AND NITRIDES

PEDRO BENAVENTE DONAYRE

A dissertation submitted for the degree of Master of Philosophy

Heriot-Watt University

School of Engineering and Physical Sciences

February 2018

Abstract

The main focus of this thesis is the investigation of the catalytic transformation of biomass-derived carvone to valuable fine chemical products over supported metal catalysts and nitrides. In the continuous gas phase carvone hydrogenation (P = 1 atm, 423 K ≤ T ≤ 573 K) over Al_2O_3 supported nanoparticle Au was found to be active towards dihydrocarvone (endocyclic -C=C-), whereas Pt/Al_2O_3 was selective towards carvotanacetone (exocyclic -C=C-). Temperature had an impact on carvone adsorption at metal/support interface and products distribution. Carvacrol was found to form through carvotanacetone or directly from carvone. Exclusive carvacrol formation on Ag/Al_2O_3 was linked to the catalyst lowest recorded H_2 uptake.

The selective conversion of carvone in H_2 was studied over (Al_2O_3, C and CeO_2) supported Pd (mean size 2.8-3.0 nm), taking bulk Pd as benchmark. 100% carvacrol yield was achieved over Pd/Al_2O_3, Pd/C and bulk Pd at an inlet H_2/Carvone = 1/6, with appreciably higher rates for the supported catalysts. Carveol formation over Pd/CeO_2 was attributed to -C=O activation at surface oxygen vacancies (confirmed by O_2 titration) generated during TPR. Carvotanacetone and carvomenthone formation were observed at H_2/Carvone > 1/6. The incorporation of water (H_2O:Carvone ≤ 1:3) with hydrogen (H_2:Carvone = 1:6-2:1) increased carvacrol production rate to deliver 100% yield. A higher H_2O content lowered rate due to competition with carvone for surface active sites. Our results demonstrated the benefits of carvacrol production in continuous flow relative to conventional batch processes allowing full selective transformation under mild reaction conditions.

Liquid phase hydrogenation of carvone over model Pd/Al_2O_3 catalyst was also investigated. Dependence of reaction kinetic on range of temperatures, pressures and solvent(less) was studied. Carveol formation was observed by lowering polarity of solvents. On the contrary, promotion in the hydrogenation rates of -C=C- double bonds associated with increase in polarity of solvents. Increasing temperature favoured formation of carvacrol, whereas raising pressure inhibits its production according to the proposed mechanism of hydrogen migration/keto-enol tautomerization.

The ongoing study with nitrides (β− and γ−Mo_2N) prepared by temperature programmed treatment of MoO_3 in flow of H_2+N_2 demonstrated full selectivity towards carvacrol in hydrogen free condition. Variation in surface Mo/N molar ratio of prepared samples did not affect production rate which is controlled by surface area of Mo_2N.

Dedication

To my family:

Julio Cesar and Elena Benavente Donayre

Margarita Belekova and Sylvia Umeres Valle

Djenish Belekov and Rimma Belekova

ACADEMIC REGISTRY

Research Thesis Submission

Name*:*	Pedro Benavente Donayre		
School:	School of Engineering and Physical Sciences		
Version: *(i.e. First, Resubmission, Final)*	Final	Degree Sought:	MPhil

Declaration

In accordance with the appropriate regulations I hereby submit my thesis and I declare that:

1) the thesis embodies the results of my own work and has been composed by myself
2) where appropriate, I have made acknowledgement of the work of others and have made reference to work carried out in collaboration with other persons
3) the thesis is the correct version of the thesis for submission and is the same version as any electronic versions submitted*.
4) my thesis for the award referred to, deposited in the Heriot-Watt University Library, should be made available for loan or photocopying and be available via the Institutional Repository, subject to such conditions as the Librarian may require
5) I understand that as a student of the University I am required to abide by the Regulations of the University and to conform to its discipline.
6) I confirm that the thesis has been verified against plagiarism via an approved plagiarism detection application e.g. Turnitin.

* *Please note that it is the responsibility of the candidate to ensure that the correct version of the thesis is submitted.*

Signature of Candidate*:*	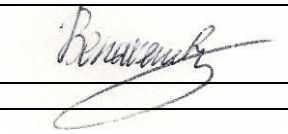	Date:	15/05/2018

Submission

Submitted By *(name in capitals):*	
Signature of Individual Submitting:	
Date Submitted:	

For Completion in the Student Service Centre (SSC)

Received in the SSC by *(name in capitals):*			
Method of Submission *(Handed in to SSC; posted through internal/external mail):*			
*E-thesis Submitted (**mandatory for final theses**)*			
Signature:		Date:	

Please note this form should be bound into the submitted thesis.

Table of Contents

Lists of Tables

Lists of Figures

Glossary

Acronyms

AAS	Atomic Absorption Spectroscopy
BET	S.Brunauer, P. H. Emmett and E. Teller theory; measurement of surface area
CVAN	Carvotanacetone
CVCOL	Carvacrol
CVMN	Carvomenthone
CVMNOL	Carvomenthol
CVN	Carvone
CVOL	Carveol
DCVN	Dihydrocarvone
FID	Flame Ionisation Detector
GHSV	Gas Hourly Space Velocity
ICP	Inductively Coupled Plasma
ICP-OES	Inductively coupled plasma-optical emission spectrometry
STEM	Scanning Transmission Electron Microscopy
TEM	Transmission Electron Microscopy
TOF	Turnover Frequency
TPD	Temperature Programmed Desorption
TPR	Temperature Programmed Reduction
XRD	X-ray Diffraction

List of Publications by the Candidate

[1] P. Benavente, F. Cárdenas-Lizana, M. A. Keane, Catal. Commun. 96 (2017) 37-40.

[2] P. Benavente, F. Cárdenas-Lizana, M. A. Keane, Catal. Today 308 (2018) 45-49.

List of Presentations by the Candidate

[1] *Selective production of carveol from biomass-derived carvone over Pd/Al_2O_3*, Poster presentation at the **EPS Poster Event**, Heriot-Watt University, October 2015.

[2] *Selective hydrogenation of biomass-derived carvone over Pd/Al_2O_3 under mild reaction conditions*, Oral presentation at the **3rd IMPEE Conference**, Heriot-Watt University, August 2015.

Chapter 1

Introduction and Objective of Research

1.1 From Convectional to Sustainable Chemical Production. Circular Economy

Exponential increase in world population triggers production of chemicals to satisfy consumption needs. Chemical industries are still heavily relied on fossil hydrocarbons [1] that are known to result in serious environmental degradations [2]. Introduction of new environmental policies requires development of sustainable chemical processing [3] to decrease waste production, energy consumption and chemical toxicity [4].

Implementation of Circular Economy (the concept of closing material loops to preserve products, parts, and materials in the industrial system and extract their maximum utility [5]) aims to decrease human footprint by integration of economic activity and environmental wellbeing in a sustainable way [6]. Such concept has been adopted throughout the globe [5], with Zero Waste strategy implemented by the UK [7] tends to minimize waste production.

1.2 Carvone as a bio alternative

To satisfy environmental concerns and consumer needs there is a requirement to exploit the potentials of renewable raw materials. Carvone is a valuable bio stock material [8], containing three reactive functionality (exo-/endocyclic -C=C- and carbonyl -C=O group) can be catalytically utilize to a number of valuable fine chemical products [8] in hydrogen mediated reactions. Carvone normally produced at low cost *via* biowaste transformation of citruses peels or by steam distillation of spearmint oil [9]. Up to now not many studies of carvone transformation has been reported, with majority considering high reaction conditions and/or use of toxic chemicals [10–16]. Nevertheless, achievement of highly selective carvone transformation is a current challenge.

1.3 Objective of Research

The aim of this research was to investigate sustainable selective processes for the continuous production of valuable chemicals through catalytic transformation of biosourced carvone over bulk (nitrides) and supported (Pt, Pd, Au, Ag) catalysts.

Catalyst characterisation has involved ICP, TPR, H_2/O_2 chemisorption, H_2 TPD, (S)TEM and XRD measurements. The work presented in **Chapter 2** examines effect of metal (Pt, Au, Ag) on gas phase transformation of carvone over a series of alumina supported catalysts. The effect of the support and H_2 content in the feed was considered in **Chapter 3**. The continuous gas phase hydrogenation of carvone was investigated over Pd supported on non-reducible (Al_2O_3), reducible (CeO_2) and carbon supported catalysts. Operation under hydrogen lean conditions results in the formation of carvacrol while hydrogenated products (mainly carvotanacetone and carvomenthone) were obtained at increase hydrogen partial pressures. This work is extended in **Chapter 4** where we consider the use of H_2O as a hydrogen source for reaction over Pd/Al_2O_3. In order to further explore the potential of Pd/Al_2O_3, we considered in **Chapter 5** the hydrogenation of carvone in liquid phase. The thesis ends (**Chapter 6**) with preliminary results obtained over bulk molybdenum nitrides that promote carvacrol formation in the absence of hydrogen.

1.4 References

[1] S. Singh, B.R. Bakshi, Chapter Twelve - Chemical Engineering and Biogeochemical Cycles: A Techno-Ecological Approach to Industry Sustainability, in: G. Ruiz-Mercado, H. Cabezas (Eds.), Sustainability in the Design, Synthesis and Analysis of Chemical Engineering Processes, Butterworth-Heinemann, Oxford, 2016: pp. 275–294.

[2] L. Liu, S.Y. Cheng, J.B. Li, Y.F. Huang, Energy Sources, Part A Recover. Util. Environ. Eff. 29 (2007) 1069–1080.

[3] I.T. Horváth, Chem. Rev. 118 (2018) 369–371.

[4] M. Gavrilescu, Y. Chisti, Biotechnol. Adv. 23 (2005) 471–499.

[5] T. Zink, R. Geyer, J. Ind. Ecol. 21 (2017) 593–602.

[6] A. Murray, K. Skene, K. Haynes, J. Bus. Ethics 140 (2017) 369–380.

[7] C. Cole, M. Osmani, M. Quddus, A. Wheatley, K. Kay, Resour. Conserv. Recycl. 89 (2014) 64–75.

[8] W. Schwab, C. Fuchs, F.-C. Huang, Eur. J. Lipid Sci. Technol. 115 (2013) 3–8.

[9] J.L. Bicas, A.P. Dionísio, G.M. Pastore, Chem. Rev. 109 (2009) 4518–4531.

[10] I.M.J. Vilella, S.R. de Miguel, O.A. Scelza, J. Mol. Catal. A Chem. 284 (2008) 161–171.

[11] C.I. Melo, R. Bogel-Łukasik, E. Bogel-Łukasik, J. Supercrit. Fluids 61 (2012) 191–198.

[12] S.R. de Miguel, M.C. Román-Martínez, D. Cazorla-Amorós, E.L. Jablonski, O.A. Scelza, Catal. Today 66 (2001) 289–295.

[13] G.C. Torres, S.D. Ledesma, E.L. Jablonski, S.R. de Miguel, O.A. Scelza, Catal. Today 48 (1999) 65–72.

[14] S.R. de Miguel, M.C. Román-Martínez, E.L. Jablonski, J.L.G. Fierro, D. Cazorla-Amorós, O.A. Scelza, J. Catal. 184 (1999) 514–525.

[15] E.I. Klabunovskii, L.F. Godunova, L.K. Maslova, Bull. Acad. Sci. USSR, Div. Chem. Sci. 21 (1972) 1020–1024.

[16] C.I. Melo, R. Bogel-Łukasik, M.G. da Silva, E. Bogel-Łukasik, Green Chem. 13 (2011) 2825–2830.

Chapter 2

Continuous Carvone Transformation over Al_2O_3 Supported Pt, Au and Ag

In this Chapter role of Al_2O_3 supported Pt, Au and Ag was evaluated the in continuous gas phase conversion of carvone (T = 423 – 573 K; P = 1 atm). Catalytic performance is correlated to critical catalyst characterisation data.

2.1 Introduction

The global demand in consumption of fine chemicals that rely on non-renewable fossil fuels and environmental concerns associated with commercial processes has triggered a reconsideration of alternative production routes using renewable raw materials. With a worldwide production of 1×10^{11} tons year^{-1} biomass represents a potential alternative [1]. Carvone is a polyunsaturated monoterpenoid (-C=O group, exo- and endo- C=C) obtained at low cost by steam distillation of spearmint oil or nitrosochlorination of citrus-derived limonene [2]. Reaction of carvone with hydrogen results in the formation of a range products (see **Figure 2.1**) with applications in the flavoring, food processing and pharmaceutical industries [3]. Although numbers of reported products formed by hydrogen attack of exo-, endo -C=C or both functionalities resulted in carvotanacetone, carvomenthone, dihydrocarvone and carvomenthol formation, respectively (**path I-II** in **Figure 2.1**), carvacrol – carvone isomer was also reported among them. Isomerization process in carvone is not well studied where carvacrol formation was reported through hydrogenated product – carvotanacetone [4,5] in the presence of hydrogen over Pd catalysts (**path IIIB** in **Figure 2.1**). The reaction has been typically carried out in batch operation under conditions of high pressures (>50 atm) and temperatures (>523 K) with organic solvents (*e.g.* toluene, hexane, alcohols) over bulk/supported metal catalysts [4–10].

In pressurised batch operation Pt and Au promote the formation of carvotanacetone and dihydrocarvone, respectively, with highest reported selectivity exceeded 50% for both products [6,8,11]. Conclusions regarding preferential hydrogen attack of exocyclic -C=C- by Pt catalysts was not explained by authors and only suggested to be link to high catalytic activity of the metal [6,8]. Despite the reported

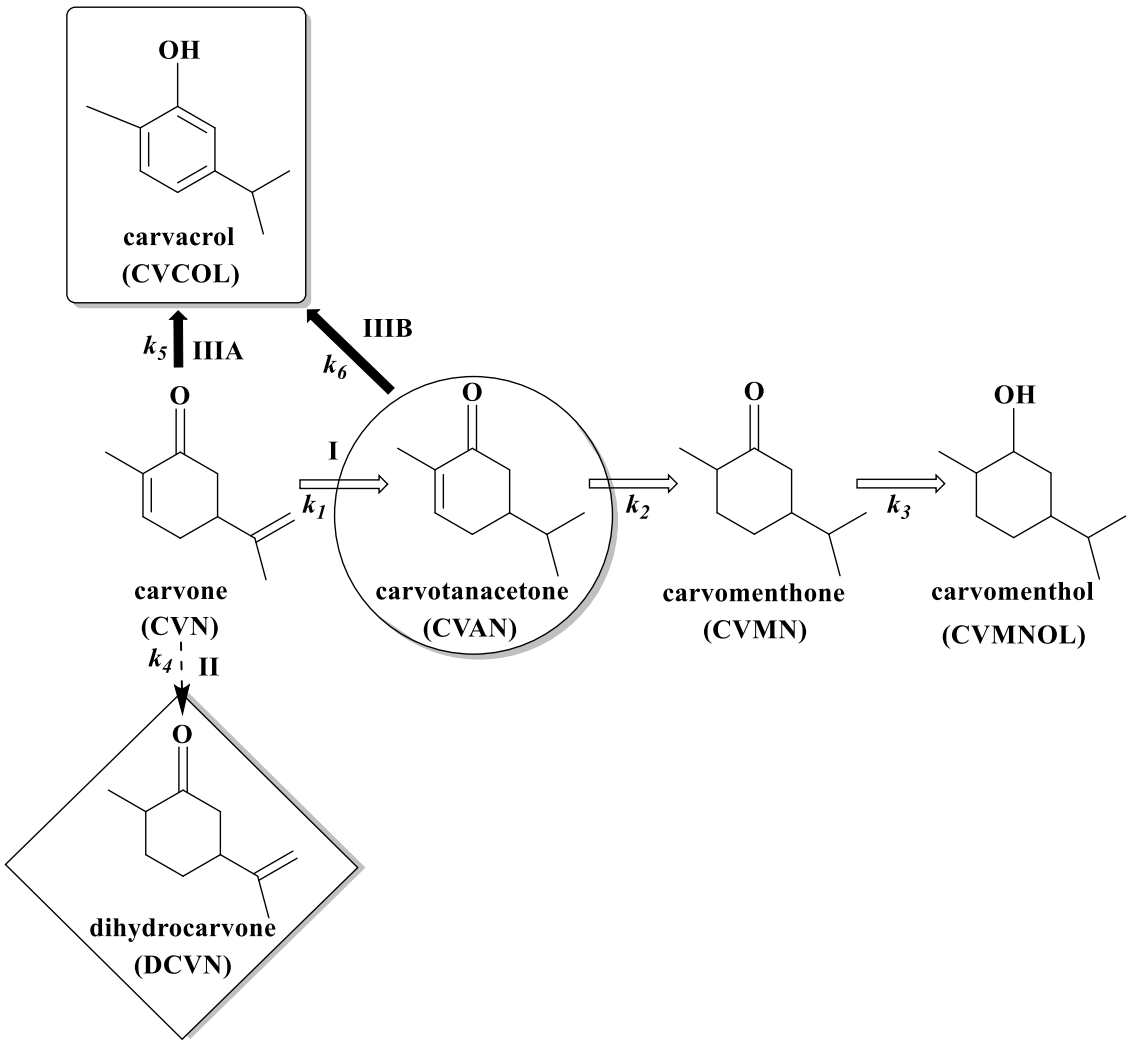

Figure 2.1: Reaction pathways in the conversion of carvone to carvotanacetone (CVAN) carvomenthone (CVMN), carvomenthol (CVMNOL) (path I, open arrows), dihydrocarvone (DCVN) (path II, dashed arrow) and carvacrol (CVCOL) (path III, solid arrows).

selective gold behavior towards hydrogenation of carbonyl group in unsaturated ketones [12], Demidova and co-workers [11] reported formation of dihydrocarvone with the yield of 56%, that they explained based on conjugation effect of -C=C- with carbonyl group that influenced carvone adsorption on the catalyst surface, however no comparison with other metals has been made. Gold was also reported to promotes isomerization of allylbenzene to 2-methylstyrene [13], limone to terpinolene [14] while Pt was also extensively studied in isomerization reaction of linear alkanes to iso-alkanes (skeletal isomerization) and double bond isomerization (H-shift) in alkenes [15]. Recent studies demonstrate that oxide–metal interfaces are responsible for changes in the catalytic activity and selectivity due to charge transfer between the metal and the oxide support [16]. An example of metal/support interaction is an electron transfer from Al_2O_3

to generate $Au^{\delta-}$ [17]. Elsewhere [18] has been proposed and reported [19] by the number of research that the electronic character of Au nanoparticles can influence activation of the -C=O group with enhanced selectivity for carbonyl group (relative to -C=C-) reduction over $Au^{\delta-}$ in the conversion of α,β-unsaturated ketones to α,β-unsaturated alcohols. Small number of studies considered temperature effect [4,5,9] over Pt, Pd, Rh catalysts. The results showed that increasing in temperature (283-323 K) resulted in formation of carvomenthone as principal product, with yield more than 90% can be accounted based on increased hydrogen concertation in the solution with temperature. Increase in the solubility for organic solvents (e.g. toluene, hexane, alcohols) can be explained based on the weaker solvation enthalpy in compare to water, making dissolution of a gas endothermic process [20]. In all cases, researchers observed increase in total rate. Nanoparticle Ag catalyst has never been applied in carvone hydrogenation but results obtained for a number of unsaturated ketones (cinnamaldehyde, citral, crotonaldehyde, prenal, acrolein) [21] suggested that Ag as a promising alternative. The majority of the work has focused on batch systems, however operating in continuous flow at atmospheric pressure without a solvent offers advantages in terms of sustainability and enhancing catalytic activity and/or selectivity [22].

In this work we investigated reaction mechanism of solvent-free carvone with hydrogen in continuous process by evaluating effect of metal (Pt, Au and Ag) supported on Al_2O_3 and temperature in the hydrogenation and isomerization processes.

2.2 Experimental

2.2.1 Catalyst Preparation and Activation

The support (γ-Al_2O_3), Au ($HAuCl_4$ (99.999%)) and Ag ($AgNO_3$ (99.99%)) precursors and (0.7% wt.) Pt/Al_2O_3 catalyst were purchased from Sigma-Aldrich. Synthesis of Au/Al_2O_3 and Ag/Al_2O_3 by deposition-precipitation followed a prior procedure [23,24]. Samples were sieved to mean diameter = 75 μm, activated in 60 cm^3 min^{-1} H_2 at 5 K min^{-1} to 573 K for Au and Ag/Al_2O_3 samples and to 773 K for Pt/Al_2O_3, with further passivation in 1% v/v O_2/He at ambient temperature prior to *ex*-situ characterisation.

2.2.2 Catalyst Characterisation

Metal content was measured by ICP-OES (Vista-Pro, Varian Inc.). Catalyst activation by temperature programmed reduction (TPR, in 5% v/v H_2/N_2 at 5 K min^{-1} to 573 K for Au and Ag/Al_2O_3 samples and to 773 K for Pt/Al_2O_3), H_2 (at 423 and 573 K) chemisorption using a pulse (10-50 µl) titration procedure and total specific surface area (SSA, in 30% v/v N_2/He using the single point BET method) measurements were conducted on the commercial CHEM-BET 3000 (Quantachrome) according to procedures described elsewhere [23,24]. Measurements of BET surface area, using single point measurement, were performed at the liquid nitrogen temperature and followed method/calculation described elsewhere [25–28]. Results were reproducible to ±5%. Metal particle morphology was determined by scanning transmission electron microscopy (STEM, JEOL 2200FS field emission gun-equipped TEM), employing Gatan Digital Micrograph 1.82 for data acquisition/manipulation. Samples for analysis were dispersed in acetone and deposited on a holey carbon/Cu grid (300 Mesh). Surface area-weighted mean metal sizes ($d_{(S)TEM}$) were determined from a count of up to 1000 individual particles according to:

$$d_{(S)TEM} = \frac{\sum_i n_i d_i^3}{\sum_i n_i d_i^2} \qquad \textbf{(2.1)}$$

where n_i is the number of particles of diameter d_i. Standard deviation of the size counting was within 10%.

2.2.3 Catalytic Procedure

2.2.3.1 Materials

Carvone (98%), carvacrol (98%), dihydrocarvone (99%), carveol (98%), ethylidenecyclohexane (99%), ethylcyclohexane (99%), cyclohexane (99%), cyclohexanone (99%) and bicyclohexyl (99%) were obtained from Sigma-Aldrich. Vinylcyclohexane (97%), cyclohexene (99%) and cyclohexanol (99%) were purchased from Fisher. Carvotanacetone, carvomenthone and carvomenthol were synthesised following published methods [29]. All gases (H_2, N_2, O_2 and He) were ultra-high purity (BOC, 99.9%).

2.2.3.2 Catalytic System

Reactions were conducted at atmospheric pressure and isothermal conditions (423 – 573 K) *in situ* after activation in a continuous flow fixed bed vertical tubular glass reactor (15 mm i.d.). A layer of borosilicate glass beads served as preheating zone where the organic reactant was vaporised and reached reaction temperature before contacting the catalyst. Temperature was continuously monitored by a thermocouple inserted in a thermowell within the catalyst bed. The organic reactant (carvone, vinylcyclohexane, cyclohexene or cyclohexanone) was delivered *via* a glass/teflon air-tight syringe and teflon line using a microprocessor controlled infusion pump (Model 100 kd Scientific) at a fixed calibrated flow rate. A co-current flow of N_2, H_2 or H_2+N_2 with reactant (N_2/Reactant and H_2/Reactant = 12/1 – 20/1 mol mol^{-1}) was maintained at $GHSV = 3 \times 10^3 - 2 \times 10^4$ h^{-1}. Metal (n, mol_{metal}) to reactant (F, $mol_{reactant}$ h^{-1}) ratio spanned the range $5 \times 10^{-6} - 5 \times 10^{-4}$ h. In blank tests, reactions in the absence of catalyst or hydrogen and/or support alone did not result in any measurable conversion. The reactor effluent was frozen in a liquid N_2 trap for analysis using a Perkin-Elmer Auto System XL gas chromatograph with split/splitless injector, FID and Stabilwax capillary column (RESTEK). Data acquisition/manipulation used the TotalChrom data system. Fractional carvone conversion (X) is given by:

$$X = \frac{[\text{Carvone}]_{in} - [\text{Carvone}]_{out}}{[\text{Carvone}]_{in}} \quad \textbf{(2.2)}$$

with selectivity to carvacrol ($S_{Carvacrol}$):

$$S_{\text{Carvacrol}}\ (\%) = \frac{[\text{Carvacrol}]_{out}}{[\text{Carvone}]_{in} - [\text{Carvone}]_{out}} \times 100 \quad \textbf{(2.3)}$$

Repeated reactions with different samples from the same batch of catalyst delivered raw data reproducibility and carbon mass balances within ±5%. Reactant consumption rate (R) was obtained from:

$$R(\text{h}^{-1}) = \frac{X_0 \times F}{n} \quad \textbf{(2.4)}$$

where initial fractional conversion (X_0) was extracted from time on-stream measurements [23]. Kinetic modelling was carried out using Berkley Madonna Version 8.0.1 (for Windows).

2.3 Results and Discussion

2.3.1 Catalyst Characterisation

The metal loading, SSA, particle size (from (S)TEM analysis) and H_2 chemisorption values for the Al_2O_3 supported catalysts are presented in **Table 2.1**. The three catalysts exhibit a SSA (126-220 m^2 g^{-1}), that fell in the surface area intervals characterised by γ-Al_2O_3 [30]. All studied samples present pseudo-spherical metal nanoparticles (**Figure 2.2(I)**). Pt, Au and Ag/Al_2O_3 had similar metal content (0.5 – 1.1%) and mean metal diameter (1.7 – 4.4 nm) (**Table 2.1**). Catalysts bear metal nanoparticles in the 1-8 nm size range (**Figure 2.2(II)**).

Table 2.1: Metal content, specific surface area (SSA), metal particle size from (S)TEM analysis (d_{STEM}), H_2 chemisorption and carvone consumption rate (R) at X_0 ~ 0.3 over Al_2O_3 supported Pt, Au and Ag.

Catalyst	Metal loading (% wt.)	SSA (m^2 g^{-1})	$d_{(S)TEM}$ (nm)	H_2 uptake (mmol g_{metal}^{-1})	$R \times 10^2$ (h^{-1})
Pt/Al_2O_3	0.7	126	1.7	3.1[a]; 2.7[b]	244[a]; 134[b]
Au/Al_2O_3	1.1	147	3.6	0.3[a]; 0.6[b]	13[a]; 5[b]
Ag/Al_2O_3	0.5	220	4.4	-[a; c]; 0.07[b]	-[a; c]; 1[b]

[a]at 423 K; [b]at 573 K; [c]below detection limit.

The TPR profiles for Au and Ag (profiles **(II)** and **(III)** in **Figure 2.2**) exhibit a single positive peak (H_2 release) at 450 K where the associated H_2 consumption matched that required for the reduction of the precursor to the metallic form. An equivalent response in terms of metal reduction has been reported previously, with a single reduction peak in the range 436 - 503 K [31]. The TPR for Pt/Al_2O_3 (**Figure 2.2(I)**) shows two consumption peaks at 473 K and 643 K. First peak associated with lower temperature

may be due to the bulk phase reduction of the platinum species PtO, and PtO_2, including Pt_sO (surface platinum oxide) [32,33]. The second peak at high temperature can be attributed to highly dispersed particle with strong interaction with the support as previously reported [34]. Hydrogen chemisorption on Pt/Al_2O_3 (**Table 2.1**) was one and two order of magnitude greater than that obtained for the Au and Ag catalysts, respectively, and can be attributed to the greater capacity of

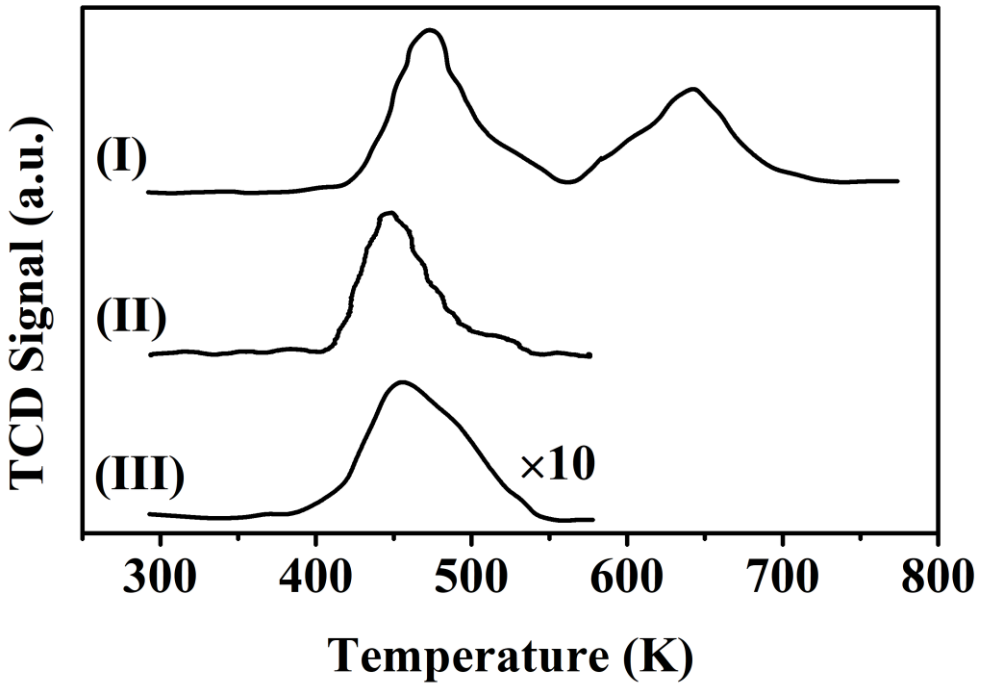

Figure 2.2: Temperature programmed reduction (TPR) profiles for Al_2O_3 supported (I) Pt, (II) Au and (III) Ag.

Pt to dissociate H_2 [35]. Hydrogen dissociation is exothermic process [36] driven by kinetic (adsorption on metal) and thermodynamic factor (temperature of the process). Over Pt H_2 uptake decreased with temperature (3.1 → 2.7 mmol g_{metal}^{-1}) which is consisted with previously reported [35]. The presence of the high activation energy barrier for hydrogen dissociative adsorption on Au and Ag due to the filled d band is well recognized [37]. Hydrogen chemisorption on Au/Al_2O_3 is an activated process with an increased uptake (by 2 fold) with temperature (**Table 2.1**) [35].

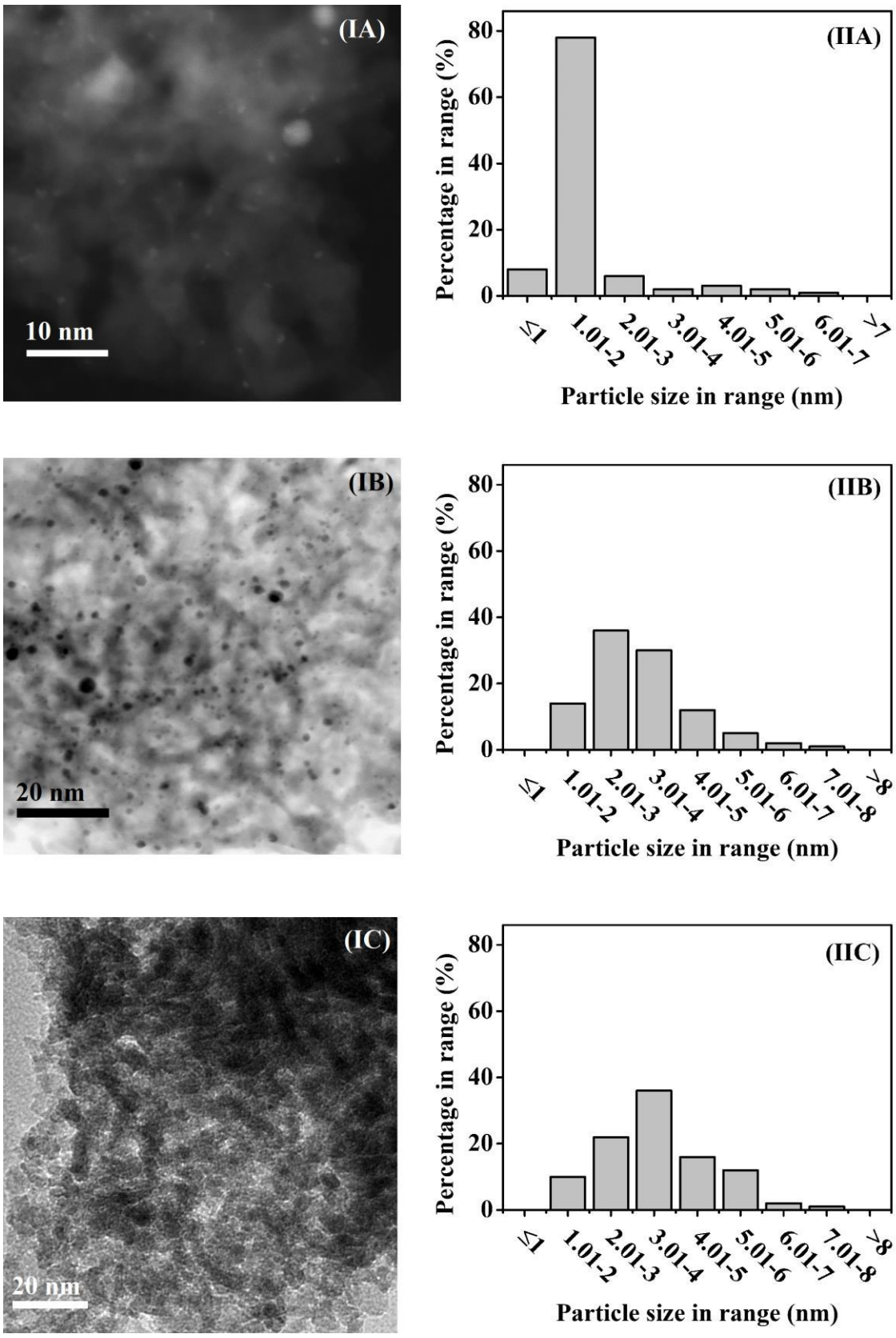

Figure 2.3: (I) Representative (S)TEM images with (II) metal size histograms for Al_2O_3 supported (A) Pt, (B) Au and (C) Ag.

2.3.2 Catalysis results

A mass balance was applied assuming pseudo-first order kinetics for each reaction step:

$$\frac{dn_{CVN}}{dt} = -n_{CVN} \times (k_1 + k_4 + k_5) \quad \textbf{(2.5)}$$

$$\frac{dn_{CVAN}}{dt} = n_{CVN} \times k_1 - n_{CVAN} \times (k_2 + k_6) \quad \textbf{(2.6)}$$

$$\frac{dn_{CVMN}}{dt} = n_{CVAN} \times k_2 - n_{CVMN} \times k_3 \quad \textbf{(2.7)}$$

$$\frac{dn_{DCVN}}{dt} = n_{CVN} \times k_4 \quad \textbf{(2.8)}$$

$$\frac{dn_{CVCOL}}{dt} = n_{CVN} \times k_5 + n_{CVAN} \times k_6 \quad \textbf{(2.9)}$$

where n_i represents number of moles of compound i, k_j is the pseudo-first order rate constant for step j and $t=n_{metal}/F$ has the physical meaning of contact time. It should be stressed that uniqueness of presented model was tested based on differences (deviation) between experimental and predicted (modelling) results of applied above kinetic equations. In this case deviation did not exceed 10% [38,39]. Taking the reaction over Pt/Al_2O_3 at 423 K as a representative, the results of a non-linear regression of the experimental data to the kinetic model are shown in **Figure 2.3**. The resultant rate constant values k_j (min^{-1}) are given in **Table 2.2**. In all cases rate over Pt was one order of magnitude higher in compare to Au (**Table 2.2**) and with no reaction detected over Ag at 423 K can be link to H_2 uptake (**Table 2.1**). The experimentally determined and predicted product compositions converge with the amount of metal (n_{metal}) are presented in **Figure 2.4**. It was found that selectivity response was largely sensitive to the amount of metal. Thermodynamics finding [40] suggested greater stability of conjugated endo-cyclic carbon-carbon double bond and carbonyl functionalities in carvone, with decreasing reactivity based on Gibbs free energy [41]: exo -C=C- > endo -C=C- > -C=O. For both, Pt/Al_2O_3 and Au/Al_2O_3, **path I** of sequential CVAN to CVMN with further formation to CVMNOL ($\boldsymbol{k_1>k_2>k_3}$, note $\boldsymbol{k_3}$ is not shown) is consistent with previous findings where formation of unsaturated and saturated ketones was reported [8]. Only Au promoted formation of dihydrocarvone (k_4

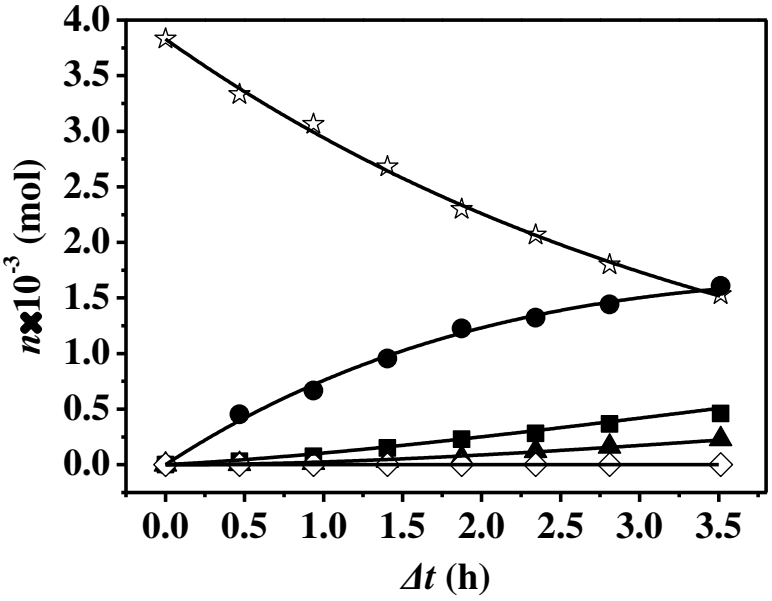

Figure 2.4: Mol of CVN (☆), CVAN (●), CVMN (▲), DCVN (◇) and CVCOL (■) as a function of contact time (Δt) for reaction over Pt/Al_2O_3. *Note*: lines represent fit to eqns (2.5-2.9). *Reaction conditions*: P = 1 atm, T = 423 K, H_2/Carvone = 20/1, $n/F = 9 \times 10^{-6} - 7 \times 10^{-5}$ h, $GHSV = 2 \times 10^4$ h^{-1}.

Table 2.2: Rate constants for carvone hydrogenation over Al_2O_3 supported Pt and Au.

Steps		$k \times 10^2$, h^{-1}			
		423 K		573 K	
		Pt	Au	Pt	Au
k_1	CVN→CVAN	244	11	40	0.7
k_2	CVAN→CVMN	62	10	38	0.6
k_4	CVN→DCVN	-[a]	2	-[a]	0.9
k_5	CVN→CVCOL	-[a]	-[a]	94	3
k_6	CVAN→CVCOL	93	10	-[a]	-[a]
k_1/k_2	CVAN/CVMN	4.0	1.1	1.0	1.2
k_2/k_6	CVMN/CVCOL	0.6	1	-	-
$(k_1+k_4)/k_5$	Hydrogenated product(s)/isomerization	-	-	0.4	0.5
k_4/k_1	DCVN/CVAN	-	0.2	-	1.3

CVN = carvone; CVAN = carvotanacetone; CVMN = carvomenthone; CVMNOL = carvomenthol; DCVN = dihydrocarvone; CVCOL = carvacrol.
[a]no activity

= 2 × 10^2 h^{-1}, **path II**) with selectivity nearly 10% at all the range of moles of the catalyst (*i.e.* conversion). Since the carvone molecule is polarised at the oxygen being partial negative charged with the ring carbon bonded to O bears the lowest electron density of all the carbons in the ring [42], it has been suggested that the adsorption takes place between $C^{\delta+}$ and partly negatively charged metal nanoparticles *via* electrostatic effects. The presence of electron rich $Au^{\delta-}$ nanoparticles caused by support→metal electron transfer, have been previously reported in the literature [43], destabilize conjugated structure of endo -C=C- and -C=O. Such destabilization leads to the adsorption of -C=C- on the support. Indeed negative charged Au particles was reported previously influencing course of reactions [43]. Au catalytic response was also observed in preferable carvomenthone formation relative to carvotanacetone (k_1/k_2) over Au (4 fold lower) in comparison with Pt. Skrzyńska and co-workers [44] reported presence of metallic Pt species with δ=0 in commercial Pt/Al_2O_3 (1% wt, 4 nm) similar to the sample used in our study.

Formation of carvacrol was found to proceed *via* dehydroisomerization of carvotanacetone (**path IIIB** in **Figure 2.1**) being formed on metal/support interface. Such phenomena is widely accepted where interactions between the metal and the support can dramatically influence catalytic activity [45]. The enhancement of activity is often attributed to sites along the metal/support boundary, where the adsorbed species interact with both the metal and the support [46]. We suggested that new formed intermediate with saturated exo-cyclic -C=C- is formed on metal followed by C–H bond cleavage at the ring forms a double unsaturated ring intermediate. In the works of Shimizu [47] dehydrogenation of alcohols has been proposed took place with C-H dissociation on the metal (Pt, Au). Further in theoretical study of alcohol dehydrogenations, Lyalin *et. al.* [48] found a decrease in barrier for H-elimination due to the formation of the additional adsorption sites at metal/support interface. As suggested above destabilize structure of newly formed intermediate triggers isomerization know as keto-enol tautomerization involving hydrogen migration from neighbouring carbon to oxygen allowed to obtain carvacrol. In the work of An [49] it was concluded that oxide-metal interface acts to promote selective n-hexane isomerization over supported Pt. According to **Figure 2.4(IB)** twice higher CVCOL selectivity over Au compare with Pt can be accounted to high hydrogen surface concentration on the latter metal (**Table 2.1**) that inhibits C–H bond cleavage. Interestingly, that over Pt being known as hydrogenation/dehydrogenated catalyst,

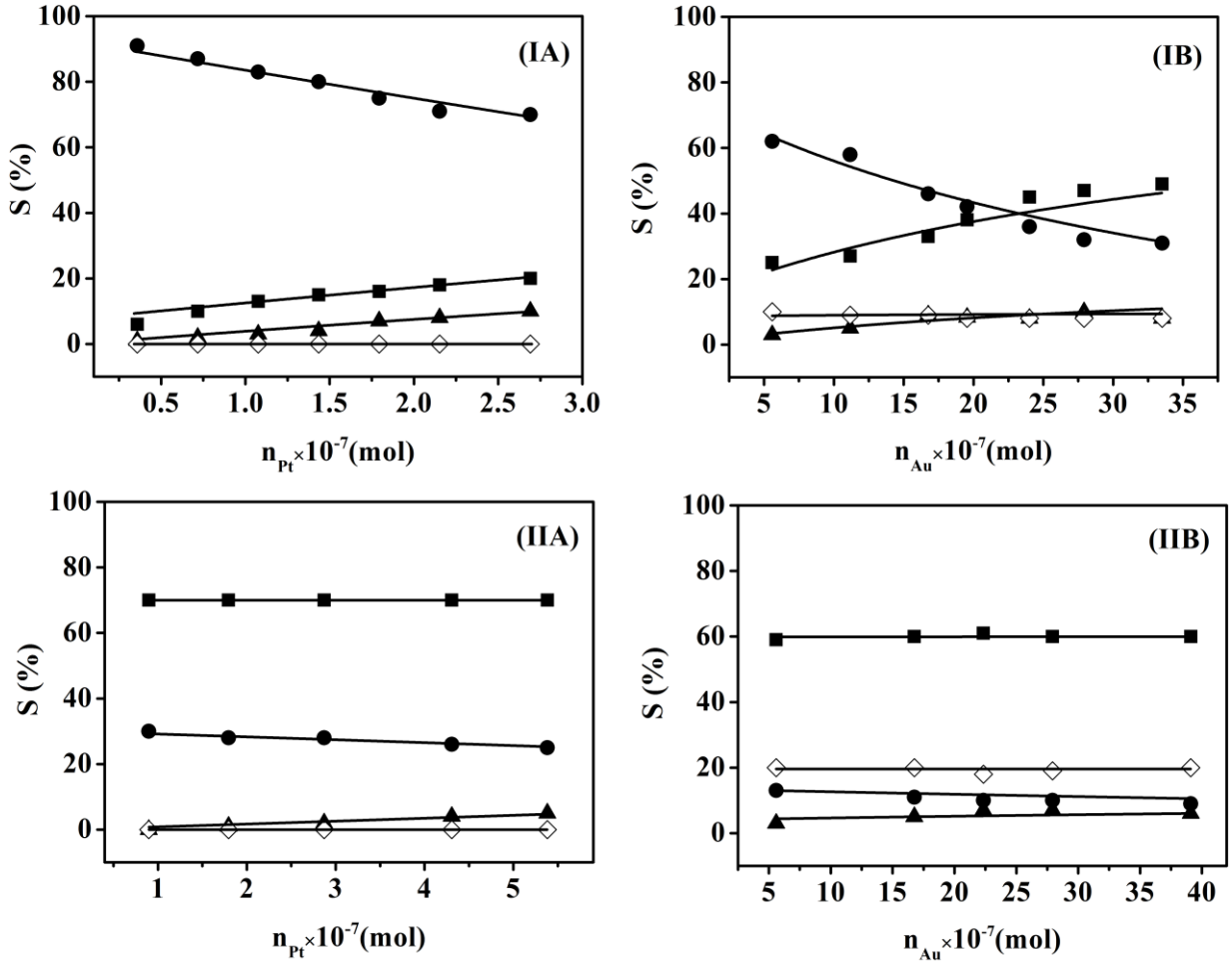

Figure 2.5: Variation of selectivity to CVAN (●), CVMN (▲), DCVN (◇) and CVCOL (■) with mol of metal for reaction at (I) 423 K and (II) 573 K over (A) Pt/Al_2O_3 and (B) Au/Al_2O_3. *Reaction conditions*: P = 1 atm, H_2/Carvone = 20/1, $n/F = 5\times10^{-6} - 5\times10^{-4}$ h, $GHSV = 8 \times 10^3 - 2 \times 10^4$ h^{-1}.

CVAN was favourably transformed to CVCOL rather than to CVMN (k_2/k_6 = 0.6) in compare with Au (k_2/k_6 = 1) despite the higher H_2 uptake ability can be accounted based on adsorption on metal/support boundaries.

Evaluating effect of temperature, we observed the drop in total rate (**Table 2.1**). We examined the effect of reaction temperature on conversion of exo -C=C-, endo -C=C- and -C=O in isolation by studying the catalytic response of vinylcyclohexane, cyclohexene and cyclohexanone and the reactions are presented in **Figure 2.5**.

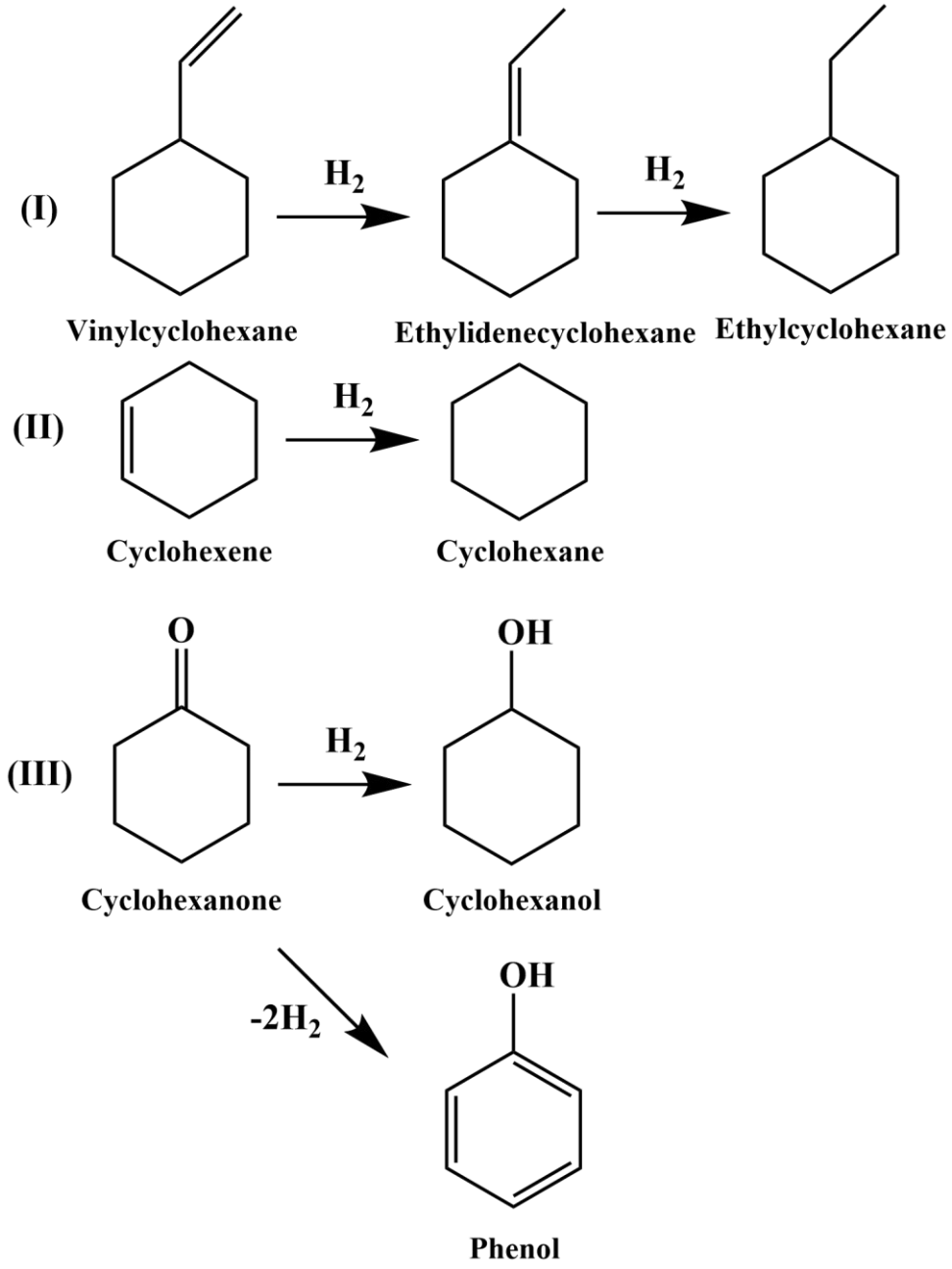

Figure 2.6: Reaction scheme for hydrogenation of (I) vinylcyclohexane, (II) cyclohexene and (II) cyclohexanone.

We observe a decrease in hydrogenation rate for vinylcyclohexane and cyclohexene (**Table 2.3**) with reaction temperature that can be explained by lower surface coverage. Additionally literature consists of examples evaluating temperature effect on activity for hydrogenation of cyclic, acyclic alkene and aromatic [50–52] where an increase in temperature resulted in lower surface coverage. Less conclusions can be drawn from reaction with cyclohexanone with no visible changes in rate being 2 order of magnitude lower in comparison with -C=C-.

Table 2.3: Consumption rate of vinylcyclohexane, cyclohexene and cyclohexanone over Al_2O_3 supported Pt and Au. ***Reaction conditions:*** **P = 1 atm, T = 423 – 573 K, H_2/Reactant = 12-13, n/F = 6×10^{-6} – 4×10^{-4} h, $GHSV$ = 9×10^{3} – 2×10^{4} h^{-1}.**

Reactant	423 K		573 K	
	Pt	Au	Pt	Au
	$R \times 10^2$ (h^{-1})			
Vinylcyclohexane	842	31	577	29
Cyclohexene	780	11	488	7
Cyclohexanone	21	2	25	3

It was found that reaction with cyclohexene gave one sole product of hydrogenation – cyclohexane (**Figure 2.6**), in case of cyclohexanone we observe formation of dehydrated by-product ($S_{bicylohexane}\geq90\%$) at 573 K. Reaction of vinylcyclohexane additionally yielded by-product - ethylidenecylohexane. Formation of this by-product is possible proceeded *via* an allyl intermediate that is formed by a hydrogen addition as previously reported for cyclic/acyclic alkenes over metals [53–55]. This intermediate undergoes hydrogen (double bond) migration as a result of H elimination giving ethylidenecylohexane or insertion of a second H to generate the alkane - ethylcyclohexane. Content of by-product increased by S = 10 – 15% (from 15 to 25% for Pt and 35 to 50% over Au) with temperature. The reason for this can be attributed to surface phenomena; it can be suggested that -C=C- can be adsorbed via σ- and/or π-complex [56] where the σ-bonded species inhibit hydrogenation by competitive adsorption [57] and as follow facilitates double bond migration [53].

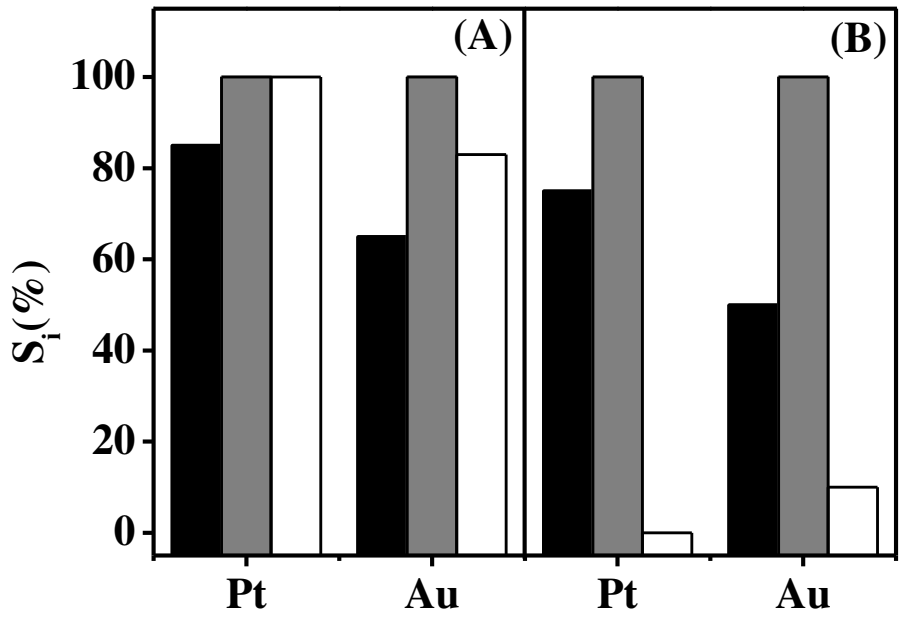

Figure 2.7: Selectivity to ethylcyclohexane (black bars), cyclohexane (grey bars) and cyclohexanol (open bars) for reaction over Pt/Al_2O_3 and Au/Al_2O_3 at (A) 473 K and (B) 573 K. ***Reaction conditions:*** ***P*** **= 1 atm,** ***T*** **= 423 – 573 K, H_2/Reactant = 12-13,** ***n/F*** **= 6×10^{-6} – 4×10^{-4} h,** ***GHSV*** **= 9×10^3 – 2×10^4 h^{-1}.**

We also observed the significant change in reaction pathway at 573 K. It was shown that carvacrol is a major product (S≥60%) and its content is independent from amount of metal (**Figure 2.4(II)**) suggesting its direct formation according with **path IIIA** of **Figure 2.1**. Comparing rates of formation for hydrogenated product(s) with isomerization we can draw conclusion that both catalysts (Pt and Au over Al_2O_3) behave similarly in direct isomerization (***$(k_1+k_4)/k_5$*** *= 0.4-0.5).* Carvacrol formation was suggested proceed by double bond migration of carvone similar to vinylcyclohexane through the exo -C=C- group interaction with catalyst [58]. Hydrogen prior dissociated on metal form reactive atomic hydrogen that attacks the exo-double bond. This results in the formation of an allyl intermediate that undergoes H elimination with bond migration and keto-enol tautomerisation to generate carvacrol. Comparing steps of hydrogenation endo- *vs* exo -C=C- (***k_4*** and ***k_1*** respectfully) one can see that ***k_1*** dropped more than 10 time in compare to ***k_4*** (only 2 times) over Au (**Table 2.2**) can suggest higher rate of desorption for exo *vs* endo -C=C-. Although decrease in rates for carvone substitutes were proportional for each group one can not discount an effect caused by conjugated -C=O group on carvone molecule. The unique selectivity response towards

carvacrol as exclusive product over Ag can be linked to surface hydrogen availability being the lowest among studied catalysts but effective to avoid full hydrogenation of exo -C=C-, *i.e.* formation of CVAN.

2.4 Conclusions

We examined continuous carvone transformation over nanoparticle Pt, Au and Ag/Al_2O_3 at T = 423 – 573 K and P_{H_2} = 1 atm. Adsorption of reactant was suggested took place on metal-support interface. Formation of main hydrogenated products (carvotanacetone, carvomenthone and dihydrocarvone) and carvone isomer – carvacrol was shown be influenced by metal partial charge (due to support interaction) and reaction temperature. Under the same reaction condition, negatively charged Au nanoparticles favoured formation of dihydrocarvone (S=10-20%). Carvotanacetone formation was preferential over neutrally charged Pt supported on Al_2O_3. Formation of carvacrol was found to proceed *via* carvotanacetone dehydroisomerization or carvone double bond migration. Increase in temperature had resulted in decrease in strength of carvone adsorption over studied catalysts. Adsorbability additionally was confirmed over carvone's substitutes having one functionality. Ag/Al_2O_3 ability to generate carvacrol as sole product was linked to the lowest reported H_2 uptake among the studied catalysts.

2.5 References

[1] M. Fantini, Biomass Availability, Potential and Characteristics, in: M. Rabaçal, A.F. Ferreira, C.A.M. Silva, M. Costa (Eds.), Biorefineries: Targeting Energy, High Value Products and Waste Valorisation, Springer International Publishing, Cham, 2017: pp. 21–54.

[2] J.L. Bicas, A.P. Dionísio, G.M. Pastore, Chem. Rev. 109 (2009) 4518–4531.

[3] W. Schwab, C. Fuchs, F.-C. Huang, Eur. J. Lipid Sci. Technol. 115 (2013) 3–8.

[4] E.I. Klabunovskii, L.F. Godunova, L.K. Maslova, Bull. Acad. Sci. USSR, Div. Chem. Sci. 21 (1972) 1020–1024.

[5] C.I. Melo, R. Bogel-Łukasik, M.G. da Silva, E. Bogel-Łukasik, Green Chem. 13 (2011) 2825–2830.

[6] I.M.J. Vilella, S.R. de Miguel, O.A. Scelza, J. Mol. Catal. A: Chem. 284 (2008) 161–171.

[7] C.I. Melo, R. Bogel-Łukasik, E. Bogel-Łukasik, J. Supercrit. Fluid. 61 (2012) 191–198.

[8] S.R. de Miguel, M.C. Román-Martínez, D. Cazorla-Amorós, E.L. Jablonski, O.A. Scelza, Catal. Today 66 (2001) 289–295.

[9] G.C. Torres, S.D. Ledesma, E.L. Jablonski, S.R. de Miguel, O.A. Scelza, Catal. Today 48 (1999) 65–72.

[10] S.R. de Miguel, M.C. Román-Martínez, E.L. Jablonski, J.L.G. Fierro, D. Cazorla-Amorós, O.A. Scelza, J. Catal. 184 (1999) 514–525.

[11] Y.S. Demidova, E. V Suslov, O.A. Simakova, I.L. Simakova, K.P. Volcho, N.F. Salakhutdinov, D.Y. Murzin, Catal. Today 241 (2015) 189–194.

[12] P. Mäki-Arvela, J. Hájek, T. Salmi, D.Y. Murzin, Appl. Catal. A: Gen. 292 (2005) 1–49.

[13] V. V Smirnov, S.A. Nikolaev, G.P. Murav'eva, L.A. Tyurina, A.Y. Vasil'kov, Kinet. Catal. 48 (2007) 265–270.

[14] R.J. Grau, P.D. Zgolicz, C. Gutierrez, H.A. Taher, J. Mol. Catal. A: Chem. 148 (1999) 203–214.

[15] I. Lee, F. Zaera, J. Phys. Chem. B 109 (2005) 2745–2753.

[16] E. Gross, G.A. Somorjai, Top. Catal. 56 (2013) 1049–1058.

[17] G.M. Veith, A.R. Lupini, S.J. Pennycook, G.W. Ownby, N.J. Dudney, J. Catal. 231 (2005) 151–158.

[18] C. Milone, R. Ingoglia, L. Schipilliti, C. Crisafulli, G. Neri, S. Galvagno, J. Catal. 236 (2005) 80–90.

[19] T.K. Hari, Z. Yaakob, Chinese J. Chem. Eng. 23 (2015) 327–336.

[20] S. Garde, A.E. García, L.R. Pratt, G. Hummer, Biophys. Chem. 78 (1999) 21–32.

[21] Y. Yuan, S. Yao, M. Wang, S. Lou, N. Yan, Curr. Org. Chem. 17 (2013) 400–413.

[22] H. Ishitani, Y. Furiya, S. Kobayashi, Bioorg. Med. Chem. 25 (2017) 6229–6232.

[23] M. Li, Y. Hao, F. Cárdenas-Lizana, M.A. Keane, Catal. Commun. 69 (2015) 119–122.

[24] Y. Hao, Palladium and gold catalysts for sustainable chemical processing, PhD Dissertation, M.A. Keane, Chemical Engineering, Heriot-Watt Univ., 2015: pp. 112–132.

[25] S. Lowell, J.E. Shields, The single point BET method BT - Powder Surface Area and Porosity, in: S. Lowell, J.E. Shields (Eds.), Springer Netherlands, Dordrecht, 1984: pp. 30–35.

[26] A.D. Bokare, R.C. Chikate, C. V Rode, K.M. Paknikar, Environ. Sci. Technol. 41

(2007) 7437–7443.

[27] X. Ma, J. Gong, S. Wang, N. Gao, D. Wang, X. Yang, F. He, Catal. Commun. 5 (2004) 101–106.

[28] R.N. Reddy, R.G. Reddy, J. Power Sources 132 (2004) 315–320.

[29] C. Petrier, J.-L. Luche, Tetrahedron Lett. 28 (1987) 2351–2352.

[30] M. Akia, S.M. Alavi, M. Rezaei, Z.-F. Yan, J. Porous Mater. 17 (2009) 85–90.

[31] A.C. Gluhoi, X. Tang, P. Marginean, B.E. Nieuwenhuys, Top. Catal. 39 (2006) 101–110.

[32] J.E. Park, B.B. Kim, E.D. Park, Korean J. Chem. Eng. 32 (2015) 2212–2219.

[33] M.S. Zanuttini, M.A. Peralta, C.A. Querini, Ind. Eng. Chem. Res. 54 (2015) 4929–4939.

[34] C. Meephoka, C. Chaisuk, P. Samparnpiboon, P. Praserthdam, Catal. Commun. 9 (2008) 546–550.

[35] E. Bus, J.T. Miller, J.A. van Bokhoven, J. Phys. Chem. B 109 (2005) 14581–14587.

[36] G.C. Bond, Chemisorption and Reactions of Hydrogen, in: Metal-Catalysed Reactions of Hydrocarbons, Springer, Boston, MA, 2005: pp. 93–152.

[37] H.A. Michelsen, C.T. Rettner, D.J. Auerbach, The Adsorption of Hydrogen at Copper Surfaces: A Model System for the Study of Activated Adsorption, in: R.J. Madix (Ed.), Surface Reactions, Springer-Verlag, Berlin, 2012: pp. 185–235.

[38] N.M. Bertero, A.F. Trasarti, C.R. Apesteguía, A.J. Marchi, Appl. Catal. A: Gen. 394 (2011) 228–238.

[39] S. P. Bressa, O. M. Martínez, G. F. Barreto, Ind. Eng. Chem. Res. 42 (2003) 2081–2092.

[40] R.A. Kjonaas, S.P. Mattingly, J. Chem. Educ. 82 (2005) 1813–1814.

[41] A. Zsigmond, F. Notheisz, P. Kluson, T. Floris, Chemoselective and Enantioselective Hydrogenations on Immobilized Complexes, in: P. Barbaro, F. Liguori (Eds.), Heterogenized Homogeneous Catalysts for Fine Chemicals Production Catalysis by Metal Complexes, Springer, Dordrecht, 2010: pp. 283–359.

[42] H. Deka, M.D. Saikia, H.K. Srivastava, ChemistrySelect 2 (2017) 5248–5258.

[43] F. Wang, G. Lu, Catal. Lett. 134 (2010) 72–77.

[44] E. Skrzyńska, S. Zaid, J.-S. Girardon, M. Capron, F. Dumeignil, Appl. Catal. A: Gen. 499 (2015) 89–100.

[45] P. Mehta, J. Greeley, W.N. Delgass, W.F. Schneider, ACS Catal. 7 (2017) 4707–4715.

[46] K. Hayek, R. Kramer, Z. Paál, Appl. Catal. A: Gen. 162 (1997) 1–15.

[47] K. Kon, S.M.A.H. Siddiki, K. Shimizu, J. Catal. 304 (2013) 63–71.

[48] A. Lyalin, K. Shimizu, T. Taketsugu, J. Phys. Chem. C 121 (2017) 3488–3495.

[49] K. An, S. Alayoglu, N. Musselwhite, K. Na, G.A. Somorjai, J. Am. Chem. Soc. 136 (2014) 6830–6833.

[50] C. Zhao, W. Gan, X. Fan, Z. Cai, P.J. Dyson, Y. Kou, J. Catal. 254 (2008) 244–250.

[51] H. Potgieter, R. Bekker, A. Govender, E. Rohwer, J. Chromatogr. A 1445 (2016) 118–125.

[52] R.M. Rioux, B.B. Hsu, M.E. Grass, H. Song, G.A. Somorjai, Catal. Lett. 126 (2008) 10–19.

[53] M. Retajczyk, A. Wróblewska, Catalysts 7 (2017) 273–286.

[54] W. Ludwig, A. Savara, S. Schauermann, Dalt. Trans. 39 (2010) 8484–8491.

[55] K. Hashimoto, Y. Masuda, H. Kominami, ACS Catal. 3 (2013) 1349–1355.

[56] G.C. Bond, The Chemisorption of Hydrocarbons, in: Metal-Catalysed Reactions of Hydrocarbons, Springer, Boston, MA, 2005: pp. 153–207.

[57] M.A. Keane, P.M. Patterson, Ind. Eng. Chem. Res. 38 (1999) 1295–1305.

[58] A.M. Doyle, S.K. Shaikhutdinov, H.-J. Freund, J. Catal. 223 (2004) 444–453.

Chapter 3

Selective Production of Carvacrol from Carvone over Supported Pd Catalysts

Taking commercial and laboratory-synthesised Pd catalysts we compared support effects and evaluate the effect of hydrogen content in the feed in carvone transformation. This Chapter has been published in Journal of Catalysis Communications (see publication No. 1). Co-authors F.C.L. and M.A.K. directed the project and co-wrote the chapter.

3.1 Introduction

Carvone is a terpenoid obtained at low cost by steam distillation of spearmint oil or nitrosochlorination of citrus-derived limonene [1]. Carvone contains three reducible functionalities, a carbonyl group and an endo- and exo-cyclic -CH=CH-. Reaction of carvone with hydrogen generates valuable chemicals (**Figure 3.1**) in the pharmaceutical, food and agriculture sectors [2]. Reaction selectivity is challenging and most methodologies are non-selective, generating product mixtures [3-6]. Current carvacrol production includes (i) supercritical (300 bar) CO_2 extraction from oregano essential oils [7] and (ii) industrial scale isopropylation of *o*-cresol with propylene over activated alumina at 633 K and 50 bar [8]. The requirements for high operating pressures and temperatures (>523 K) are major drawbacks. Application of supported metal catalysts to promote carvone → carvacrol (in H_2) is an alternative but studies to date are sparse and inconclusive with work focused on batch systems in organic solvents (*e.g.* toluene, hexane, alcohols) [3,6,9-13]. Solvent-free continuous processing at atmospheric pressure offers advantages in terms of throughput and sustainability. The carvone → carvacrol reaction mechanism is still a matter of debate. Klabunovskii *et al.* [13] proposed a classical Horiuti-Polanyi mechanism for reaction over Pd with carvotanacetone as reaction intermediate (**Figure 3.1**, path **(IA)**). Supported Pt catalysts do not promote carvacrol formation [3,10-12] and selectivities reported for the most selective Pd catalysts [13,14] are low (≤38%).

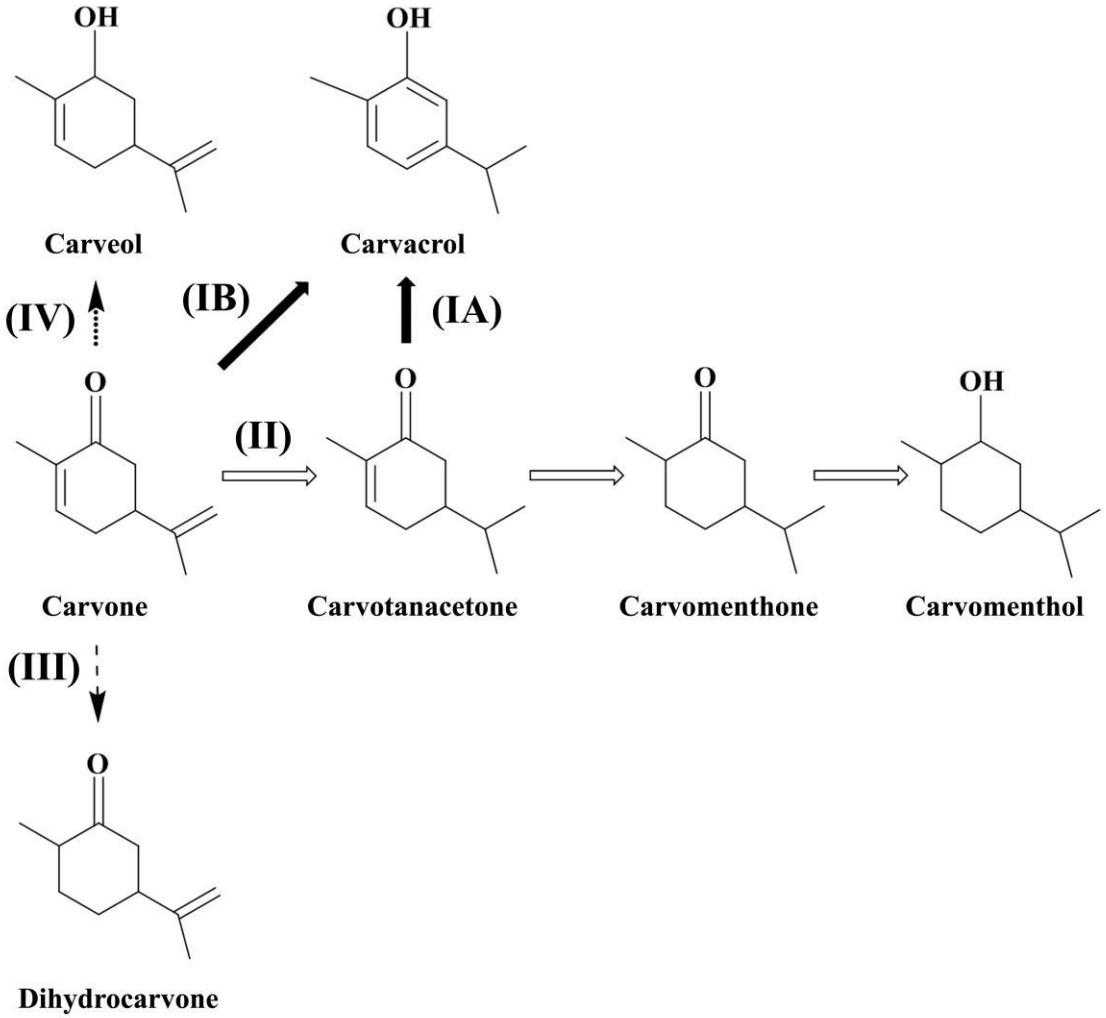

Figure 3.1: Reaction pathways in the conversion of carvone to (target) carvacrol (path I, solid arrows), carvomenthol (path II, open arrows), dihydrocarvone (path III, dashed arrow) and carveol (path IV, dotted arrow).

The redox and acid-base properties of the metal support can influence catalytic activity/selectivity in the reduction of carbonyl and/or unsaturated groups where stronger -C=O (*vs.* -CH=CH-) polarisation on surface Lewis acid sites promotes unsaturated alcohols [15]. Preferential carbonyl and -CH=CH- reduction has been reported over Pd on reducible (CeO_2, TiO_2) [16] and non-reducible (Al_2O_3) oxides [17], respectively. In this study we set out to identify the critical variable(s) that control carvone → carvacrol by examining commercial and laboratory-synthesised Pd catalysts. We compare the catalytic action of (unsupported) bulk Pd with Pd on (non-reducible Al_2O_3 and reducible CeO_2) oxides and carbon. We evaluate the effect of H_2 content in the feed as a critical process variable.

3.2 Experimental

3.2.1 Catalyst Preparation and Activation

Ceria, 1.2% wt. Pd/Al_2O_3, 1.1% wt. Pd/C and PdO were obtained from Sigma-Aldrich. Synthesis of Pd/CeO_2 by deposition-precipitation followed a prior procedure [18]. Samples were sieved to mean diameter = 75 μm, activated in 60 cm^3 min^{-1} H_2 at 10 K min^{-1} to 573 K and passivated in 1% v/v O_2/He at ambient temperature prior to *ex-situ* characterisation.

3.2.2 Catalyst Characterisation

Palladium content was measured by ICP-OES (Vista-Pro, Varian Inc.). Catalyst activation by temperature programmed reduction (TPR, in 5% v/v H_2/N_2 at 10 K min^{-1} to 573 K), H_2 (at 423 K) and O_2 (at ambient temperature) chemisorption and total specific surface area (SSA, in 30% v/v N_2/He using the single point BET method) measurements were conducted on the commercial CHEM-BET 3000 (Quantachrome) unit as described elsewhere [19]; results were reproducible to ±7%. Palladium particle morphology was determined by scanning transmission electron microscopy (STEM, JEOL 2200FS field emission gun-equipped TEM), employing Gatan Digital Micrograph 1.82 for data acquisition/manipulation. Samples for analysis were crushed and deposited (dry) on a holey carbon/Cu grid (300 Mesh). Surface area-weighted mean Pd sizes (d_{STEM}) were determined from a count of 800 particles [19]. Metal size for bulk Pd was determined by H_2 chemisorption at 298 K [20].

3.2.3 Catalytic Procedure

3.2.3.1 Materials

Carvone (98%), carvacrol (98%), dihydrocarvone (99%) and carveol (98%) were obtained from Sigma-Aldrich. Carvotanacetone, carvomenthone and carvomenthol were synthesised following published methods [21]. All gases (H_2, N_2, O_2 and He) were ultra-high purity (BOC, 99.9%).

3.2.3.2 Catalytic System

Reactions were conducted at atmospheric pressure and isothermal conditions (423 K) *in situ* after activation in a continuous flow fixed bed vertical tubular glass reactor (15 mm i.d.). A layer of borosilicate glass beads served as preheating zone where the organic reactant was vaporised and reached reaction temperature before

contacting the catalyst. Temperature was continuously monitored by a thermocouple inserted in a thermowell within the catalyst bed. The organic reactant was delivered *via* a glass/teflon air-tight syringe and teflon line using a microprocessor controlled infusion pump (Model 100 kd Scientific) at a fixed calibrated flow rate. A co-current flow of N_2, H_2 or H_2+N_2 with carvone (N_2/Carvone = 20/1 mol mol^{-1}, H_2/Carvone = 1/6 – 20/1 mol mol^{-1}) was maintained at gas hourly space velocity (*GHSV*) = $2 \times 10^4 - 1 \times 10^5$ h^{-1}. Palladium (*n,* mol$_{Pd}$) to reactant (*F,* mol$_{Carvone}$ h^{-1}) ratio spanned the range $1 \times 10^{-5} - 5 \times 10^{-2}$ h. In blank tests, reactions in the absence of catalyst did not result in any measurable conversion. The reactor effluent was frozen in a liquid N_2 trap for analysis using a Perkin-Elmer Auto System XL gas chromatograph with split/splitless injector, FID and Stabilwax capillary column (RESTEK). Data acquisition/manipulation used the TotalChrom data system. Fractional carvone conversion (X) is given by:

$$X = \frac{[\text{Carvone}]_{in} - [\text{Carvone}]_{out}}{[\text{Carvone}]_{in}} \tag{3.1}$$

with selectivity to carvacrol ($S_{Carvacrol}$):

$$S_{\text{Carvacrol}}\ (\%) = \frac{[\text{Carvacrol}]_{out}}{[\text{Carvone}]_{in} - [\text{Carvone}]_{out}} \times 100 \tag{3.2}$$

and yield ($Y_{Carvacrol}$):

$$Y_{\text{Carvacrol}}\ (\%) = X \times S_{\text{Carvacrol}} \tag{3.3}$$

Catalytic activity is also quantified in terms of reactant consumption rate (R, mol$_{Carvone}$ mol$_{Pd}^{-1}$ h^{-1}) at initial conversion X_0, extracted from time on-stream measurements [22]. Turnover frequency (*TOF*, rate per active site) was determined from particle size measurements [22] and defined by

$$TOF\ (\text{h}^{-1}) = \frac{R}{D} \tag{3.4}$$

where D is the metal dispersion (surface metal per total metal atoms) was obtained from

$$D = \frac{S_{Metal} \times M_{Metal}}{A_{Metal} \times N_{Avogadro}} = \frac{(6 / d_{\mathrm{STEM}} \times \rho_{Metal}) \times M_{Metal}}{A_{Metal} \times N_{Avogadro}} \quad \textbf{(3.5)}$$

where d_{STEM} resulted from STEM measurements, S_{Metal} is the metal atom surface area, ρ_{Metal} metal density, M_{Metal} metal atomic mass, A_{Metal} metal atom surface area and $N_{Avogadro}$ the Avogadro number.

Repeated reactions with different samples from the same batch of catalyst delivered raw data reproducibility and carbon mass balances within ±5%.

3.3 Results and Discussion

3.3.1 Catalyst Characterisation

Physicochemical properties of the catalysts in this study are given in **Table 3.1**. The commercial and laboratory synthesised samples display a range of SSA (3-870 m^2 g^{-1}). The TPR profiles (**Figure 3.2**) exhibit a negative peak (H_2 release) at 350-383 K due to decomposition of Pd hydride formed by H_2 absorption at ambient temperature [20]. The lower hydride Pd/H ratio for supported (0.06-0.04) relative to bulk Pd (0.67) is consistent with nano-scale metal particles as is the shift to lower decomposition temperatures [20]. TPR of Pd/CeO_2 (**Figure 3.2(IV)**) presents a positive peak at the final isothermal hold (573 K), suggesting partial CeO_2 reduction (at the metal-support interface) with the formation of oxygen vacancies [23]. This was confirmed by O_2 titration post-TPR where O_2 uptake (160 μmol g^{-1}) is comparable with values in the literature [24]. Hydrogenation performance is determined by the capacity of Pd for H_2 adsorption/dissociation [20]. Hydrogen chemisorption at reaction temperature (**Table 3.1**) was close to detection limits for bulk Pd and appreciably lower than that recorded for the supported systems. Uptake was equivalent for Pd/Al_2O_3 and Pd/C and measurably higher for Pd/CeO_2. Differences in H_2 chemisorption can be due to variations in metal dispersion [19]. The three supported catalysts present pseudo-spherical Pd particles in the 1-6 nm range (**Figures 3.3(I)**) with a similar size distribution (**Figures 3.3(II)**) and mean (d_{STEM} ~ 3 nm, **Table 3.1**). Greater H_2 chemisorption on Pd/CeO_2 can be linked to partial support reduction with the generation of sites for H_2 adsorption. Wang *et al*. [25] have recently discussed the formation of active sites at the interface of metal nanoparticles strongly interacting with reducible

Table 3.1: Palladium content, specific surface area (SSA), H_2 chemisorption (at 423 K), mean Pd size (d_{STEM}), carvone consumption rate (R) and turnover frequency (TOF) and carvacrol, carvotanacetone and carvomenthone selectivity ($S_{Product}$) at X_0 ~ 0.3 for different inlet H_2/Carvone.

Catalyst	Pd content (% wt.)	SSA ($m^2\ g^{-1}$)	H_2 uptake (mmol g_{Pd}^{-1})	d_{STEM} (nm)	H_2/Carvone = 1/6		$S_{Carvotanacetone}/S_{Carvomenthone}$ (%)		
					R ($mol_{Carvone}\ mol_{Pd}^{-1}\ h^{-1}$) / TOF (h^{-1})	$S_{Carvacrol}$ (%)	H_2/Carvone		
							1/1	5/1	10/1
Pd	-	3	<0.04	-	$5 / 7 \times 10^{2a}$	100	30/0	29/13	28/14
Pd/Al_2O_3	1.2	145	1.7	3.0	$8 \times 10^3 / 2 \times 10^4$	100	12/1	15/4	21/8
Pd/C	1.1	870	2.0	2.8	$8 \times 10^3 / 2 \times 10^4$	100	13/1	17/2	27/7
Pd/CeO_2	0.5	37	9.0	3.0	$9 \times 10^3 / 2 \times 10^4$	90	13/0	18/2	24/3

[a]*TOF* obtained using Pd size (=130 nm) from H_2 chemisorption (see Experimental section).

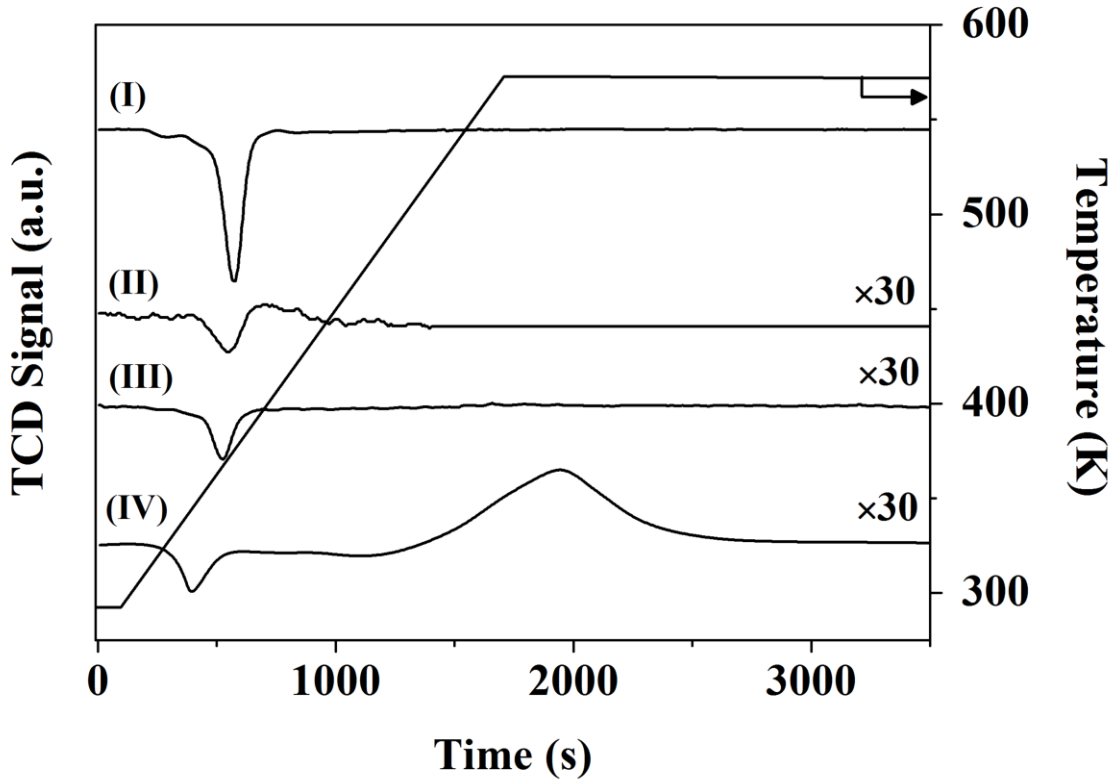

Figure 3.2: Temperature programmed reduction (TPR) profiles for (I) PdO, (II) Pd/Al_2O_3, (III) Pd/C and (IV) Pd/CeO_2.

CeO_2. Tu and Cheng [26] reported a synergistic effect between Pd and CeO_2 that resulted in stronger H_2 adsorption and increased uptake.

3.3.2 Gas Phase Conversion of Carvone

Reaction thermodynamics establishes greater stability of conjugated endo-cyclic -CH=CH- and carbonyl functionalities in carvone [27] with the following order of decreasing reactivity based on Gibbs free energy [28]: exo -CH=CH- > endo -CH=CH- > -C=O. This can account for the reported formation of unsaturated and saturated ketones (**Figure 3.1** (path **(II)**)) as principal products in the hydrogenation of carvone [6]. Variations in H_2 content in the feed (represented as inlet H_2/Carvone) were tested in order to probe reaction pathway. A range of H_2/Carvone ratios was considered, from 0 (reaction in N_2) to sub- (H_2/Carvone = 1/6), stoichiometric (= 1/1) and H_2 in excess (= 20/1) for the reduction of a single carvone functionality. Under all reaction conditions, formation of dihydrocarvone (endo -CH=CH- reduction, path **(III)**) and carvomenthol (-C=O reduction in carvomenthone, path **(II)**) was negligible with selectivities ≤6%.

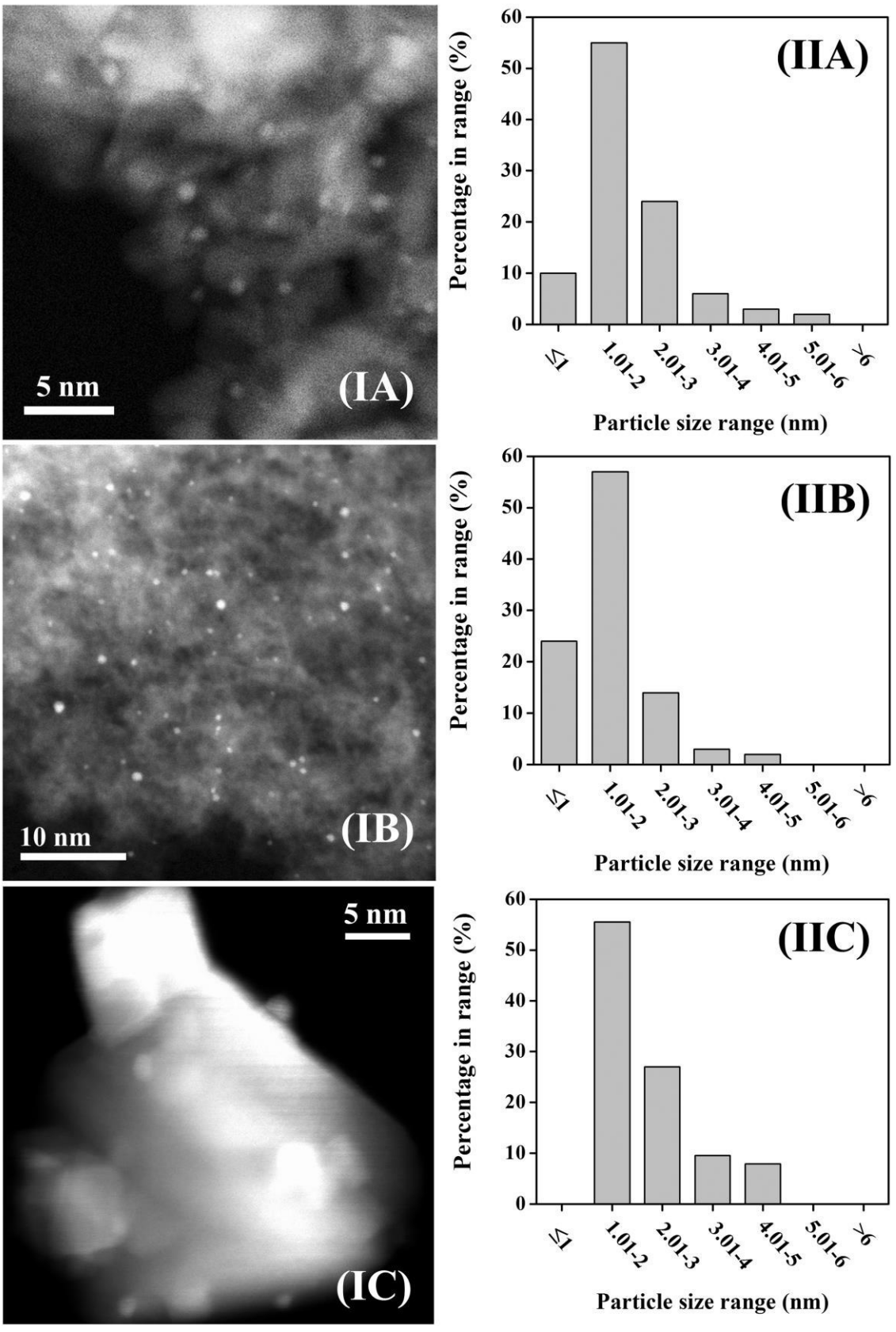

Figure 3.3: (I) Representative STEM images with (II) Pd size histograms for (A) Pd/Al_2O_3, (B) Pd/C and (C) Pd/CeO_2.

Reaction in N_2 did not result in any measurable conversion of carvone. Under hydrogen lean conditions (H_2/Carvone = 1/6), we achieved full selectivity to the target carvacrol for reaction over bulk Pd, Pd/Al_2O_3 and Pd/C (**Table 3.1** and **Figure 3.4(I)**).

This result is significant given the reports in batch liquid phase carvone hydrogenation where low selectivity to carvacrol (≤38%) was obtained over unsupported Pd [13] and (C and Al_2O_3) supported Pd [13,14]. Variations in contact time can govern selectivity [29] and the exclusivity to carvacrol achieved in this study may result from the lower contact time (0.03-0.2 s) in continuous operation.

Negligible conversion of carvotanacetone was recorded for reactions in N_2 or H_2 lean conditions. This indicates direct carvacrol formation from carvone *via* hydrogen migration and keto-enol tautomerisation, following path **(IB)** in **Figure 3.1**. Catalytic inactivity for carvone reaction in N_2 suggests that carvacrol formation requires H_2 in the feed. This is in line with recent work by Zhang *et al.* [30] who reported formation of phenols over Pd/C *via* hydrogen treatment of substituted 2-cychlohexenones. Naito and Tanimoto [31] provided direct evidence for intramolecular double-bond migration in propene hydrogenation over Pd/SiO_2 while Musolino *et al.* [32] established a hydrogen requirement for double bond migration in *cis*-2-butene-1,4-diol → 2-hydroxytetrahydrofuran transformation over Pd/C.

Pd/CeO_2 exhibited different behaviour in promoting carveol formation (S = 10%) *via* -C=O hydrogenation (path **(IV)** in **Figure 3.1**). This can be attributed to the involvement of surface oxygen vacancies where the carbonyl group is activated at Ce^{3+} sites for hydrogen attack to generate carveol. Neri *et al.* [16] proposed preferential formation of an unsaturated alcohol from an unsaturated aldehyde over Pd on reducible oxides (TiO_2, ZnO, Fe_2O_3), which they ascribed to reactant activation on the support. Calaza *et al.* [33] demonstrated (by TPD, RAIRS and DFT) carbonyl activation at oxygen vacancies on CeO_2. We observed an initial decline in conversion that attained steady state for all the systems (see inset to **Figure 3.4(I)** for Pd/Al_2O_3). Similar reaction rates (and *TOF*) were obtained for the three supported Pd catalysts, which were appreciably greater than bulk Pd (**Table 3.1**) and can be linked to H_2 uptake capacity under reaction conditions. At an inlet H_2/Carvone =1/6, carvacrol yield was proportional to Pd content (**Figure 3.4(II)**) to reach 100% in the case of Pd, Pd/Al_2O_3 and Pd/C. The lower yield over Pd/CeO_2 was due to carveol formation. An increase in H_2/Carvone resulted in decreased carvacrol selectivity where the data for all the catalysts converged on a common trend line (**Figure 3.4(I)**). Loss of carvacrol selectivity with increasing H_2

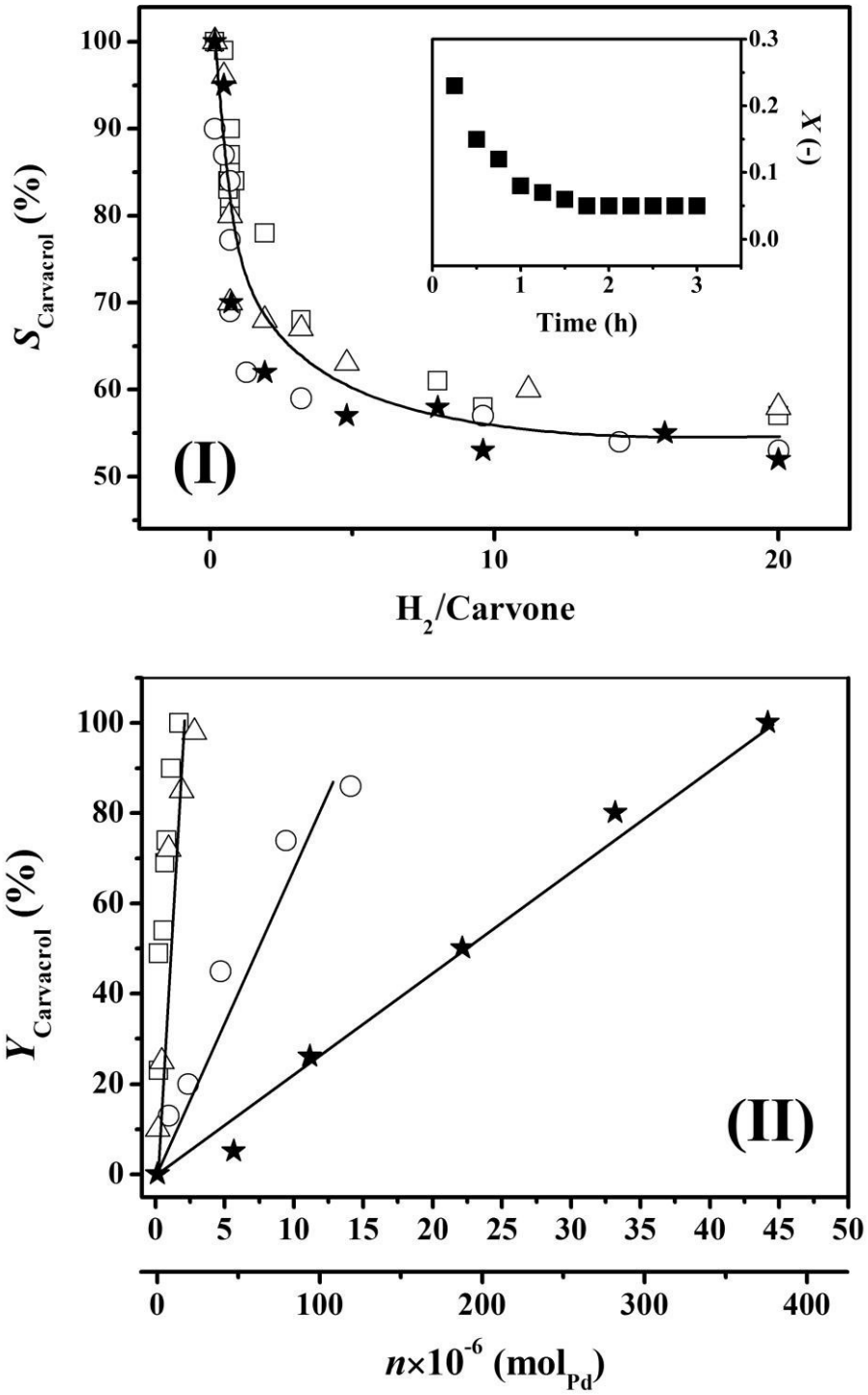

Figure 3.4: (I) Effect of inlet H_2/Carvone on selectivity to carvacrol ($S_{Carvacrol}$). *Inset*: variation of carvone fractional conversion (X) with time on-stream over Pd/Al_2O_3 (■); (II) variation of carvacrol yield ($Y_{Carvacrol}$) with Pd content in the catalyst bed (n) for reaction over Pd (★), Pd/Al_2O_3 (□), Pd/C (△) and Pd/CeO_2 (○). *Note*: Bottom x-coordinate in (II) refers to Pd (★). *Reaction conditions*: T = 423 K, H_2/Carvone = 1/6 – 20/1, n/F = $1 \times 10^{-5} – 5 \times 10^{-2}$ h, $GHSV$ = $2 \times 10^4 – 1 \times 10^5$ h^{-1}.

content was accompanied by formation of carvotanacetone and carvomenthone, which were promoted at higher H_2/Carvone (**Table 3.1**). Olefin conversion over transition metal catalysts proceeds through an allyl intermediate that is formed by a hydrogen addition [34]. This intermediate can undergo (i) H elimination with bond migration or (ii) insertion of a second H to generate the alkane [34]. The switch from double bond migration (path **(IB)** in **Figure 3.1**) to hydrogenation (path **(II)**) is sensitive to H_2/Carvone, which is consistent with the literature [32]. Hydrogen elimination is favoured under conditions of low surface hydrogen (H_2/Carvone = 1/6). Increased H_2 content facilitates H insertion, directing the reaction to preferential hydrogenation. Carveol formation over Pd/CeO_2 was insensitive to H_2/Carvone.

3.4 Conclusions

We have established exclusive formation of carvacrol at full carvone conversion over Pd/Al_2O_3 and Pd/C (mean Pd size = 2.8-3.0 nm) at an inlet H_2/Carvone = 1/6. Under the same reaction conditions, bulk Pd with lower H_2 uptake capacity delivered 100% carvacrol yield at a lower rate. Reaction over Pd/CeO_2 promoted formation of carveol due to -C=O activation at oxygen vacancies created during TPR. Hydrogenation to carvotanacetone and carvomenthone was promoted at higher H_2/Carvone (>1/6).

3.5 References

[1] J. L. Bicas, A. P. Dionísio, G. M. Pastore, Chem. Rev. 109 (2009) 4518-4531.

[2] W. Schwab, C. Fuchs, F.-C. Huang, Eur. J. Lipid Sci. Technol. 115 (2013) 3-8.

[3] I. M. J. Vilella, S. R. de Miguel, O. A. Scelza, J. Mol. Catal. A: Chem. 284 (2008) 161-171.

[4] L. J. Lemus-Yegres, M. Pérez-Cadenas, M. C. Román-Martínez, C. S.-M. de Lecea, Micropor. Mesopor. Mater. 139 (2011) 164-172.

[5] V. P. Sivcev, K. P. Volcho, N. P. Salakhutdinov, V. I. Anikeev, J. Supercrit. Fluid. 80 (2013) 9-14.

[6] C. I. Melo, Alternative Solvents in Carvone Hydrogenation, MSc Thesis, E. Bogel-Łukasik, Chemical Engineering, Universidade Nova de Lisboa, Lisbon, 2011, pp. 53.

[7] A. Ocaña-Fuentes, E. Arranz-Gutiérrez, F. J. Señorans, G. Reglero, Food Chem. Toxicol. 48 (2010) 1568-1575.

[8] G. D. Yadav, S. B. Kamble, J. Chem. Technol. Biotechnol. 84 (2009) 1499-1508.

[9] C. I. Melo, R. Bogel-Łukasik, E. Bogel-Łukasik, J. Supercrit. Fluid. 61 (2012) 191-198.

[10] S. R. de Miguel, M. C. Román-Martínez, D. Cazorla-Amorós, E. L. Jablonski, O. A. Scelza, Catal. Today 66 (2001) 289-295.

[11] G. C. Torres, S. D. Ledesma, E. L. Jablonski, S. R. de Miguel, O. A. Scelza, Catal. Today 48 (1999) 65-72.

[12] S. R. de Miguel, M. C. Román-Martínez, E. L. Jablonski, J. L. G. Fierro, D. Cazorla-Amorós, O. A. Scelza, J. Catal. 184 (1999) 514-525.

[13] E. I. Klabunovskii, L. F. Godunova, L. K. Maslova, B. Acad. Sci. USSR Chem. Sci. 21 (1972) 1020-1024.

[14] C. I. Melo, R. Bogel-Łukasik, M. G. da Silva, E. Bogel-Łukasik, Green Chem. 13 (2011) 2825-2830.

[15] S. Handjani, E. Marceau, J. Blanchard, J.-M. Krafft, M. Che, P. Mäki-Arvela, N. Kumar, J. Wärnå, D. Y. Murzin, J. Catal. 282 (2011) 228-236.

[16] G. Neri, G. Rizzo, L. de Luca, A. Donato, M. G. Musolino, R. Pietropaolo, Appl. Catal. A: Gen. 356 (2009) 113-120.

[17] B. C. Campo, M. A. Volpe, C. E. Gigola, Ind. Eng. Chem. Res. 48 (2009) 10234-10239.

[18] N. S. Babu, N. Lingaiah, N. Pasha, J. V. Kumar, P. S. S. Prasad, Catal. Today 141 (2009) 120-124.

[19] M. Li, X. Wang, Y. Hao, F. Cárdenas-Lizana, M. A. Keane, Catal. Today 279 (2017) 19-28.

[20] F. Cárdenas-Lizana, Y. Hao, M. Crespo-Quesada, I. Yuranov, X. Wang, M. A. Keane, L. Kiwi-Minsker, ACS Catal. 3 (2013) 1386-1396.

[21] C. Petrier, J.-L. Luche, Tetrahedron Lett. 28 (1987) 2351-2352.

[22] M. Li, Y. Hao, F. Cárdenas-Lizana, H. H. P. Yiu, M. A. Keane, Top. Catal. 58 (2015) 149-158.

[23] N. C. Nelson, J. S. Manzano, A. D. Sadow, S. H. Overbury, I. I. Slowing, ACS Catal. 5 (2015) 2051-2061.

[24] S. Salasc, V. Perrichon, M. Primet, N. Mouaddib-Moral, J. Catal. 206 (2002) 82-90.

[25] Y.-G. Wang, D. Mei, V.-A. Glezakou, J. Li, R. Rousseau, Nature Commun. 6 (2015) 1-8.

[26] C. Tu, S. Cheng, ACS Sust. Chem. Eng. 2 (2014) 629-636.

[27] R. A. Kjonaas, S. P. Mattingly, J. Chem. Educ. 82 (2005) 1813-1814.

[28] P. Barbaro, F. Liguori, Heterogenized Homogeneous Catalysts for Fine Chemicals Production: Materials and Processes, Springer, Dordrecht, 2010.

[29] Y. Hao, M. Li, F. Cárdenas-Lizana, M. A. Keane, Catal. Lett. 146 (2016) 109-116.

[30] J. Zhang, Q. Jiang, D. Yang, X. Zhao, Y. Dong, R. Liu, Chem. Sci. 6 (2015) 4674-4680.

[31] S. Naito, M. Tanimoto, J. Catal. 102 (1986) 377-385.

[32] M. G. Musolino, C. M. S. Cutrupi, A. Donato, D. Pietropaolo, R. Pietropaolo, Appl. Catal. A: Gen. 243 (2003) 333-346.

[33] F. C. Calaza, Y. Xu, D. R. Mullins, S. H. Overbury, J. Am. Chem. Soc. 134 (2012) 18034-18045.

[34] W. Ludwig, A. Savara, S. Schauermann, Dalton Trans. 39 (2010) 8484-8491.

Chapter 4

Promotional Effect of Water in the Clean Continuous Production of Carvacrol from Carvone

In the previous Chapter, it was shown that selective carvacrol formation required limited amount of hydrogen. In this Chapter, we consider the effect of water as a hydrogen source in the conversion of carvone over Pd/Al_2O_3. This chapter has been published in Catalysis Today Journal (see publication No. 2). F.C.L. and M.A.K. directed the project and co-wrote the chapter.

4.1 Introduction

Biomass offers an alternative carbon source to supplant current dependence on crude oil and natural gas for the production of fine chemicals [1]. Biomass upgrading can enhance process sustainability but is still at an early stage of development [2]. The flavour and fragrance industry is based on terpenes [3], which are derived from the paper pulp and citric juice industries [4]. Natural terpenes contain -C=C- bonds and chemo-catalytic isomerisation can produce more valuable products [5]. Reviews by Swift in 2004 [3], Corma *et al.* in 2007 [5], Schwab and co-workers in 2013 [4] and Sanchez *et al.* in 2016 [6] covered terpene isomerisation by homogeneous catalysts in batch liquid systems where product selectivity was identified as the main challenge. Heterogeneous catalysis reduces separation costs and the volume of toxic waste [4] while operation in continuous flow offers clear benefits in terms of reduced downtime and higher throughput [7]. Carvacrol is a mono-terpenoid phenol used as a flavoring agent and intermediate for the production of drugs, fungicides and pesticides [6]. The main routes to carvacrol include (i) supercritical (300 bar) CO_2 extraction from oregano essential oils [8] and (ii) isopropylation of *o*-cresol with propylene over activated alumina at 50 bar and 633 K [9]. The requirements for high operating temperatures and pressures are major drawbacks. Carvacrol generation from carvone in hydrogen over supported metal catalysts is an alternative but studies to date are limited and inconclusive with work focused on batch systems in organic solvents (*e.g.* toluene, alcohols) [10-16].

Carvone transformation in hydrogen generates a range of products (**Figure 4.1**). The formation of unsaturated (carvotanacetone) and saturated (carvomenthone) ketones and alcohol (carvomenthol) occurs *via* path **(II)**; the endo-cyclic double bond and carbonyl functionalities are more resistant to attack [17,18]. We have reported the results of continuous catalytic carvone hydrogenation over bulk and (oxide and carbon) supported Pd catalysts where Pd/Al_2O_3 delivered the highest combined activity and carvacrol selectivity [19]. In that work, we established carvone → carvacrol transformation in hydrogen and a dependence of isomerisation (to carvacrol, path **(IA)** in **Figure 4.1**) *vs*. hydrogenation (path **(II)**) on H_2 content in the feed.

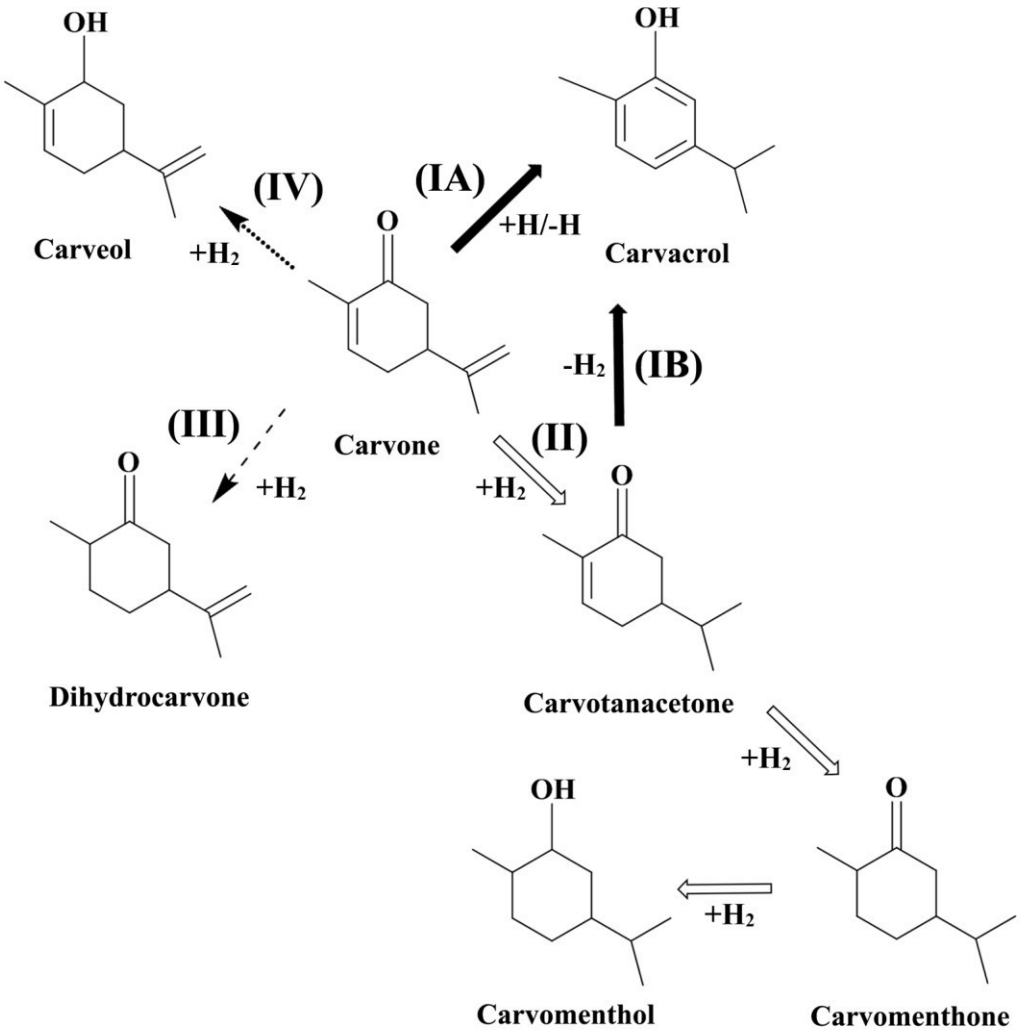

Figure 4.1: Reaction pathways in the conversion of carvone to (target) carvacrol (path I, solid arrows), carvomenthol (path II, open arrows), dihydrocarvone (path III, dashed arrow) and carveol (path IV, dotted arrow).

Water has been shown to impact on gas phase catalytic hydrogenation [20] and isomerisation mechanisms [21], which are critical steps in carvone transformation (**Figure 4.1**). A promoting effect of water has been reported in the hydrogenation (of carbonyl (acetone → isopropanol [22] and acetic acid → ethanol [20]) and -C=C- functionalities [23]) and isomerisation (oleic acid → isostearates [24,25]). We could not find any report that has examined the role of water in the catalytic transformation of a reactant containing both -C=C- and -C=O groups. Cao *et al.* [26] provided theoretical evidence that water can lower the energy barrier in the isomerisation of fulminic acid (HCNO) and isocyanic acid (HNCO). Water has, however, been found to have no effect or to inhibit hydrogenation (levulinic acid [27] and maleic anhydride [28]) and isomerisation (oleic acid [29]). In this study, we evaluate the effect of water in determining the selective continuous gas phase conversion of carvone to carvacrol over Pd/Al_2O_3.

4.2 Experimental

4.2.1 Catalyst Activation and Characterisation

A commercial (Sigma-Aldrich) 1.2% wt. Pd/Al_2O_3 was sieved to mean diameter = 75 μm and activated in 60 cm^3 min^{-1} H_2 at 10 K min^{-1} to 573 K. The sample was passivated in 1% v/v O_2/He at ambient temperature for *ex*-situ characterisation. Palladium content was measured by ICP-OES (Vista-Pro, Varian Inc.). Temperature programmed reduction (TPR, in 5% v/v H_2/N_2 at 10 K min^{-1} to 573 K), H_2 chemisorption (at 298 K) and total specific surface area (SSA, in 30% v/v N_2/He using the single point BET method) measurements were conducted on the commercial CHEM-BET 3000 (Quantachrome) unit as described elsewhere [30]; results were reproducible to ±7%. Bulk catalyst structure was determined by X-ray diffraction (XRD) analysis, using a Bruker/Siemens D500 incident X-ray diffractometer with Cu Kα radiation (0.02º $step^{-1}$ at 5 s $step^{-1}$ over the range $20º \leq 2\theta \leq 90º$). Palladium particle morphology was determined by scanning transmission electron microscopy (STEM, JEOL 2200FS field emission gun-equipped TEM), employing Gatan Digital Micrograph 1.82 for data acquisition/manipulation. Samples for analysis were crushed and deposited (dry) on a holey carbon/Cu grid (300 Mesh). Surface area-weighted mean Pd sizes (d) were measured from a count of 800 particles [30]. For comparison purposes, Pd size was also determined from H_2 chemisorption (at 298 K) [31]

considering dissociative adsorption (Pd:H stoichiometry = 1:1) and assuming spherical morphology [32].

4.2.2 Catalytic Procedure

Carvone (98%), carvacrol (98%), dihydrocarvone (99%) and carveol (98%) were obtained from Sigma-Aldrich and used as supplied. Carvotanacetone, carvomenthone and carvomenthol were synthesised following published methods [33]. All gases (H_2, N_2, O_2 and He) were ultra-high purity (BOC, 99.9%). Reactions were conducted at atmospheric pressure and isothermal conditions (423 K) *in situ* after activation in a continuous flow fixed bed vertical tubular glass reactor (15 mm i.d.). A layer of borosilicate glass beads served as preheating zone where the organic reactant was vaporised and reached reaction temperature before contacting the catalyst. Temperature was continuously monitored by a thermocouple inserted in a thermowell within the catalyst bed. The organic reactant and H_2O were delivered *via* two glass/teflon air-tight syringes and teflon lines using two microprocessor controlled infusion pumps (Model 100 kd Scientific). A co-current flow of N_2, H_2 or H_2+N_2 with carvone (N_2:Carvone = 20:1 mol mol^{-1}, H_2:Carvone = 1:6 – 20:1 mol mol^{-1}) or H_2O+carvone (H_2O:Carvone = 1:12 – 6:1 mol mol^{-1}) was maintained at $GHSV = 1 \times 10^6$ min^{-1}. Palladium (n, mol$_{Pd}$) to reactant (F, mol$_{Carvone}$ min^{-1}) ratio spanned the range 2×10^{-3} – 2×10^{-1} min. In blank tests, reactions in the absence of catalyst or over the Al_2O_3 support alone did not result in any measurable conversion. The reactor effluent was frozen in a liquid N_2 trap for analysis using a Perkin-Elmer Auto System XL gas chromatograph with split/splitless injector, FID and Stabilwax capillary column (RESTEK). Data acquisition/manipulation used the TotalChrom data system. Fractional carvone conversion (X) is given by:

$$X = \frac{[\text{Carvone}]_{in} - [\text{Carvone}]_{out}}{[\text{Carvone}]_{in}} \quad \textbf{(4.1)}$$

with selectivity to carvacrol ($S_{Carvacrol}$):

$$S_{\text{Carvacrol}}\ (\%) = \frac{[\text{Carvacrol}]_{out}}{[\text{Carvone}]_{in} - [\text{Carvone}]_{out}} \times 100 \quad \textbf{(4.2)}$$

Catalytic activity is also quantified in terms of carvacrol production rate (R, min^{-1}), extracted from time on-stream measurements [34]. Repeated reactions with different samples from the same batch of catalyst delivered raw data reproducibility and carbon mass balances within ±5%.

4.3 Results and discussion

4.3.1 Catalyst Characterization

The physico-chemical characteristics of the Pd/Al_2O_3 catalyst are given in **Table 4.1**.

Table 4.1: Physico-chemical characteristics of the Pd/Al_2O_3 catalyst.

Pd loading (% wt.)	1.2
SSA (m^2 g^{-1})	145
TPR T_{max} (K)	375
Pd mean size (nm)	2.4[a] / 3.0[b]

[a]from H_2 chemisorption at 298 K.

[b]from STEM analysis (d).

Temperature programmed reduction (TPR) generated the profile shown in **Figure 4.2(A)** with H_2 release (negative peak) at 375 K due to the decomposition of Pd hydride formed by room temperature H_2 absorption [35]. The XRD diffractogram of the activated catalyst (**Figure 4.2(B)**) shows two broad peaks at 2θ = 45.8º and 66.8º characteristic of the main planes of cubic γ-Al_2O_3 (JCPDS-ICDD Card No. 10-0425). The total specific surface area (SSA = 145 m^2 g^{-1}) is consistent with γ-Al_2O_3 [36]. The absence of reflections due to Pd (main reflection at 2θ = 40.1º for (111); JCPDS-ICDD Card No. 05-0681) suggests the presence of Pd nanoparticles (≤3 nm) below XRD detection limits [37]. A Pd particle size of 2.4 nm was obtained from H_2 chemisorption. The representative STEM image in **Figure 4.2(C)** further confirms the occurrence of Pd as nano-particles (≤6 nm, see **Figure 4.2(D)**) with a mean size of 3 nm.

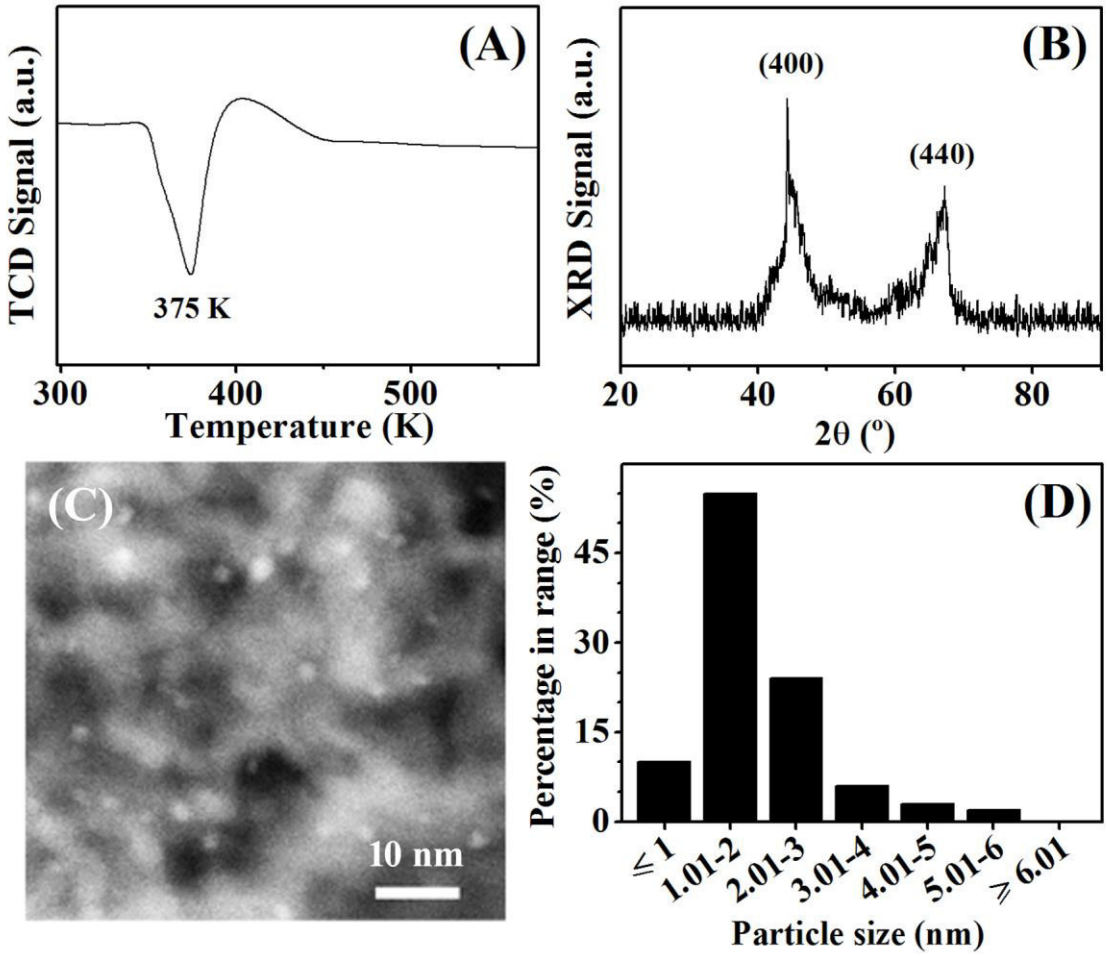

Figure 4.2: (A) TPR profile, (B) XRD diffractogram with main planes for γ-Al_2O_3 from JCPDS-ICDD reference (Card No. 10-0425) and (C) representative STEM image with (D) Pd particle size distribution for Pd/Al_2O_3.

4.3.2 Gas Phase Catalytic Conversion of Carvone

The formation of carvacrol can occur either *via* direct conversion of carvone (path **(IA)** in **Figure 4.1**) or through transformation of the carvotanacetone intermediate (path **(IB)**). There was no detectable carvone conversion for reaction in N_2 (without H_2 or H_2O), a result that deviates from the reported formation of several products (including carvacrol) over Pd/C in batch operation (for up to 12 h) at 506 K [38]. The shorter contact time (0.2 s) and lower reaction temperature (423 K) employed in this work did not result in carvone to carvacrol transformation in the absence of hydrogen or water in continuous gas phase operation.

At a low hydrogen content in the feed (H_2:Carvone = 1:6), we achieved full selectivity to carvacrol (**Figure 4.3(A)**) over Pd/Al_2O_3. This is an important result considering the reported low carvacrol selectivity (≤38%) in batch systems over Pd catalysts [15,39]. To probe reaction pathway, carvone and carvotanacetone were used as

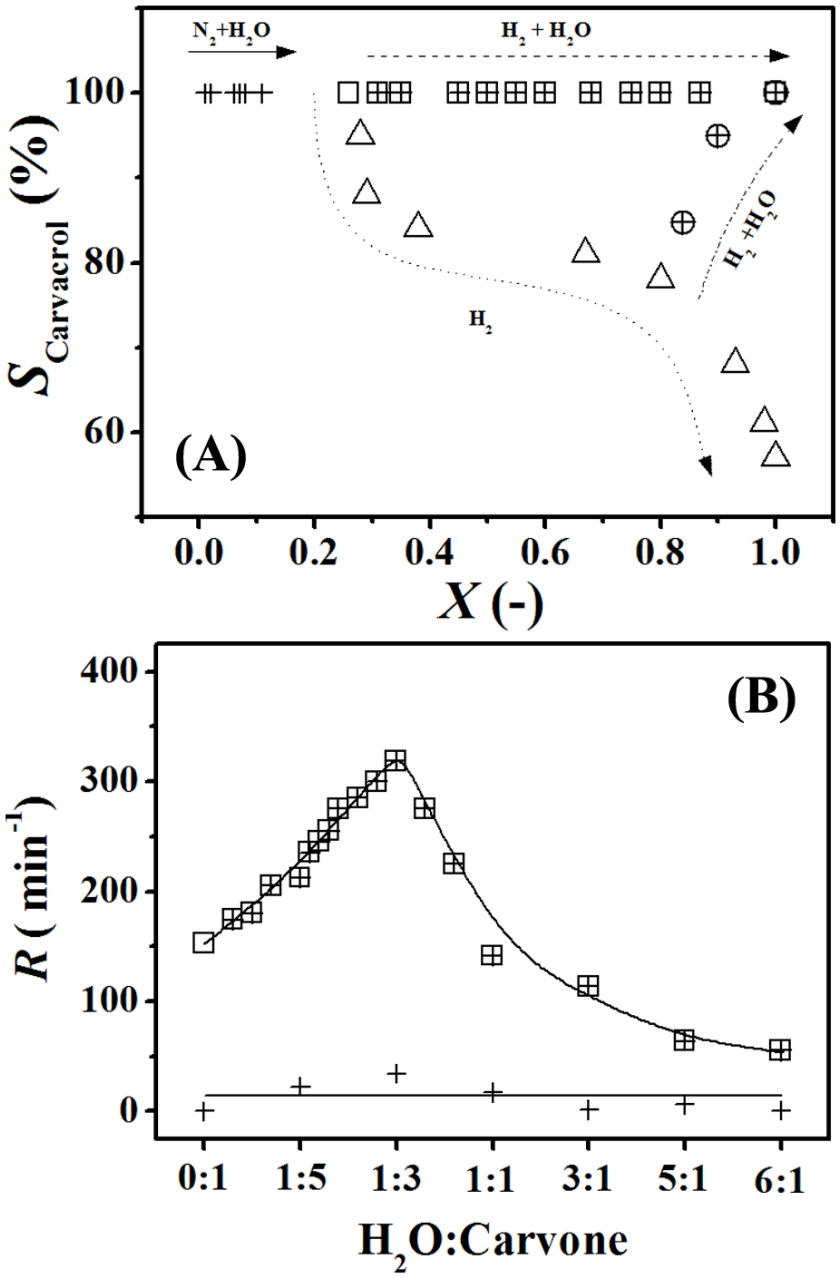

Figure 4.3: (A) Carvacrol selectivity ($S_{Carvacrol}$, %) as a function of fractional conversion (X) of carvone and (B) variation in carvacrol production rate (R, min^{-1}) with inlet H_2O:Carvone molar ratio for reactions in H_2 (H_2:Carvone = 1:6 (□) and = 1:2-20:1 (△)) and H_2O (H_2O:Carvone = 1:12-1:6 in N_2 (+) and in H_2 (H_2:Carvone = 1:6, ⊞ and = 2:1, ⊕)). *Note*: Arrows in (A) illustrate $S_{Carvacrol}$ *vs.* X dependence for reactions with increased H_2 in the feed (dotted line) and the effect of adding water for reactions in N_2 (solid line) at H_2:Carvone = 1:6 (dashed line) and 2:1 (dashed-dotted line). *Reaction conditions*: T = 423 K, n/F = $2 \times 10^{-3} - 2 \times 10^{-1}$ min, $GHSV$ = 1×10^6 min^{-1}.

reactants under the same reaction conditions. Negligible carvotanacetone conversion (<5%) for reaction over Pd/Al_2O_3 in H_2 suggests that carvacrol formation through path **(IB)** is not promoted. Carvacrol formation can proceed by carvone interaction with Pd

sites *via* the exo -C=C- group [40] (**Figure 4.4(A)**). Dissociative adsorption of H_2 on Pd [41] generates reactive atomic hydrogen that attacks the exo-double bond. This results in the formation of an allyl intermediate that undergoes H elimination with bond migration and keto-enol tautomerisation to generate carvacrol [42,43]. At higher H_2:Carvone (= 1:2-20:1) the increase in surface hydrogen from H_2 dissociation [44] favours H insertion [19] that directs the reaction along path **(II)** with the formation of carvotanacetone ($S_{\text{Carvotanacetone}} \leq 25\%$) and carvomenthone ($S_{\text{Carvomenthone}} \leq 10\%$).

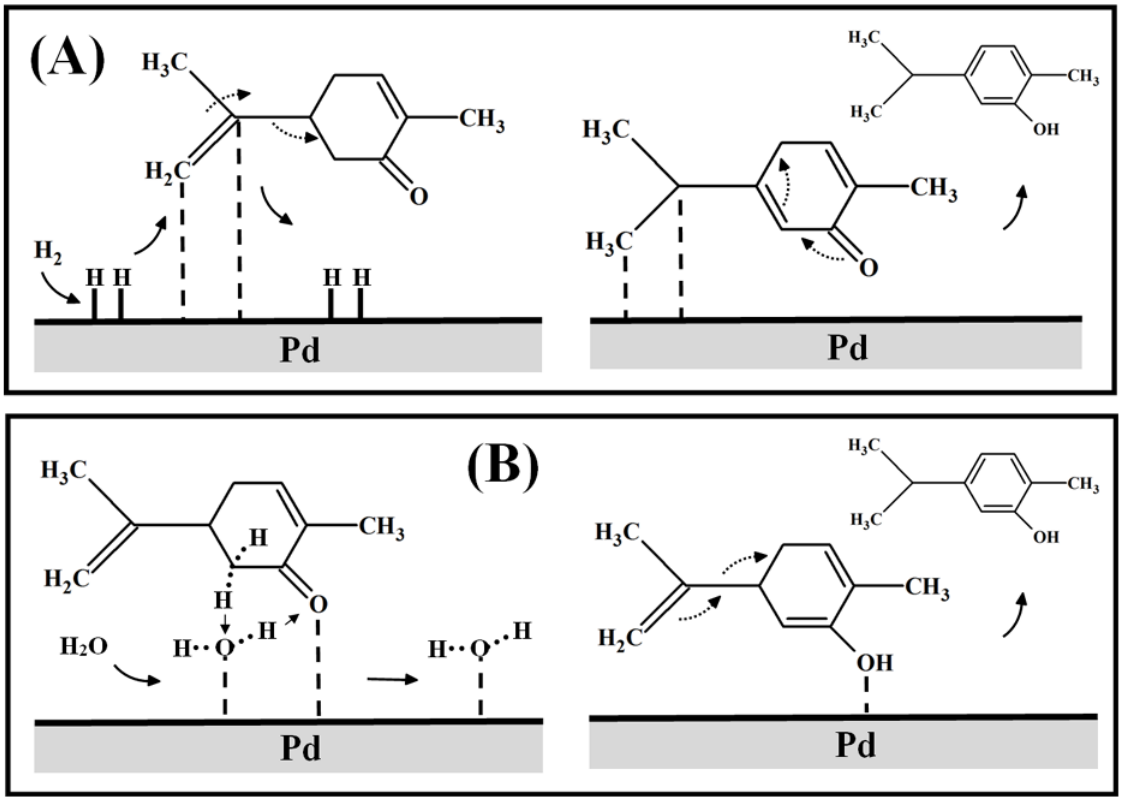

Figure 4.4: Proposed carvone adsorption/activation and reaction with (A) H_2 and (B) H_2O.

Reaction in H_2O (without H_2) gave carvacrol as the only detected product. Strauss *et al.* [45,46] reported carvone isomerisation in water with no catalyst using a pressurised microwave batch reactor operated at 523 K. Water has been deemed essential for carvacrol isomerisation (at 373 K) with homogeneous Rh catalysts, where there was no conversion under anhydrous conditions; no explanation was provided to account for this [43]. We envision a reaction mechanism (**Figure 4.4(B)**) where water adsorbs associatively on Pd through the oxygen atom [22,47] and can coordinate with carvone, acting as both hydrogen donor and acceptor [21]. A surface water-carvone complex is formed with proton donation from O-H to the carbonyl-oxygen [48,49] and

back donation from carvone to the water oxygen (Lewis base [21]). Enolisation of the carbonyl function favours aromatisation *via* migration of the isopropenyl double bond to generate carvacrol. A higher rate was evident for reaction in hydrogen (H_2:Carvone = 1:6) compared with water (in N_2, **Figure 4.3(B)**) where fractional carvone conversion was less than 0.15 and carvacrol production rate was insensitive to H_2O:Carvone molar ratio.

We considered the combined effect of H_2O and H_2 in terms of rate and carvacrol selectivity. Varying H_2O:Carvone (from pure carvone (0:1) to 1:3) under hydrogen lean conditions (H_2:Carvone = 1:6), reaction over Pd/Al_2O_3 was fully selective to carvacrol to give 100% yield (**Figure 4.3(A)**). The presence of H_2O served to significantly raise carvacrol production rate (150 min^{-1} → 320 min^{-1}), which increased with increasing water content (**Figure 4.3(B)**). Ngo *et al.* [24] also reported water promotion in the isomerisation of oleic acid to isostearates over zeolites but they did not propose a possible cause. At H_2O:Carvone = 1:3, the rate was appreciably greater than that recorded for reaction in H_2 without H_2O (150 min^{-1}) or in H_2O without H_2 (35 min^{-1}). We propose that double bond migration following exo -C=C- bond hydrogen addition is facilitated by an increased reactivity of the ring due to water-assisted -C=O group enolisation with a resultant increase in carvacrol production rate. We examined the effect of water addition at higher H_2:Carvone (= 2:1) under conditions where hydrogenation is promoted ($S_{Cavotanacetone}$ = 14%). Incorporation of H_2O suppressed hydrogenation (path **(II)** in **Figure 4.1**) and shifted the reaction along path **(IA)** with exclusive isomerisation to carvacrol to reach 100% yield (**Figure 4.3(A)**). The coordination of water with carvone through the -C=O functionality favours ketone enolisation and inhibits carvotanacetone formation (path **(II)** (**Figure 4.1**)) directing the reaction to carvacrol *via* path **(IB)**, *i.e.* carvone isomerisation is promoted in water under conditions of excess hydrogen.

The rate of carvacrol production declined at a higher H_2O content (H_2O:Carvone > 1:3) regardless of H_2:Carvone (see **Figure 4.3(B)** for H_2:Carvone = 1:6), a result that suggests inhibited carvone uptake/activation due to competition for surface active sites. Chen *et al.* [22] demonstrated that increased surface coverage by water (≥5% coverage) lowers the heat of ketone adsorption, impeding activity. Our results demonstrate the advantages of switching from conventional batch systems to a continuous catalytic process where: (i) the reaction can be operated under mild reaction conditions (423 K and atmospheric pressure); (ii) 100% yield of carvacrol is achieved in a hydrogen lean

feed with water as promoter; (iii) sole formation of cavacrol reduces production costs associated with downstream separation of undesired by-products.

4.4 Conclusions

We have evaluated the promotional effect of H_2O in the continuous gas phase conversion of carvone to carvacrol over Pd/Al_2O_3 (mean Pd size = 3 nm from STEM). Exclusive carvacrol formation was observed in H_2O and an inlet H_2:Carvone = 1:6. At higher H_2 content (H_2:Carvone = 1:2-20:1), hydrogenation to carvotanacetone and carvomenthone was promoted. Where H_2O:Carvone $\leq$ 1:3 (at H_2:Carvone = 1:6-2:1), carvacrol production rate was greater than conversion in hydrogen alone to give 100% carvacrol yield. This is linked to the effect of water on keto-enol tauromerisation that favours double bond migration. Higher H_2O content (H_2O:Carvone > 1:3) lowered activity due to competition for surface sites with carvone. The results of this work establish viable use of water to promote continuous isomerisation and enable full transformation of carvone to carvacrol.

4.5 References

[1] Y. Jiang, X. Wang, Q. Cao, L. Dong, J. Guan, X. Mu, in: M. Xian (Ed.), Sustainable Production of Bulk Chemicals, Springer Netherlands, Dordrecht, 2016, pp. 19-49.

[2] Z. Ma, L. Wei, W. Zhou, L. Jia, B. Hou, D. Li, Y. Zhao, RSC Adv. 5 (2015) 88287-88297.

[3] K. A. D. Swift, Top. Catal. 27 (2004) 143-155.

[4] W. Schwab, C. Fuchs, F.-C. Huang, Eur. J. Lipid Sci. Technol. 115 (2013) 3-8.

[5] A. Corma, S. Iborra, A. Velty, Chem. Rev. 107 (2007) 2411-2502.

[6] L. M. Sanchez, H. J. Thomas, M. J. Climent, G. P. Romanelli, S. Iborra, Catal. Rev. 58 (2016) 497-586.

[7] I. M. Mándity, S. B. Ötvös, F. Fülöp, ChemistryOpen 4 (2015) 212-223.

[8] A. Ocaña-Fuentes, E. Arranz-Gutiérrez, F. J. Señorans, G. Reglero, Food Chem. Toxicol. 48 (2010) 1568-1575.

[9] G. D. Yadav, S. B. Kamble, J. Chem. Technol. Biotechnol. 84 (2009) 1499-1508.

[10] I. M. J. Vilella, S. R. de Miguel, O. A. Scelza, J. Mol. Catal. A: Chem. 284 (2008) 161-171.

[11] C. I. Melo, R. Bogel-Łukasik, E. Bogel-Łukasik, J. Supercrit. Fluid. 61 (2012) 191-198.

[12] S. R. de Miguel, M. C. Román-Martínez, D. Cazorla-Amorós, E. L. Jablonski, O. A. Scelza, Catal. Today 66 (2001) 289-295.

[13] G. C. Torres, S. D. Ledesma, E. L. Jablonski, S. R. de Miguel, O. A. Scelza, Catal. Today 48 (1999) 65-72.

[14] S. R. de Miguel, M. C. Román-Martínez, E. L. Jablonski, J. L. G. Fierro, D. Cazorla-Amorós, O. A. Scelza, J. Catal. 184 (1999) 514-525.

[15] E. I. Klabunovskii, L. F. Godunova, L. K. Maslova, B. Acad. Sci. USSR Chem. Sci. 21 (1972) 1020-1024.

[16] C. I. Melo, Alternative Solvents in Carvone Hydrogenation, Chemical Engineering, Universidade Nova de Lisboa, Lisbon (2011) pp. 53.

[17] R. A. Kjonaas, S. P. Mattingly, J. Chem. Educ. 82 (2005) 1813-1814.

[18] P. Barbaro, F. Liguori, Heterogenized Homogeneous Catalysts for Fine Chemicals Production: Materials and Processes, Springer, Dordrecht, 2010.

[19] P. Benavente, F. Cárdenas-Lizana, M. A. Keane, Catal. Commun. 96 (2017) 37-40.

[20] H. Olcay, Y. Xu, G. W. Huber, Green Chem. 16 (2014) 911-924.

[21] E. Bosch, J. M. Lluch, J. Bertran, Can. J. Chem. 68 (1990) 666-673.

[22] H. Chen, J. Zhao, S. Li, J. Xu, J. Shen, Chin. J. Catal. 36 (2015) 380-388.

[23] L. Nikoshvili, E. Shimanskaya, A. Bykov, I. Yuranov, L. Kiwi-Minsker, E. Sulman, Catal. Today 241, Part B (2015) 179-188.

[24] H. L. Ngo, A. Nuñez, W. Lin, T. A. Foglia, Eur. J. Lipid Sci. Technol. 109 (2007) 214-224.

[25] T. Tomifuji, H. Abe, Y. Matsumura, Y. Sakuma, Process for the Preparation of Branched Chain Fatty Acids and Alkyl Esters Thereof, US5677473 A, 1997.

[26] J. Cao, Z. X. Wang, L. J. Gao, F. Fu, J. Mol. Model. 21 (2015) 66/01-66/08.

[27] W. Bonrath, A. M. C. F. Castelijns, J. G. de Vries, R. P. M. Guit, J. Schütz, N. Sereinig, H. W. L. M. Vaessen, Catal. Lett. 146 (2016) 28-34.

[28] Y. Yu, W. Zhan, Y. Guo, G. Lu, S. Adjimi, Y. Guo, J. Mol. Catal. A: Chem. 395 (2014) 392-397.

[29] L. Ha, J. Mao, J. Zhou, Z. C. Zhang, S. Zhang, Appl. Catal. A: Gen. 356 (2009) 52-56.

[30] M. Li, X. Wang, Y. Hao, F. Cárdenas-Lizana, M. A. Keane, Catal. Today 279 (2017) 19-28.

[31] F. Cárdenas-Lizana, D. Lamey, S. Gómez-Quero, N. Perret, L. Kiwi-Minsker, M. A. Keane, Catal. Today 173 (2011) 53-61.

[32] F. Cárdenas-Lizana, Y. Hao, M. Crespo-Quesada, I. Yuranov, X. Wang, M. A. Keane, L. Kiwi-Minsker, ACS Catal. 3 (2013) 1386-1396.

[33] C. Petrier, J.-L. Luche, Tetrahedron Lett. 28 (1987) 2351-2352.

[34] M. Li, Y. Hao, F. Cárdenas-Lizana, H. H. P. Yiu, M. A. Keane, Top. Catal. 58 (2015) 149-158.

[35] L. L. Jewell, B. H. Davis, Appl. Catal. A: Gen. 310 (2006) 1-15.

[36] I. Chorkendorff, J. W. Niemantsverdriet, Concepts of Modern Catalysis and Kinetics, Wiley-VCH, Weinheim, 2003.

[37] J. Liu, Microsc. Microanal. 10 (2004) 55-76.

[38] E. C. Horning, J. Org. Chem. 10 (1945) 263-266.

[39] C. I. Melo, R. Bogel-Łukasik, M. G. da Silva, E. Bogel-Łukasik, Green Chem. 13 (2011) 2825-2830.

[40] A. M. Doyle, S. K. Shaikhutdinov, H. J. Freund, J. Catal. 223 (2004) 444-453.

[41] G. Prelazzi, M. Cerboni, G. Leofanti, J. Catal. 181 (1999) 73-79.

[42] W. Ludwig, A. Savara, S. Schauermann, Dalton Trans. 39 (2010) 8484-8491.

[43] H. M. Colquhoun, J. Holton, D. J. Thompson, M. V. Twigg, New Pathways for Organic Synthesis: Practical Applications of Transition Metals, Springer US, New York, 2012.

[44] S. J. Blanksby, G. B. Ellison, Acc. Chem. Res. 36 (2003) 255-263.

[45] J. An, L. Bagnell, T. Cablewski, C. R. Strauss, R. W. Trainor, J. Org. Chem. 62 (1997) 2505-2511.

[46] X.-J. Bi, L. T. Higham, J. L. Scott, C. R. Strauss, Aust. J. Chem. 59 (2006) 883-886.

[47] J. M. Heras, G. Estiú, L. Viscido, Appl. Surf. Sci. 108 (1997) 455-464.

[48] H. Wan, A. Vitter, R. V. Chaudhari, B. Subramaniam, J. Catal. 309 (2014) 174-184.

[49] B. Ren, M. Zhao, L. Dong, G. Li, Catal. Commun. 50 (2014) 92-96.

Chapter 5

Liquid Phase Hydrogenation of Carvone over model Pd/Al_2O_3: An Evaluation of Temperature, Pressure and Solvent Effects

Based on results of previous Chapters (3 and 4), Pd/Al_2O_3 was chosen as a model catalyst to evaluate carvone conversion in batch liquid phase operation. The effect of temperature, pressure and solvent were considered.

5.1 Introduction

Hydrogenation of the polyunsaturated (-C=O group, exo- and endocyclic -C=C-) mono-terpenoid carvone generates a number of commercial products used in flavouring [1], pharmaceutical [2] and food processing industry [3]. Most literature funding [4–7] suggests that (**Figure 5.1**) reduction of the exo -C=C- bond generates carvotanacetone, which can undergo further hydrogenation to carvomenthone (reduction of endo -C=C- bond) and carvomenthol (reduction of -C=O) (**path I**). Reduction of the endo -C=C- bond leads to dihydrocarvone (**path II**). Carveol can be obtained from reduction of -C=O (carbonyl) group (**path III**). Reduction of external -C=C- function is the thermodynamically favoured step [8].

Palladium is a common catalytic metal used in the hydrogenation of polyunsaturated hydrocarbons [9] which can drive reaction of carvone hydrogenation according with **paths I-IV** [4–7].

Catalytic liquid phase hydrogenation of carvone, is the three-phase system, requires diffusion of reactants to the bulk solvent (gas/liquid), to catalytic surface (liquid layer at external catalyst surface, liquid/solid) and within the pores. These mass transfer limitations in carvone hydrogenation have never been considered in the literature; however, they play an important role on a rate of a reaction. Not many examples can be found in the literature especially for polyunsaturated aldehyde/ketone evaluating transport effects on selectivity.

Small number of studies considered temperature (283-323 K) and pressure effect (1-160 atm) [4,10,11] over Pd, Pt, Rh catalysts. The results showed that increasing in temperature or pressure resulted in formation of carvomenthone as principal product, with yield more than 90%. In all cases, researchers observed increase in total rate.

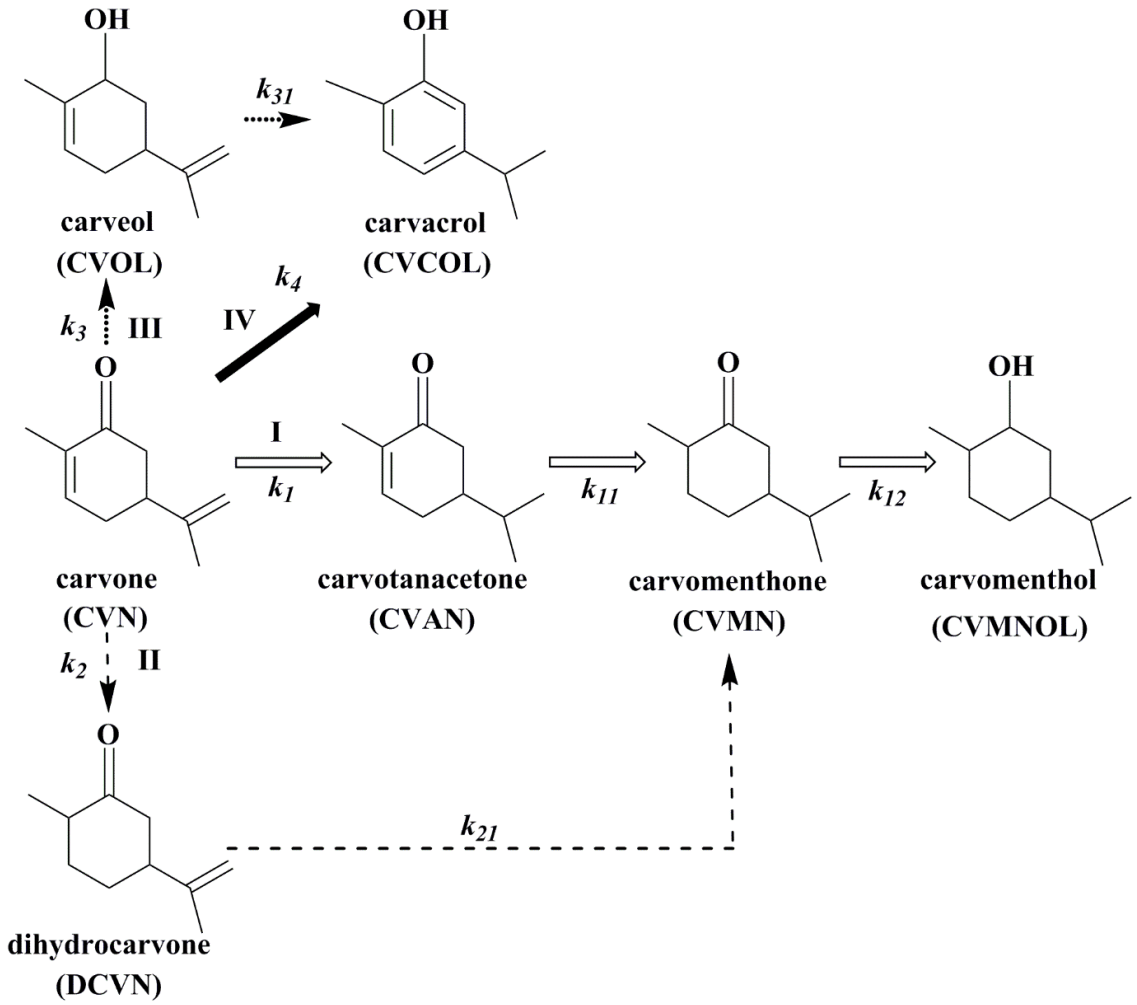

Figure 5.1: Reaction pathways involved in the conversion of carvone to carvomenthol (path I, open arrows), dihydrocarvone (path II, dashed arrow), carveol (path III, dotted arrow) and carvacrol (path IV, solid arrow).

Solvent effects have never been evaluated for carvone hydrogenation. In catalytic hydrogenation solvent effects have been attributed to polarity (μ), dielectric constant (ε), hydrogen solubility (L), catalyst–solvent interactions and reactant solvation in the bulk liquid-phase [12–16]. For instance, in hydrogenation of acetophenone [17] rate decreased with increasing ε of C_1-C_3 alcohols, such effect was linked to solvation effects that impact on reactant adsorption. Drelinkiewicza [18] *et al*. concluded that acetophenone hydrogenation was more influenced by the solvent polarity than H_2 solubility. Arai [19] *et al.* pointed out the influence of pressure on solvent (50 atm H_2 and 170 atm CO_2) in the hydrogenation of three different α, β unsaturated aldehydes, using supercritical CO_2 and ethanol over Pt/Al_2O_3 catalyst. They reported high catalytic activity and selectivity close to 90% to the unsaturated alcohol. The explanation given

for the enhancement in the selectivity is that the dielectric constant of *sc*CO_2 increases with an increase in pressure. Also it has been reported by Ando [20] *et al*. for Co/Al_2O_3 catalyst that during the hydrogenation of unsaturated aldehydes, acetals can be formed if the solvent is an alcohol (ethanol). It can be concluded the polar solvents enhance the -C=O (*vs.* -C=C-) bond hydrogenation and favoured the formation of unsaturated alcohol, due to the presence of hydrogen bonds between the solvent and solute [21–23].

The main challenge of hydrogenation of carvone is still unselective process leading majorly towards carvotanacetone or carvomenthone regardless reaction conditions. A clear understanding of reaction pathway and sensitivity to process variables is required in order to tune reaction towards desirable product(s) selectively. In this study we examine the effects of mass transfer limitations, temperature (273-323 K), pressure (1-35 atm) and solvents (polar and nonpolar), taking Pd/Al_2O_3 as a model catalyst.

5.2 Experimental

5.2.1 Catalytic Activation

Pd/Al_2O_3, (1.2% wt.) was obtained from Sigma-Aldrich. Prior to use, the catalyst was sieved (ATM fine test sieves) to mean particle diameter = 75 μm and activated in 60 cm^3 min^{-1} H_2 at 10 K min^{-1} to 573 K [24] to ensure full reduction of the supported metal precursor. The sample was passivated in 1% v/v O_2/He at ambient temperature before reactions. Main catalyst characterisation was established elsewhere [24–26].

5.2.2 Catalytic Procedure

5.2.2.1 Materials

Solutions of carvone (98%, Sigma-Aldrich) in methanol (99.9%, Sigma-Aldrich), ethanol (95%, Sigma-Aldrich), hexane (>98.5%, Sigma-Aldrich), toluene (>99%, Sigma-Aldrich), benzene (≥99.9%, Sigma-Aldrich) and 1-hexanol (98%, Fisher Chemicals) were used as reactant. All the gases (H_2 and He) were ultrahigh purity (>99.99%, BOC).

5.2.2.2 Ambient Pressure System

Reactions were performed in a commercial stirred glass reactor (Ken Kimble Reactors Ltd.) equipped with a H_2 supply at a constant (Bronkhorst mass-flow-controlled) volumetric flow rate (100 cm^3 min^{-1}). A Teflon impeller provided agitation

in the range of stirring speed (100 – 800 rpm). A recirculator (Grant GP200) was used to stabilise reaction temperature (273 – 323 ±1 K) using ethanol/water as a coolant. At the beginning of each experiment the catalyst and 100 cm^3 pure or diluted (25×10^{-2} M) carvone were charged and agitated in a He flow (50 cm^3 min^{-1}), temperature was allowed to stabilise (15 min) with H_2 introduction (t=0 for reaction). The initial molar reactant to Pd ratio spanned range 1×10^3 – 28×10^3. In blank tests, runs conducted in He did not result in any measurable conversion. Samples were taken by syringe/in-line filters that allowed the controlled removal of aliquots (≤1 cm^3) of reactant/products.

5.2.2.3 Pressurized System

Reactions above ambient pressure (2 – 35 bar) were carried out in a commercial batch stirred stainless steel reactor 75 cm^3 autoclave (Parr reactor) equipped with a H_2 supply system (GCE-Druva). The temperature was maintained at 300 ± 1 K by a process controller (Scientific & Medicine Products Ltd). At the beginning of each run, the diluted carvone solution (40 cm^3, 25×10^{-2} M) and catalyst were charged and flushed three times with He. The system was then heated to reaction temperature, instantly purged with H_2 in order to remove He, stirring was engaged (620 rpm) and the system pressurized with H_2 (t = 0 for reaction). The initial molar reactant to Pd ratio was set at 5×10^3. Liquid sampling system followed the procedure given above.

5.2.2.4 Analytical Method and Activity/Selectivity Measurements

The composition of the reaction/product mixture was analysed by gas chromatography (Perkin-Elmer Auto System XL) equipped with a programmed split/splitless injector and a flame ionization detector, employing a Stabilwax (fused silica) 30 m × 0.32 mm i.d. 0.25 μm film thickness capillary column (RESTEK). Data acquisition/manipulation was performed using the TotalChrom Workstation Version 6.1.2 (for Windows) chromatography data system. Conversion of carvone (X) is given by:

$$X(\%) = \frac{[Carvone]_0 - [Carvone]}{[Carvone]_0} \times 100 \qquad \textbf{(5.1)}$$

with selectivity to (*e. g.*) carvacrol:

$$S_{Carvacrol}(\%) = \frac{[Carvacrol]}{[Carvone]_0 - [Carvone]} \times 100 \qquad \textbf{(5.2)}$$

where subindex '0' refers to initial concentration. Initial carvone consumption rate (R) was determined from a linear regression of the temporal carvone concentration profiles at X < 25% [25]. Repeated reactions with different samples from the same batch of catalyst delivered raw data reproducibility and carbon mass balances within ±7%.

H_2 solubility L (mol dm^{-3}) at reaction conditions was extracted from the open literature [27–30].

A set of first order rate equations describing the possible pathways (**Figure 5.1**) of carvone consumption (k_1 – k_4; kinetic constants of *i*-step (h^{-1})) were solved using Berkley Madonna Version 8.0.1 (for Windows). Data fitting of experimental and predictable points are within acceptable [17,31] deviation did not exceed 10%. Total rate of the reaction r (h^{-1}) was calculated as a sum of k_i of carvone consumption (**Figure 5.1**).

5.3 Results and Discussion

Before to entering to any reaction results influence of catalyst characterization over studied model Pd/Al_2O_3 should be addressed. This particularly catalyst was studied before under similar reaction condition with main characterization data available elsewhere [24–26]. Since Pd under ambient condition in the present of hydrogen exceeded 0.02 atm species of Pd hydride will be formed. As what was previously shown in the temperature-program reduction profile of studied catalyst (**Profile I** in **Figure 5.2** [25]). One should be made clear that the presence of this species, based on DFT calculation study of acetylene hydrogenation over Pd, show essentially no change in the calculated reaction energetics between reactant and products [32], with no significant influence on a surface reaction [33] meaning the presence of Pd hydrides will not be addressed in the this study.

5.3.1 Mass Transport Constrains

Transport in a bulk solvent can be dropped since both reactants are soluble in solvents. It can be concluded that the available H_2 is sufficiently high that any restrictions to transport through the bulk solution are not significant [34]. We have examined the effect of variations in agitation speed and catalyst particle size on initial reaction rate as two well-established diagnostic methodologies to avoid external and internal mass transfer limitations [35–37]. The initial rate of carvone consumption was determined from the linear variation of concentration with time, as shown in

Figure 5.2(I). A more effective agitation of the reaction mixture can enhance the rate of mass transfer of reactants to the catalyst. An increase in stirring speed from 100 to 500 rpm resulted in an increase in rate (**Figure 5.2(A)**), which remained unchanged at greater stirring speeds, demonstrating minimal mass transfer contributions to hydrogenation rate at liquid/solid interface.

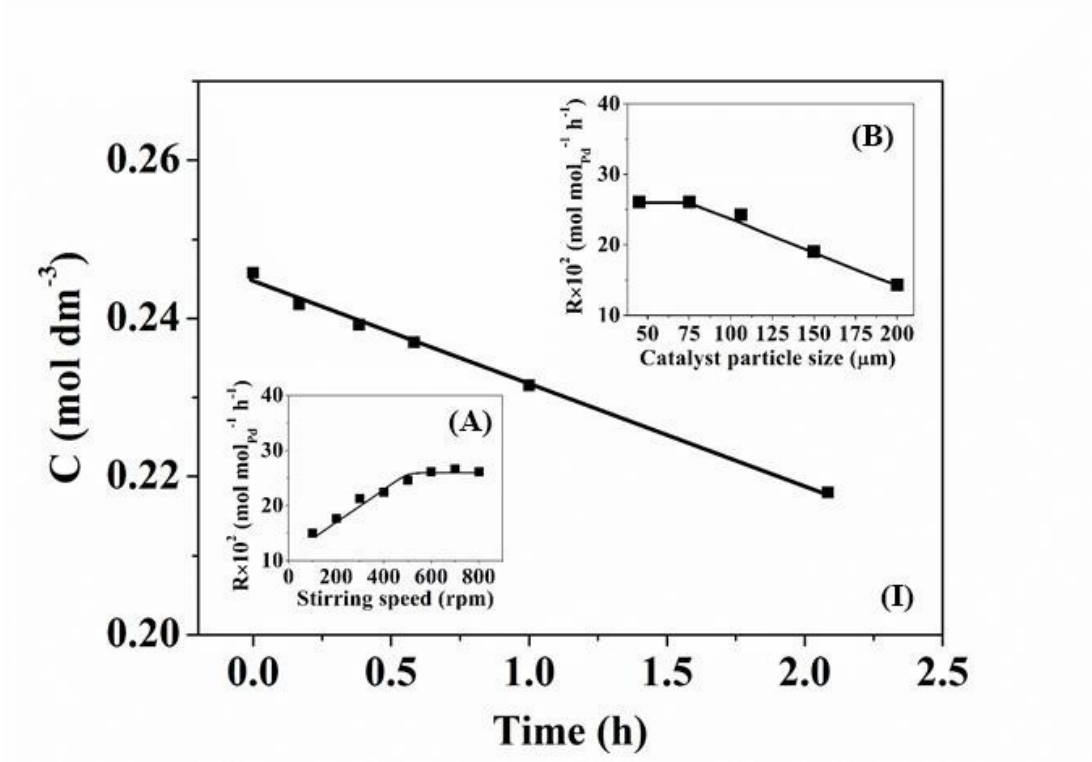

Figure 5.2: (I) Carvone concentration as a function of time; dependence of initial rate (R) of carvone consumption in ethanol at 300 K with (A) stirring speed and (B) catalyst particle size for reaction over Pd/Al_2O_3.

Internal mass transfer can be minimized by decreasing catalyst particle size [38], *i.e.* increasing catalyst surface area. As can be seen from the **Figure 5.2(B)**, initial rate obtained with catalyst particle larger than 75 μm delivered lower rates. As a general rule, Boudart has shown that mass-transport effects play a dominant role when the grain size is greater than 100 μm [38].

We observed no significant effect on the conversion-selectivity relationship (**Figure 5.3(A)**) in variations of stirring speed and particle size under condition of physical and chemical control.

Based on these results, stirring speed was set at 620 rpm and particle 75 μm used in subsequent tests. Initial specific rate (per mol Pd) was constant over a range of

catalyst masses (**Figure 5.3(B)**) and increased with increasing temperature. Such dependence confirms chemical control where external or internal transport limitations do not contribute to the catalytic response [39].

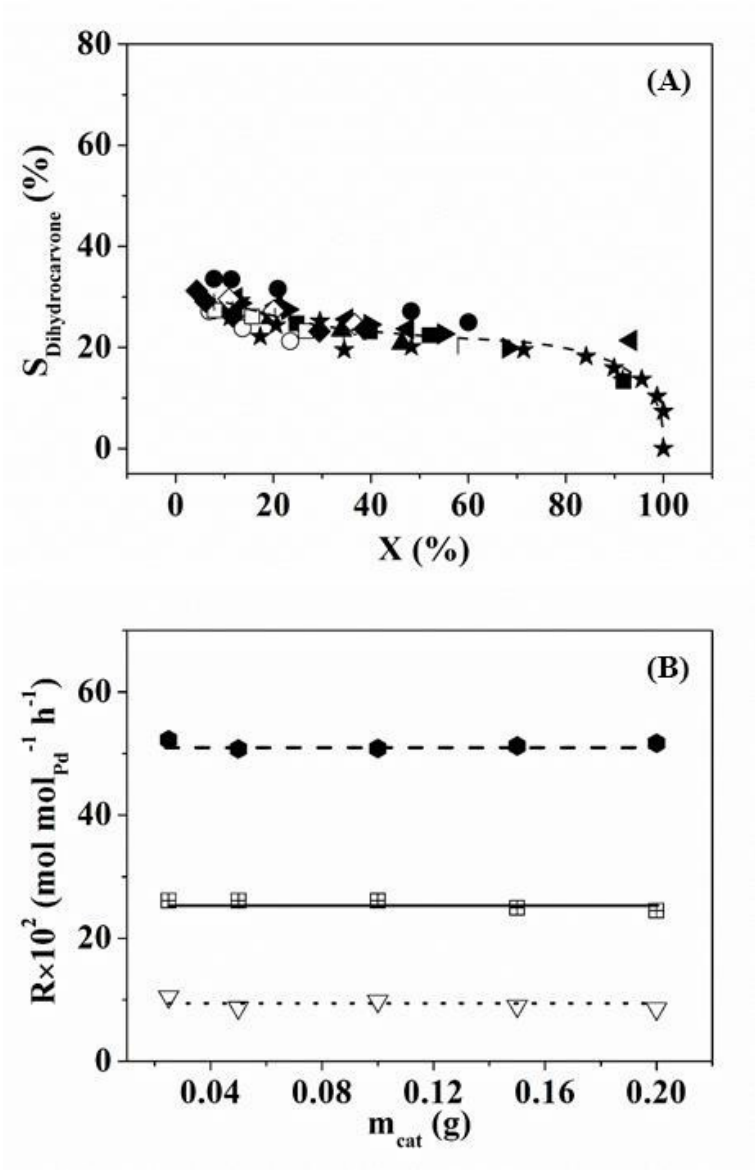

Figure 5.3: (A) Variation of dihydrocarvone selectivity with carvone. at different stirring speeds (○ - 100 rpm; □ - 200 rpm; ◇ - 300 rpm; ■ - 400 rpm; ▲ - 500 rpm; ★ - 600 rpm; ▶ - 700 rpm; ◀ - 800 rpm) and catalyst particle size (● – 45 µm; ▬ – 106 µm ; ◆ - 200 µm); (B) Dependence of rate (R) of carvone consumption in ethanol with mass of catalyst at different temperatures; ▽ - 273 K; ⊠ - 300 K; ⬢ - 323 K.

5.3.2 Catalytic results. Temperature and Pressure effects

5.3.2.1 Reaction under Atmospheric pressure

Figure 5.4 represents concentration response of reactant/products with time based on experimental points and estimated (based on first order reaction) kinetic curves at 300K. Complete carvone consumption was achieved after 5 hours with total rate of 728 h^{-1} (equals to sum of $k_1+k_2+k_3+k_4$) (**Table 5.1**). It should be noted that carveol (k_3), a product of carbonyl hydrogenation (**path III, Figure 5.1**), was detected in trace quantities ($<7\times10^{-4}$ M). As thermodynamics stated carbonyl group would be the least favourable among -C=C- in hydrogenation of polyunsaturated ketone [8].

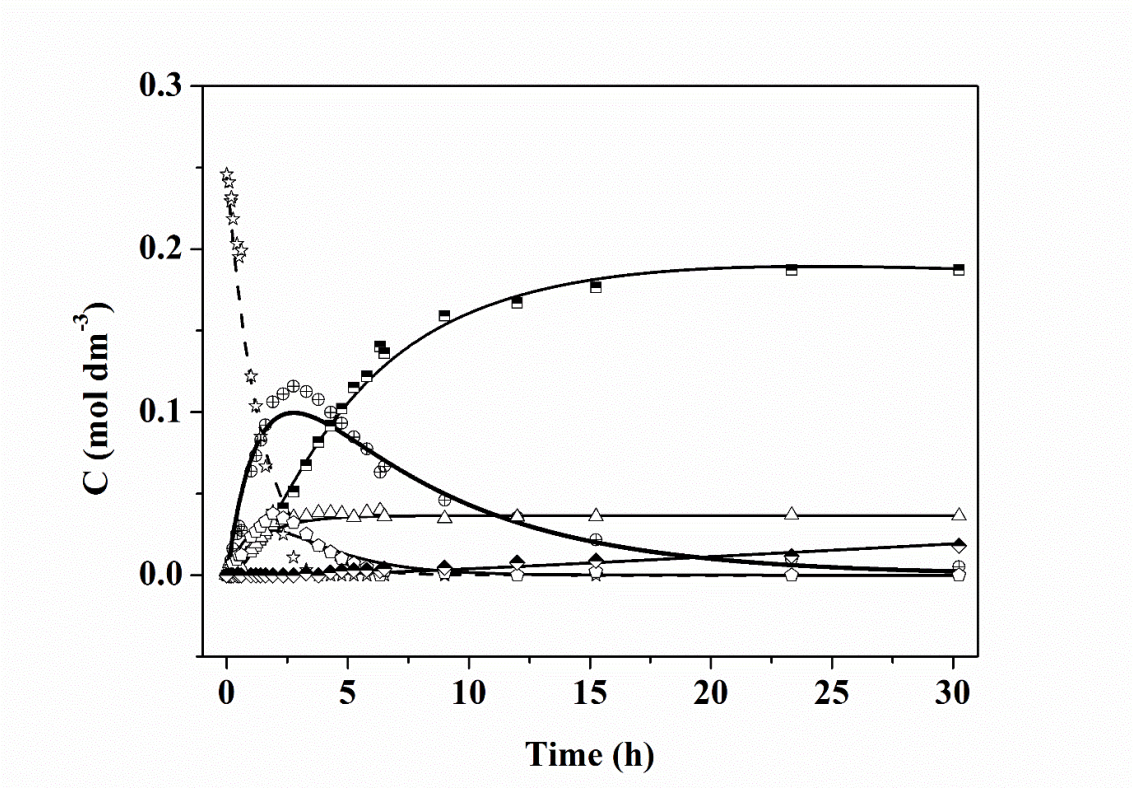

Figure 5.4: Experimental and calculated kinetic curves for temporal variation of concentration at 300 K and 1 atm in ethanol; ☆ – Carvone; ⊕-Carvotanacetone; ⬒- Carvomenthone; ◆- Carvomenthol; ⬠- Dihydrocarvone; △ - Carvacrol.

The formation of carvotanacetone (k_1) from the hydrogenation of exocyclic -C=C- group (**path I** in **Figure 5.1**) reached a maximum after 3 h with a subsequent decrease in concentration and full consumption after 25 h, sequentially giving carvomenthone (a product of endocyclic -C=C- hydrogenation via k_{11}). Carvomenthone concentration showed a time dependent increase and reached an upper limit after 15 h. Carvomenthol, the fully hydrogenated product along **path I** (k_{12}) showed an increased

formation with time. The rate constants for **path I** decrease in the order: $k_1 > k_{11} > k_{12}$ (**Table 5.1**), proofing step wise reaction mechanism.

Table 5.1: Total rate *r* ($k_1+k_2+k_3+k_4$), rates for individual steps and rate constant ratios for carvone hydrogenation in ethanol as a function of temperature (273 – 323 K) and pressure (1 – 35 atm).

	Step				
***P* (atm)**		**1**			**35**
***T* (K)**		**300**	**273**	**323**	**300**
H_2 solubility (mol dm^{-3})		0.004	0.003	0.005	0.145
r **(h^{-1})**		728	121	1267	4266
k_1	CVN → CVAN	441	66	727	2601
k_{11}	CVAN → CVMN	146	19	155	1542
k_{12}	CVMN → CVMNOL	4	0.1	10	60
k_2	CVN → DCVN	179	52	306	1237
k_{21}	DCVN → CVMN	450	41	474	2229
k_3	CVN → CVOL	0	0	0	0
k_{31}	CVOL → CVCOL	0	0	0	0
k_4	CVN → CVCOL	108	4	234	428
k_2/k_1		0.4	0.8	0.4	0.5
k_{21}/k_{11}		3.1	2.2	3.1	1.4
k_2/k_4		1.7	13.0	1.3	2.9
k_1/k_4		4.1	16.5	3.1	6.1

CVN = carvone; CVAN = carvotanacetone; CVMN = carvomenthone; CVMNOL = carvomenthol; DCVN = dihydrocarvone; CVOL = carveol; CVCOL = carvacrol.

There is no many evidence in the literature according to **path II** in the literature over Pd catalyst, however it was reported in the trace amount for Pt system under condition close to experimental (T = 313 – 363K, atmospheric pressure) [11].

Alternatively, over Au catalyst (T = 373K, P = 9atm) where Demidova [3] *et. al* obtained dihydrocarvone (62% of yield) with consecutive it hydrogenation to carvomenthone. In our case similar tendency to Au was observed over Pd in endocyclic -C=C- hydrogenation generating dihydrocarvone (**path II**) with a maximum (at 2.5 h) and subsequent consumption to carvomenthone (via k_{21}) through the reduction of remaining -C=C-.

Comparison of kinetic constants relative to hydrogenation of each of 3 functional groups showed that $k_1 > k_2 >> k_3$ which is coincided with thermodynamics finding [8] and reported literature over supported noble metals (Pd, Pt, Rh [9,10,12,39–43]) under condition close to experimental.

As can be seen from **Figure 5.4**, carvacrol formation coincides with carvone consumption and once the reactant was completely transformed there was no detectable change in carvacrol concentration. This suggests direct transformation carvone → carvacrol (k_4, **path IV**). It has been proposed that carvacrol formation occurs *via* dehydrogenation of carvotanacetone over bulk Pd (atmospheric pressure) and Pd/Al_2O_3 under supercritical conditions [4,5]. We explained such transformation due to intramolecular hydrogen transfer between the ring structure and isopropenyl group (exo -C=C-) with keto-enol tautomerisation of formed unstable intermediate based on the Horiuti-Polanyi mechanism with keto-enol tautomerization taking into account hydrogenation and isomerization of -C=C- double bonds on metal surface [40]. The mechanism consists of four steps [41]: (1) hydrogen chemisorption and dissociation on the catalyst surface; (2) the chemisorption of the -C=C- double bonds of carvone on the catalyst surface accompanied by an opening of the double bond and the formation of two new connection with the catalyst, which leads to the formation of a di-adsorbed complex (π – complex); (3) the migration of a hydrogen atom from the catalyst surface to one of the carbon atoms of the di-adsorbed complex, forming a half-hydrogenated intermediate. This intermediate can undergo in two ways: (a) formation of di-adsorbed species when hydrogen of a neighbouring carbon atom is abstracted or (b) addition of second hydrogen atom to the half-hydrogenated intermediate, leading to the saturation of double bond. It should be added that formed di-adsorbed complex (unstable intermediate) in (3(a)) will undergo to final step (4) of keto-enol tautomerization by activation of -C=O and $-C^{\alpha}-C^{\beta}H_2-$ (at carbonyl group) which leads to the formation of a three-adsorbed complex (2π complexes). These species would proceed by hydrogen transfer/elimination from C^{β} to oxygen forming carvacrol as ultimate product. Musolino

reported [42] that double bond isomerization reaction (hydrogen migration) in linear alcohols can occur in the presence of hydrogen (P_{H_2} = 1 atm) in ethanol at T = 293 K over supported Pd to generate saturated aldehydes - 2-hydroxytetrahydrofuran up to 20% yield.

5.3.2.2 Effect on Reaction kinetic

Altering reaction condition – temperature, pressure and solvents, can be expected to influence reaction rate and reaction pathways [3,4,10,17,43].

Rate constants over the temperature range 273 – 373 K are given in **Table 5.1**. It can be seen linear increase in total rate with temperature (121 – 1267 h^{-1}) which can be linked to (i) increase of hydrogen solubility (0.003 – 0.005 mol dm^{-3}) and (ii) providing system with more energy to overcome potential barrier leading to products. Conversion/selectivity plots coincided in the case of carvotanacetone and carvomenthone (**Figure 5.5(A**) and **(B)**) with no differences in activation energies, 36 *vs.* 26 kJ mol^{-1}, calculated based on Arrhenius plot (ln k = f(1/T)). Literature indicates that hydrogenation of exocyclic -C=C- requires 59 kJ mol^{-1} over Pd-bulk [4], which has same order of magnitude with our value. Carvomenthone (from dihydrocarvone) was the predominant product at full conversion (**Figure 5.4**) with k_{21}/k_{11} = 2.2 – 3.1. In terms of endo- and exo- -C=C- reduction reaction in the studied temperature range went *via* **path II** less favourable rather than *via* **path I** with temperature influence (k_2/k_1 = 0.8 – 0.4) 2 fold higher towards carvotanacetone at 323 K. Opposite we found strong temperature effect on dihydrocarvone and carvacrol. At lower temperature dihydrocarvone selectivity is more predominant in compare to the high temperature, whereas carvacrol tendency is opposite (**Figure 5.5(D)**). Evaluating k_2/k_4 showed decreasing from 13.0 to 1.3 with respect to temperature raise. Taking into account proposed mechanism and increase in energy of the system it can be suggested that step of hydrogen transfer – (3(a)) of the proposed mechanism, became more favourable in compare to hydrogenation – (3(b)). Previously in the literature increase in selectivity towards carvacrol with temperature over unsupported Pd under mild conditions in the presence of H_2 has also been noted [4]. Grau [44] *et al.* in the liquid hydrogenation of limonene at atmospheric hydrogen pressure over Pd/Al_2O_3, also observed that hydrogen migration rate compared to the hydrogenation rate is noticeable at higher temperatures.

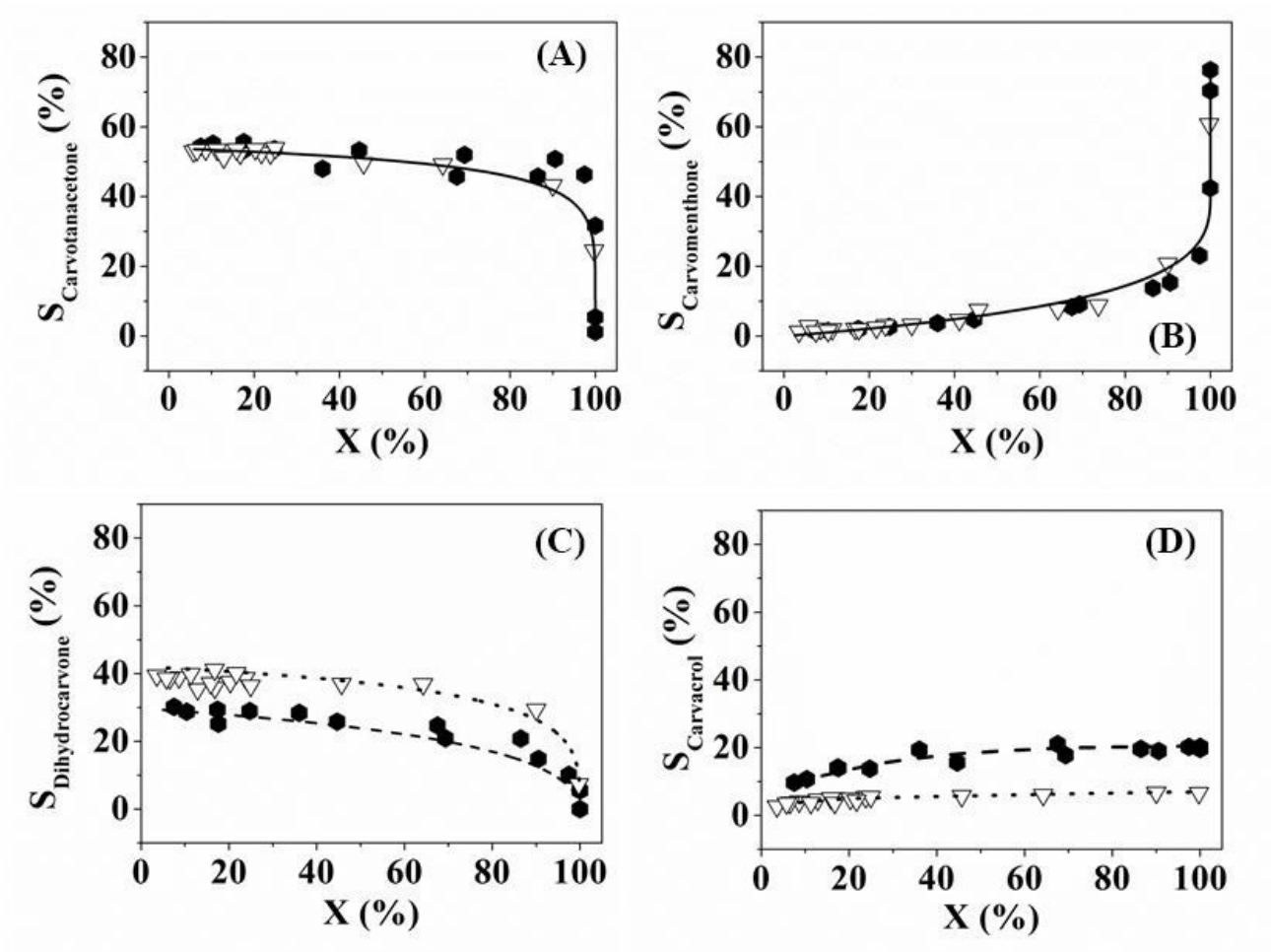

Figure 5.5: Experimental points and calculated selectivity/conversion plots ((A) carvotanacetone, (B) carvomenthone, (C) dihydrocarvone and (D) carvacrol) for reaction at 1 atm and 273 K (▽) and 323 K (●) in ethanol.

Pressure was another tested valuable that allowed to increase hydrogen solubility (L) by 36 times, thus it is known that the increase of pressure causes a linear growth of hydrogen solubility in accordance with Henry's Law and, consecutively causing the increase of hydrogen concentration on the catalyst surface. Rate of carvone consumption was directly proportional to pressure (**Figure 5.6**).

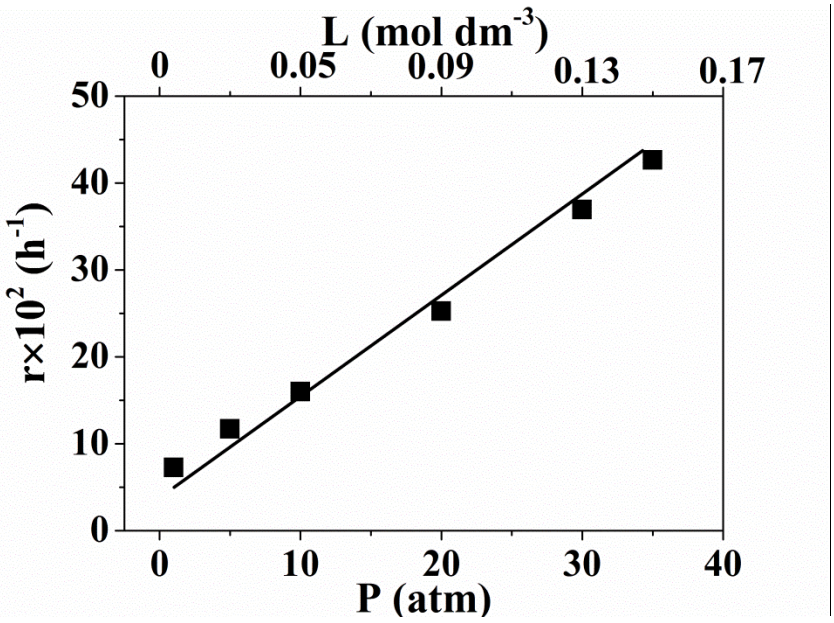

Figure 5.6: Total rate of carvone transformation (r) and hydrogen solubility (L) with pressure (1 – 35 atm) at 300 K

Rate of carvotanacetone formation in comparison to dihydrocarvone is favourable towards the reduction of exo- -C=C- at all pressures (k_2/k_1 = 0.4 – 0.5), perhaps due to greater thermodynamic stability of conjugated endo- -C=C- in compare to exo- -C=C- [8]. Selectivity/conversion response was common for carvotanacetone and carvomenthone with pressure (**Figure 5.7(A) and (B)**). Carvomenthone majorly formed *via* dihydrocarvone (k_{21}/k_{11} > 1) at all studied pressure, however, it worth to highlight that with increase in pressure contribution of carvotanacetone is raised by twice (3.1-1.4) due to preferential adsorption of letter with raise in hydrogen coverage. We also found, that once hydrogen solubility was modified from low to high content (0.004 – 0.145 mol dm^{-3}), ratio between hydrogenation (dihydrocarvone) and hydrogen transfer step (carvacrol) k_2/k_4 decrease from 1.7 to 2.9, showing that hydrogen transfer (**path IV**) became less favourable at high hydrogen concentration (**Table 6.1**), whereas hydrogenation is almost doubled. According with suggested mechanism increase in H_2

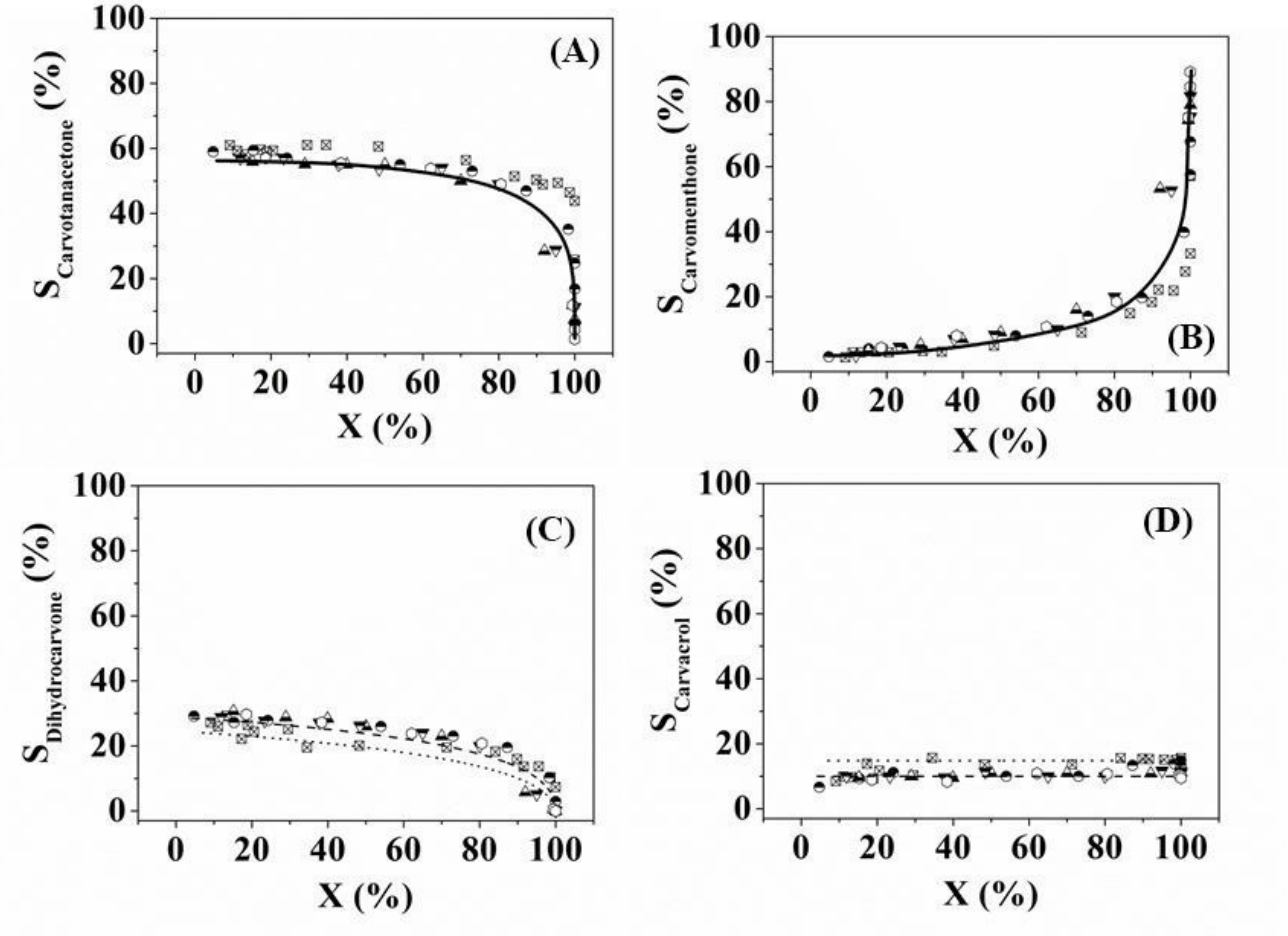

Figure 5.7: Experimental and calculated selectivity/conversion curves for (A) carvotanacetone, (B) carvomenthone, (C) dihydrocarvone and (D) carvacrol for reaction at 300 K and different pressures; ⊠ - 1 atm; ◓ - 5 atm; ▲ - 10 atm; ▽ -20 atm; ⬡ - 35 atm.

concertation on the catalyst surface would ensure saturation of double bounds (step (3(b)) in proposed mechanism) and hence dihydrocarvone and carvotanacetone are formed more likely in compare to carvacrol.

5.3.2.3 Solvent Effect

Before considering any effects relating to solvents reaction with carvone was performed in the absence of any solvents (**Figure 5.8(A)**) as the benchmark. Since pressure effect has an influence on selectivity for hydrogenation *vs.* hydrogen transfer, reaction with/without solvent was done under the similar hydrogen solubility conditions. For that purpose, we considered hydrogen solubility in cyclohexanone as the closest molecular structure to carvone available in the literature (0.004 mol dm^{-3}) [45]. **Figure 5.8(A)** shows the rate constants for the different possibilities (k_1-k_4) considered to evaluate the effect of the solvent: solventless (pure carvone), nonpolar solvent (toluene) and polar solvent (ethanol). In the absence of solvents no formation of dihydrocarvone (k_2=0) can be explained by the presence of dipole-dipole interaction and/or van-der-Walls forces between carvone molecules [46] that could hinder internal -C=C- and stabilize carvone within the ring with possible adsorption of exo -C=C- and -C=O group, giving carvotanacetone (k_1=49 h^{-1}) and carveol (k_3=10 h^{-1}), respectively.

In all three cases we observed products of external -C=C- hydrogenation (k_1) – carvotanacetone with hydrogen migration/keto-enol tautomerization (k_4) – carvacrol. In ethanol values of k_1 and k_4 is by order of magnitude higher those for solventless system and toluene, which are under the similar level, 50 and 23 h^{-1}, respectively. It can be explained based on the presence of H bonds in alcohol that facilitate hydrogen transfer from the catalyst to the substrate allowing solvent react as mediator [47]. As oppose, in solventless system and toluene, where H-bonds can not exist values are lower. Additionally, differences in formation of carvacrol in the absence of solvent and toluene can be explained based on the interaction between solute-solute (carvone-carvone) and solute-solvent (carvone-toluene) interaction, which cyclic structure of carvone/non-polar solvent tends to stabilize the carvone and inhibits hydrogen transfer within it. However, a close look, comparing ratio between hydrogen transfer step (k_4) with the rest of hydrogenation step (k_1, k_2 and k_3), reveals no differences in the values (0.2-0.3), suggesting that hydrogen migration is insensitive to solvent environments.

Electron delocalization within the ring in carvone is modified by ethanol through the solute – solvent interaction between -OH in alcohol and -C=O in carvone caused by dipole-dipole forces. More specifically intermolecular H bonds to oxygen in carbonyl

increasing the energy barrier of the transition state required for formation of carveol [48,49]. As a result formation of carveol is inhibited ($k_3=0$). Nevertheless, since the ring structure is no longer stable hydrogenation of endocyclic -C=C- is observed (k_2 = 179 h^{-1}). And opposite, in the absence of solvent and toluene, formation of dihydrocarvone was also not detected; however entry for k_3 is by more than 4-fold higher in compare to solventless system. It can be explained that toluene predominantly solvate/interacts with endocyclic -C=C- by dipole-induce dipole forces activating -C=O group [50].

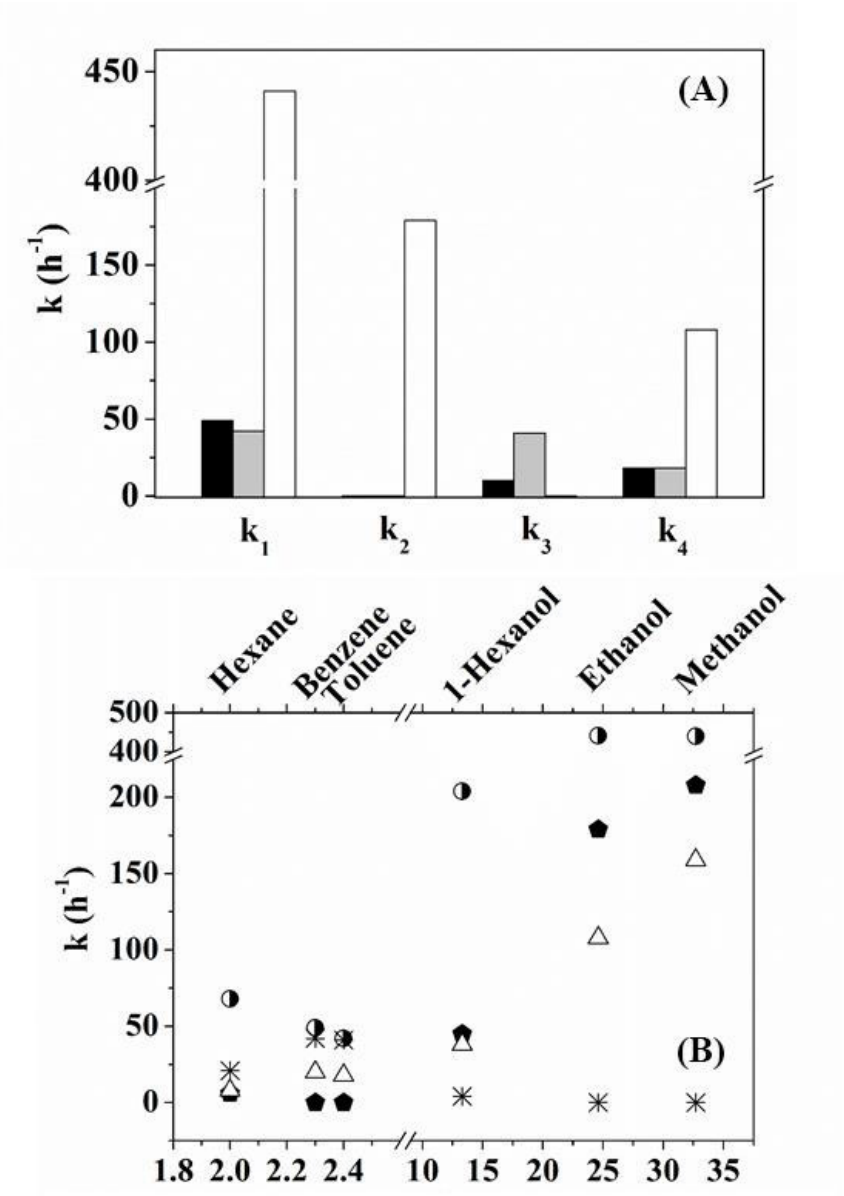

Figure 5.8: (A) Dependence of k_{1-4} (h^{-1}) in the absence of solvent, in toluene and ethanol (black, grey and white bars respectively) at 300 K and ambient pressure (H_2 solubility = 0.004 mol dm^{-3}); (B) Response on solvent dependence of ε for: ◑- k_1, ⬟ - k_2, ✳ - k_3 and △ - k_4 at 300 K and 1 atm (data for 1-Hexanol at 2 atm); H_2 solubility = 0.004 mol dm^{-3}.

Formation of carveol (hydrogenation of -C=O bond) was significantly higher previous reported ($\leq 8 \times 10^{-3}$ $mol_{carveol}$ g_{metal}^{-1} h^{-1} at 313 K and atmospheric pressure over Pt catalysts [51]) thus it was worth to study over polar and non-polar solvents. Dielectric constant (ε) is a macroscopic property, indicating of solvents ability to insulate charges from each other, was served as a measure of polarity [17]. Higher ε means higher polarity, and greater ability to stabilize charges. As can be seen from the **Figure 5.8(B)**, once reaction is taken place in polar solvent (ε = 33 – 25) no formation of carveol can be detected. Moving in the region with less polarity is allowing to obtain carveol with the rate constant of 4 h^{-1} in 1-hexanol (ε = 13). Finally over toluene (ε = 2.4) and benzene (ε = 2.3) as non-polar solvents k_3 reaches the highest values of 41 and 42 h^{-1}, respectively. In hexane, having the lowest polarity (ε = 2.0), k_3 value is twice lower in compare to aromatic solvents, which can be accounted based on structural differences of aromatic and linear nonpolar solvents. It is know, that benzene will solvate electron deficient site of the local dipoles in solute molecules [52] (carbon atom at -C=O group in carvone) by local dipole-induced dipole interaction of carvone with benzene. Ring conjugated structure of the π-electron in aromatic tends to lie away from the negative end of the local dipole [52] (oxygen atom at -C=O group in carvone). Moreover, comparison among non-polar solvents (hexane *vs* aromatics) demonstrated; (i) $k_2 > 0$ in hexane, suggesting that both functionalities in conjugated position (endo -C=C- with -C=O) does not interact with solvent; (ii) favourable reduction of exo -C=C- (k_1) in hexane that on toluene or benzene and opposite trends was observed for hydrogen transfer product (k_4). Elsewhere [50] it was suggested to separate saturated non-polar solvents from aromatic while evaluation results due to the possible reactivity/adsorption of the letter with the catalyst surfaces. Generally, steps of -C=C- hydrogenation and hydrogen migration (**Figure 5.8(B)**) tend to increase with ε of studied solvents which can also be linked to existence of intermolecular forces between solvent and solute and their influence on reaction pathways.

5.4 Conclusions

- Conditions to avoid mass transfer limitation for carvone hydrogenation over model Pd/Al_2O_3 catalyst was found to be ≥600 rpm and ≤75 μm of catalyst particle size. Variations in stirring speed and particle size had no significant effect on the conversion-selectivity relationship.

- Strong temperature influence was found in formation of dihydrocarvone (k_2) and carvacrol (k_4), with decreasing in rate constant ratio k_2/k_4 by 13 times from 273 to

323 K., which was suggested to be linked to an intermediate which can undergo hydrogen transfer and hydrogenation step.

- Raising pressure allowed to increase total rate of carvone consumption linearly. Higher pressures (35 atm) limit carvacrol formation due to greater hydrogen availability, which inhibits hydrogen elimination step according with suggested mechanism.

- Polar solvents preferentially solvate exocyclic and endocyclic -C=C- in carvone, whereas activation of carbonyl group is hindered by the solute – solvent interaction which can modify the energy barrier of the transition state required for formation of carveol. Lowering in ε of solvents is favourable for formation of carveol. On the other hand moving from nonpolar to polar solvents allowed to facilitate activation of -C=C- groups.

5.5 References

[1] A. Kumar, V. Khajuria, S. Aggarwal, Anal. Chem. Lett. 2 (2012) 373–400.

[2] R.A. Kjonaas, S.P. Mattingly, J. Chem. Educ. 82 (2005) 1813–1814.

[3] Y.S. Demidova, E. V Suslov, O.A. Simakova, I.L. Simakova, K.P. Volcho, N.F. Salakhutdinov, D.Y. Murzin, Catal. Today 241 (2015) 189–194.

[4] E.I. Klabunovskii, L.F. Godunova, L.K. Maslova, Bull. Acad. Sci. USSR, Div. Chem. Sci. 21 (1972) 1020–1024.

[5] C.I. Melo, R. Bogel-Łukasik, E. Bogel-Łukasik, J. Supercrit. Fluid. 61 (2012) 191–198.

[6] M. Cano, A.M. Benito, W.K. Maser, E.P. Urriolabeitia, New J. Chem. 37 (2013) 1968–1972.

[7] R. Mélendrez, G. del Angel, V. Bertin, M.A. Valenzuela, J. Barbier, J. Mol. Catal. A: Chem. 157 (2000) 143–149.

[8] A. Zsigmond, F. Notheisz, P. Kluson, T. Floris, Chemoselective and Enantioselective Hydrogenations on Immobilized Complexes, in: P. Barbaro, F. Liguori (Eds.), Heterogenized Homogeneous Catalysts for Fine Chemicals Production Catalysis by Metal Complexes, Springer, Dordrecht, 2010: pp. 283–359.

[9] V.D. Stytsenko, D.P. Mel'nikov, Russ. J. Phys. Chem. A 90 (2016) 932–942.

[10] C.I. Melo, R. Bogel-Łukasik, M.G. da Silva, E. Bogel-Łukasik, Green Chem. 13 (2011) 2825–2830.

[11] G.C. Torres, S.D. Ledesma, E.L. Jablonski, S.R. de Miguel, O.A. Scelza, Catal.

Today 48 (1999) 65–72.

[12] L. Gilbert, C. Mercier, Solvent effects in Heterogeneous Catalysis : Application to the Synthesis of Fine Chemicals, in: M. Guisnet, J. Barbier, J. Barrault, C. Bouchoule, D. Duprez, G. Pérot, et al. (Eds.), Studies in Surface Science and Catalysis, Elsevier, Amsterdam, 1993: pp. 51–66.

[13] J.T. Wehrli, A. Baiker, D.M. Monti, H.U. Blaser, H.P. Jalett, J. Mol. Catal. 57 (1989) 245–257.

[14] R.L. Augustine, The Stereochemistry of Hydrogenation of α,β-Unsaturated Ketones, in: D.D. Eley, H. Pines, B.W. Paul (Eds.), Advances in Catalysis, Academic Press, New York, 1976: pp. 56–80.

[15] H.U. Blaser, H.P. Jalett, J. Wiehl, J. Mol. Catal. 68 (1991) 215–222.

[16] J. Hidalgo-Carrillo, M.A. Aramendía, A. Marinas, J.M. Marinas, F.J. Urbano, Appl. Catal. A: Gen. 385 (2010) 190–200.

[17] N.M. Bertero, A.F. Trasarti, C.R. Apesteguía, A.J. Marchi, Appl. Catal. A: Gen. 394 (2011) 228–238.

[18] A. Drelinkiewicza, A. Waksmundzka, W. Makowski, J.W. Sobczak, A. Król, A. Zieba, Catal. Lett. 94 (2004) 143–156.

[19] B.M. Bhanage, Y. Ikushima, M. Shirai, M. Arai, Catal. Lett. 62 (1999) 175–177.

[20] C. Ando, H. Kurokawa, H. Miura, Appl. Catal. A: Gen. 185 (1999) L181–L183.

[21] P. Mäki-Arvela, J. Hájek, T. Salmi, D.Y. Murzin, Appl. Catal. A: Gen. 292 (2005) 1–49.

[22] I. Kun, G. Szöllösi, M. Bartók, J. Mol. Catal. A: Chem. 169 (2001) 235–246.

[23] H. Yamada, S. Goto, J. Chem. Eng. Jpn. 36 (2003) 586–589.

[24] Y. Hao, M. Li, F. Cárdenas-Lizana, M.A. Keane, Catal. Lett. 146 (2016) 109–116.

[25] S. Gómez-Quero, F. Cárdenas-Lizana, M.A. Keane, Ind. Eng. Chem. Res. 47 (2008) 6841–6853.

[26] P. Benavente, F. Cárdenas-Lizana, M.A. Keane, Catal. Commun. 96 (2017) 37–40.

[27] T.-K.-H. Trinh, J.-C. de Hemptinne, R. Lugo, N. Ferrando, J.-P. Passarello, J. Chem. Eng. Data 61 (2016) 19–34.

[28] E. Brunner, J. Chem. Eng. Data 30 (1985) 269–273.

[29] K. Radhakrishnan, P.A. Ramachandran, P.H. Brahme, R. V Chaudhari, J. Chem. Eng. Data 28 (1983) 1–4.

[30] J.V.H. d'Angelo, A.Z. Francesconi, J. Chem. Eng. Data 46 (2001) 671–674.

[31] S. P. Bressa, O. M. Martínez, G. F. Barreto, Ind. Eng. Chem. Res. 42 (2003) 2081–2092.

[32] P.A. Sheth, M. Neurock, C.M. Smith, J. Phys. Chem. B 107 (2003) 2009–2017.

[33] B. Yang, R. Burch, C. Hardacre, G. Headdock, P. Hu, J. Catal. 305 (2013) 264–276.

[34] S. Gómez-Quero, F. Cárdenas-Lizana, M.A. Keane, Am. Inst. Chem. Eng. 56 (2010) 756–767.

[35] J. Wood, L. Bodenes, J. Bennett, K. Deplanche, L.E. Macaskie, Ind. Eng. Chem. Res. 49 (2010) 980–988.

[36] C. Wan, Y. An, G. Xu, W. Kong, Int. J. Hydrogen Energy 37 (2012) 13092–13096.

[37] P.A. Rautanen, J.R. Aittamaa, A.O.I. Krause, Ind. Eng. Chem. Res. 39 (2000) 4032–4039.

[38] E. Segal, J. Catal. 52 (1978) 45–49.

[39] U.K. Singh, M.A. Vannice, Appl. Catal. A: Gen. 213 (2001) 1–24.

[40] A. Philippaerts, S. Goossens, P.A. Jacobs, B.F. Sels, ChemSusChem 4 (2011) 684–702.

[41] M. Kreich, P. Claus, Angew. Chemie Int. Ed. 44 (2005) 7800–7804.

[42] M.G. Musolino, C.M.S. Cutrupi, A. Donato, D. Pietropaolo, R. Pietropaolo, Appl. Catal. A: Gen. 243 (2003) 333–346.

[43] Z. Tian, Q. Li, J. Hou, L. Pei, Y. Li, S. Ai, J. Catal. 331 (2015) 193–202.

[44] R.J. Grau, P.D. Zgolicz, C. Gutierrez, H.A. Taher, J. Mol. Catal. A: Chem. 148 (1999) 203–214.

[45] M. Herskowitz, J. Wisniak, L. Skladman, J. Chem. Eng. Data 28 (1983) 164–166.

[46] G. Arivazhagan, A. Elangovan, R. Shanmugam, R. Vijayalakshmi, P.P. Kannan, Chem. Phys. Lett. 627 (2015) 101–106.

[47] J. Pritchard, G.A. Filonenko, R. van Putten, E.J.M. Hensen, E.A. Pidko, Chem. Soc. Rev. 44 (2015) 3808–3833.

[48] J. Lambert, R.N. Compton, T.D. Crawford, J. Chem. Phys. 136 (2012) 114512.

[49] F.A. Carey, R.J. Sundberg, Structural Effects on Stability and Reactivity, in: Advanced Organic Chemistry. Part A: Structure and Mechanisms, 5th ed., Springer, New York, 2007: pp. 253–389.

[50] J. Hájek, N. Kumar, P. Mäki-Arvela, T. Salmi, D.Y. Murzin, J. Mol. Catal. A: Chem. 217 (2004) 145–154.

[51] I.M.J. Vilella, S.R. de Miguel, O.A. Scelza, J. Mol. Catal. A: Chem. 284 (2008) 161–171.

[52] R.S. Armstrong, M.J. Aroney, R.K. Duffin, H.J. Stootman, R.J.W. Le Fevre, J. Chem. Soc. Perkin Trans. 2 (1973) 1272–1275.

Chapter 6

Summary and Future Work

The main purpose of this research project was to investigate catalytic transformation of bio derived polyunsaturated ketone – carvone to valuable products/intermediates for fine chemical industry. Isomerization and selective hydrogenation of exo-/endo- -C=C- and -C=O functionalities results in a range of products. Product distribution is sensitive to the nature of the metal (**Chapter 2**), support and hydrogen content in the feed (**Chapter 3**) with water as a suitable hydrogen source (**Chapter 3**) for reaction in continuous gas phase operation. The possibility of carvone conversion in standard batch liquid phase operation was also considered (**Chapter 5**).

6.1 Main Findings

The main results in the gas phase showed Au favours hydrogenation of endo- -C=C- to dihydrocarvone. Formation of carvacrol through transformation of carvotanacetone or carvone was observed over Pt/Al_2O_3 and Au/Al_2O_3. We demonstrate that carvacrol generation is sensitive to the hydrogen content in the feed where 100% yield can be attained over Pd/Al_2O_3 under hydrogen lean conditions (H_2:Carvone = 1/6). Use of water as a hydrogen source further enhances carvacrol production rate through a modified reaction mechanism. The nature of the solvent is a critical parameter for carvone transformation in a standard batch liquid system where non-polar solvent facilitate transformation to carveol. Increase in hydrogen availability in gas phase (H_2:Carvone>1/6) or liquid phase (P_{H_2}>1 atm) results in formation of hydrogenation products (carvotanacetone, carvomenthone).

6.2 On-going / Future work

The results in **Chapter 3** demonstrate that reaction of double bond migration was only possible in the presence of H_2 and we achieve full selectivity towards carvacrol under hydrogen lean conditions with the rate normalized per surface of 10 mol m^{-2} min^{-1}. An increase in the hydrogen content of the feed resulted in the formation of products from hydrogenation [1]. We consider here the use of alternative materials able to promote isomerisation and evaluate the role of hydrogen.

Molybdenum nitrides are known exhibit catalytic activity that are similar to noble metals (platinum-group catalysts) in isomerization of 1-butene to 2-butenes [2]. Hydrogen dissociation and activation of a molecule, which is dependent on surface area and crystallographic phase [3], can play a critical role in hydrogen-mediated reactions. There is evidence in the literature [2,4–6] that the incorporation of N in Mo creates supplementary sites that can modify reactant adsorption and alter the catalytic response. It has been suggested elsewhere [2] that activation of -C=C- taken place on the surface of Mo sites having low valence state ($Mo^{\delta+}$ with $\delta = 0 - 2$) to promote double-bond migration of 1-butene. By modifying N content it became possible to have an impact on Mo partial charge [7] and consequently to change adsorption mode. Likewise, crystallographic phase is expected to have an impact on isomerization response [7].

Table 6.1: Crystal particle size from XRD (d_{hkl}), specific surface area (SSA) and specific (per SSA) carvacrol production rate (R) for carvone conversion in N_2 and H_2 over Mo and molybdenum nitrides; *Reaction conditions*: T = 423 – 573 K, P = 1 atm, X ~ 0.1.

Catalyst	d_{hkl} (nm)	SSA ($m^2\ g^{-1}$)	T (K)	$R\times10^5$ (mol $m^{-2}min^{-1}$)
Mo	32	4	423/573[a]	-[c]
			423[b]	-[c]
			573[b]	1
β-Mo_2N	27	7	423[a]	1
			423[b]	1
			573[a]	5
			573[b]	4
γ-Mo_2N	24	46	423[a]	1
			423[b]	1
			573[a]	5
			573[b]	5

[a]Reaction in N_2 (N_2/Carvone = 20).
[b]Reaction in H_2 (H_2/Carvone = 20).
[c]no conversion detected.

Based on that we prepared number of Mo bulk (as a reference) and Mo nitrides samples with surface areas 4 – 46 $m^2 g^{-1}$ (**Table 6.1**) and different Mo/N surface ratios (*ca.* 0 – 2) [7–11] to establish the effect on carvone conversion. The process was performed in a continuous gas phase plug reactor operated at atmospheric pressure. The preparation of materials involved temperature programmed treatment of MoO_3, as a precursor, in H_2/H_2+N_2 continuous flow at atmospheric pressure in a horizontally mounted quartz reactor, followed by cooling and oxygen passivation steps [7].

XRD analysis (**Figure 6.1(A-B)**) confirms the formation of Mo (2θ = 40.5°, 58.6° and 73.7° for (110), (200) and (211) planes) β-Mo_2N (**C-D**; 2θ = 37.8°, 43.1°, 45.3°, 62.6°, 64.3°, 75.5°, 78.6° and 80.5° → (112), (200), (004), (220), (204), (312), (116) and (224)) and γ-Mo_2N (**E-F**; 2θ = 37.6°, 43.4°, 63.6°, 76.0° and 80.2°→ (111), (200), (220), (311) and (222)). The absence of additional peaks confirms the complete transformation of MoO_3 to Mo and β- and γ-Mo_2N, where the passivation step served solely to provide a superficial oxide film without bulk oxidation [8]. The three samples exhibit a similar particle size (24-32 nm (based on XRD), **Table 6.1**) that falls within the range (10-100 nm) of values previously quoted in the literature [12,13]. SSA of Mo was low (*ca.* 4 $m^2 g^{-1}$, **Table 6.1**) but comparable to previous reported Mo samples (1-13 $m^2 g^{-1}$) [12,13]. The SSA falls within the range of 2-17 and 24-193 $m^2 g^{-1}$ quoted previously for β- and γ-Mo_2N, respectively, synthesised by temperature programmed reaction in N_2/H_2 [7,8,14]. The temperature requirements for the removal of the passivating layer were analysed by TPR and the resultant profiles are presented in **Figure 6.2**. For the three samples, removal of oxygen passivated layer was demonstrated to be sufficient at 933 K.

Reaction over Mo resulted in conversion at 573 K only in the presence of H_2, with 90% selectivity to carvacrol and 10% to carvotanacetone. This catalytic behaviour is similar to that recorded over (*e.g.*) transition metals [15]. In contrast, we observed carvacrol formation in the absence of hydrogen over (β– and γ–) molybdenum nitrides (**Table 6.1**). Future work will consider catalytic response over each functionality in carvone, *i.e.* carbonyl and internal/external -C=C- (vinylcyclohexane, cyclohexene, cyclohexanone) to establish the nature of the reaction mechanism.

These preliminary results are promising and demonstrate the feasibility of an alternative hydrogen free carvacrol production over bulk molybdenum nitrides.

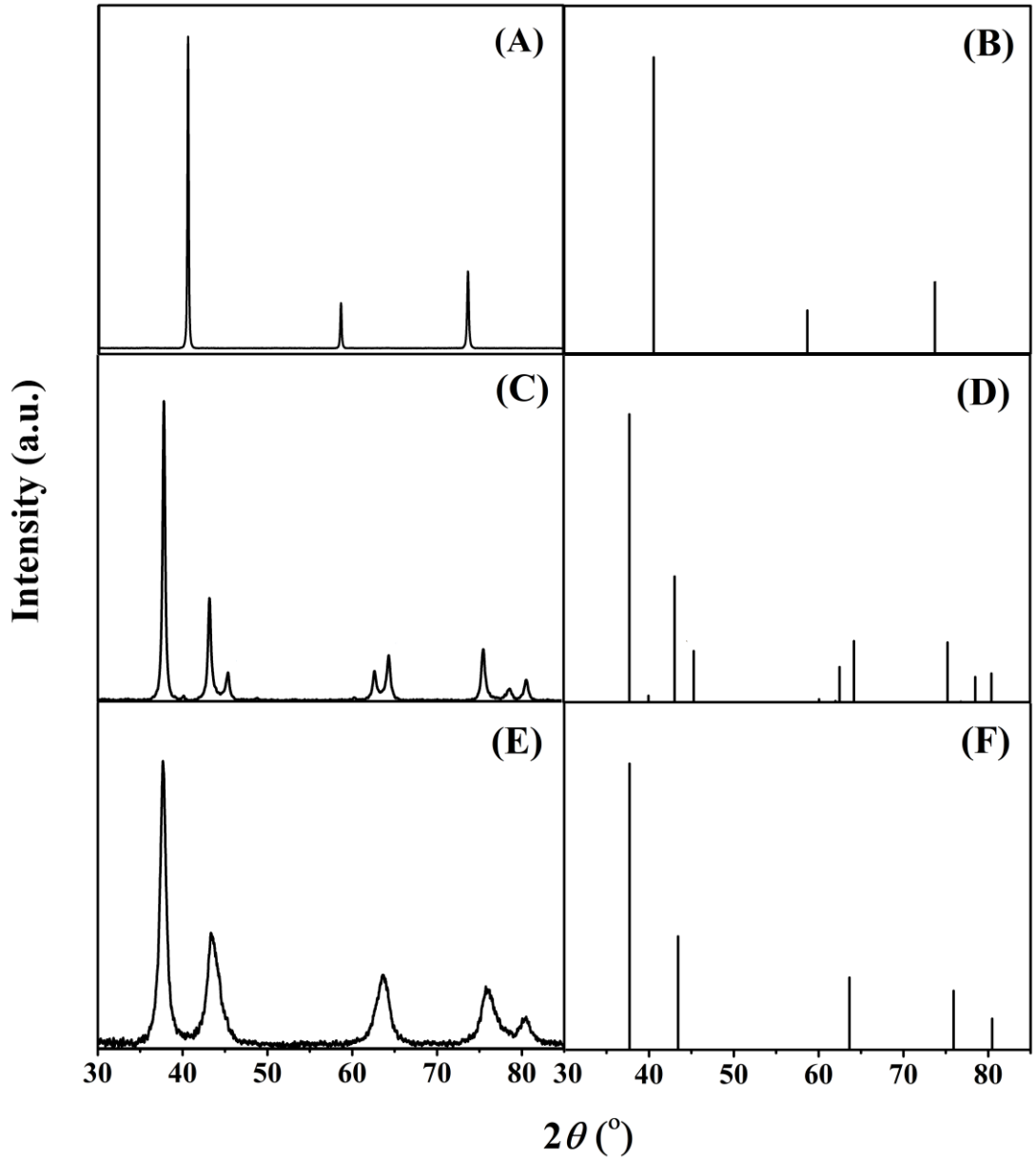

Figure 6.1: XRD patterns for (A) Mo, (C) β-Mo_2N and (E) γ-Mo_2N. *Note:* peak assignment with associated characteristic planes based on JCPDS-ICDD reference data for (B) Mo (Ref. card 42-1120), (D) β-Mo_2N (25-1368) and (F) γ-Mo_2N (25-1366).

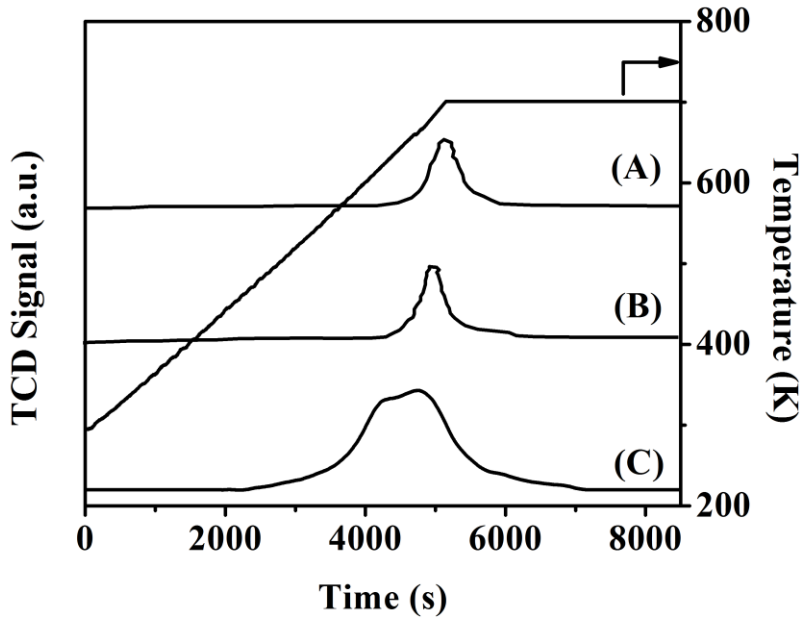

Figure 6.2: Temperature programmed reduction (TPR) profiles for (A) Mo, (B) β-Mo_2N and (C) γ-Mo_2N.

6.3 References

[1] P. Benavente, F. Cárdenas-Lizana, M.A. Keane, Catal. Commun. 96 (2017) 37–40.

[2] Z. Wu, C. Li, P. Ying, Z. Wei, Q. Xin, J. Phys. Chem. B 105 (2001) 9183–9190.

[3] Z. Wei, Q. Xin, P. Grange, B. Delmon, J. Catal. 168 (1997) 176–182.

[4] Z. Wu, S. Yang, Q. Xin, C. Li, Catal. Surv. Asia 7 (2003) 103–119.

[5] S. Yang, C. Li, J. Xu, Q. Xin, J. Phys. Chem. B 102 (1998) 6986–6993.

[6] J.F. Zhu, J.C. Guo, R.S. Zhai, X. Bao, X.Y. Zhang, S. Zhuang, Appl. Surf. Sci. 161 (2000) 86–93.

[7] N. Perret, F. Cárdenas-Lizana, D. Lamey, V. Laporte, L. Kiwi-Minsker, M.A. Keane, Top. Catal. 55 (2012) 955–968.

[8] S. Gong, H. Chen, W. Li, B. Li, Appl. Catal. A Gen. 279 (2005) 257–261.

[9] M. Nagai, Y. Goto, A. Miyata, M. Kiyoshi, K. Hada, K. Oshikawa, S. Omi, J. Catal. 182 (1999) 292–301.

[10] S.W. Gong, H.K. Chen, W. Li, B.Q. Li, Energ. Fuel. 20 (2006) 1372–1376.

[11] C.W. Colling, L.T. Thompson, J. Catal. 146 (1994) 193–203.

[12] J.-G. Choi, R.L. Curl, L.T. Thompson, J. Catal. 146 (1994) 218–227.

[13] R. Yuvakkumar, V. Elango, V. Rajendran, N. Kannan, Synth. React. Inorganic, Met. Nano-Metal Chem. 41 (2011) 309–314.

[14] D. Mckay, J.S.J. Hargreaves, J.L. Rico, J.L. Rivera, X.-L. Sun, J. Solid State Chem. 181 (2008) 325–333.

[15] P. Benavente, F. Cárdenas-Lizana, M.A. Keane, Catal. Today 308 (2018) 45–49.